The complex case of the calcareous sponge Leucosolenia complicata (Porifera: Calcarea): hidden diversity in Boreal and Arctic regions with description of a new species

Andrey I Lavrov, Irina Ekimova, Dmitry Schepetov, Alexandra Koinova, Alexander Ereskovsky

The Linnean Society of London
ZOOLOGICAL Journal of the Linnean Society

The complex case of the calcareous sponge Leucosolenia complicata (Porifera: Calcarea): hidden diversity in Boreal and Arctic regions with description of a new species

Andrey Lavrov[1,‡,*], Irina Ekimova[1,‡], Dimitry Schepetov[1,2], Alexandra Koinova[1], Alexander Ereskovsky[3,4,5]

[1]Lomonosov Moscow State University, Leninskie Gory 1-12, Moscow, Russia
[2]Biological Faculty, Shenzhen MSU-BIT University, Shenzhen, China
[3]Saint Petersburg State University, Saint Petersburg, Russia
[4]IMBE, Aix Marseille Univ, Avignon Univ, CNRS, IRD, Marseille, France
[5]N.K. Koltzov Institute of Developmental Biology RAS, Vavilov str. 26, Moscow, Russia

Journal:	*Zoological Journal of the Linnean Society*
Manuscript ID	ZOJ-03-2023-5299.R1
Manuscript Type:	Original Article
Keywords:	biogeography < Geography, molecular phylogeny < Genetics, phylogenetic systematics < Phylogenetics, species delineation < Taxonomy, species boundaries < Taxonomy, North Atlantic < Geography, ultrastructure < Anatomy, scanning electron microscopy < Techniques
Abstract:	In this study, we present the first integrative revision of the Boreal and Arctic calcareous sponges of the genus Leucosolenia with a specific focus on its biodiversity in the White Sea. The material for this work included a combination of newly collected specimens from different regions of the North-East Atlantic and the White Sea and historical museum collections. An integrative analysis was implemented based on vast morphological data (light microscopy, scanning and transmission electron microscopy), microbiome observations, ecological data, accompanied by molecular phylogenetic and species delimitation analyses based on three nuclear markers (28S rRNA, 18S rRNA and histone H3). We demonstrate that Leucosolenia complicata, previously reported from Arctic waters, is restricted to the North-East Atlantic, while in the Arctic, the Leucosolenia diversity is represented by at least four species: Leucosolenia corallorrhiza, Leucosolenia variabilis and two new species, one of which is described herein under the name Leucosolenia creepae sp. nov. The molecular phylogeny analysis supports the species identity of these species. In addition to conventional morphological characters, new informative fine morphological characters (skeleton and oscular crown organisation; cytological structure including morphotypes of symbiotic bacteria) were found, providing a baseline for further revision of this group in other regions.

Abstract

In this study, we present the first integrative revision of the Boreal and Arctic calcareous sponges of the genus *Leucosolenia* with a specific focus on its biodiversity in the White Sea. The material for this work included a combination of newly collected specimens from different regions of the North-East Atlantic and the White Sea and historical museum collections. An integrative analysis was implemented based on vast morphological data (light microscopy, scanning and transmission electron microscopy), microbiome observations, ecological data, accompanied by molecular phylogenetic and species delimitation analyses based on three nuclear markers (28S rRNA, 18S rRNA and histone H3). We demonstrate that *Leucosolenia complicata,* previously reported from Arctic waters, is restricted to the North-East Atlantic, while in the Arctic, the *Leucosolenia* diversity is represented by at least four species: *Leucosolenia corallorrhiza, Leucosolenia variabilis* and two new species, one of which is described herein under the name *Leucosolenia creepae* sp. nov. The molecular phylogeny analysis supports the species identity of these species. In addition to conventional morphological characters, new informative fine morphological characters (skeleton and oscular crown organisation; cytological structure including morphotypes of symbiotic bacteria) were found, providing a baseline for further revision of this group in other regions.

Keywords: biogeography, molecular phylogeny, phylogenetic systematics, species delineation, species boundaries, North Atlantic, ultrastructure, scanning electron microscopy

Introduction

The calcareous sponges (Class Calcarea) represent rather a small group in terms of biodiversity across all sponge taxa (<5% of diversity) (Manuel *et al.*, 2004), but are characterized by a unique mineral skeleton of calcium carbonate spicules and display great diversity in their body organisation (Borojevic *et al.*, 1990). The classification of this group is currently facing many challenges and rearrangements at all taxonomical levels due to high levels of homoplasy and convergent evolution (Manuel *et al.*, 2004; Dohrnmann *et al.*, 2006; Voigt *et al.*, 2012; Voigt & Wörheide, 2016; Alvizu *et al.*, 2018). In the course of the last two decades, the integrative taxonomy has became the most popular approach to define and describe taxa on different taxonomic levels and produce a reliable phylogeny-based classification of living organisms (Dayrat, 2005; Padial *et al.*, 2010; Schlich-Steiner *et al.*, 2010). In many cases, such studies can resolve existing taxonomic disputes strictly and definitively (Goulding & Dayrat, 2016). Molecular phylogenetics augments the ability of a researcher to find species boundaries and thus taxonomically important morphological characters. The integrative studies of calcareous sponges gave a new insight into understanding the actual diversity and evolutionary history of this group, with numerous new taxa being described during the last years (Azevedo *et al.*, 2017; Riesgo *et al.*, 2018; van Soest & de Voogd 2018; Alvizu *et al.*, 2019; Cóndor-Luján *et al.*, 2019; Sanamyan *et al.*, 2019; Chu *et al.*, 2020; Klautau *et al.*, 2020 and many others).

The Russian Arctic represents a poorly studied region with an unknown diversity of calcareous sponges. At the same time, extensive studies of Calcarea in the western part of the Arctic were carried out, thanks to which new species were described and a deep revision of the species described by that time was carried out (Rapp *et al.*, 2001; Rapp, 2006, 2015; Alvizu *et al.*, 2019). In other regions, like the Mediterranean, Caribbean and some others, the diversity of calcareous sponges has been extensively studied using molecular methods (Cavalcanti *et al.*, 2014; Klautau *et al.*, 2016, 2021; Fontana *et al.*, 2018; van Soest & de Voogd, 2018). However, contemporary studies of the Russian Arctic tend to lend heavily to traditional morphology with

limited regard for newer methods and trends in taxonomy and biogeography (Breitfuss, 1898a,b,c; Koltun, 1952; Ereskovsky, 1994a). Despite limited taxonomic studies, calcareous sponges from the White and Barents Seas are widely involved in various ecological (Ereskovsky, 1994b,c; 1995a,b), physiological and embryological (Anakina, 1997; Anakina & Korotkova, 1989; Anakina & Drozdov, 2000, 2001) researches. Two of the focus-sponges, *Leucosolenia complicata* (Montagu, 1814) and *Sycon ciliatum* (Fabricius, 1780) have become rising model species in evolutionary developmental studies (Leininger *et al.*, 2014; Fortunato *et al.*, 2014, 2015, 2016; Ereskovsky *et al.*, 2017a; Lavrov *et al.*, 2018, 2022; Lavrov & Ereskovsky, 2022; Melnikov *et al.*, 2022).

The genus *Leucosolenia* Bowerbank, 1864 (phylum Porifera, class Calcarea, subclass Calcaronea) includes more than 40 distinct species distributed worldwide, being more specious in the northern regions (Burton, 1963; Borojevic *et al.*, 2000). The history of systematics of this group is complicated by the different species conceptions proposed by various researchers since Haeckel's monograph on calcareous sponges (Haeckel, 1872). Haeckel established 21 new genera, seven of which represent an asconoid type of organisation. However, he did not consider any generic names for calcareous sponges used before him; hence, this system has undergone various modifications (Minchin, 1904). At the species-level, many of his names and his 'connection varieties' for leucosolenoid sponges were further considered synonyms of three widely distributed species: *Leucosolenia botryoides* (Ellis & Solander, 1786), *L. complicata, Leucosolenia variabilis* Haeckel, 1870 (Minchin, 1904, 1905). Further research highlighted the complications of taxonomical studies due to the absence of informative characters. As a result, some North Atlantic species, *i.e.*, *L. complicata, L. variabilis* and *L. botryoides* were believed to have a wide cosmopolitan distribution ranging from the Arctic to South Africa, New Zealand and the Antarctic (Burton, 1963). Sarà (1956) found a connection between spicular characters in these species and suggested they may hybridise, which caused even more simplification of the system with a single species, *L. botryoides* represented by different 'forms' of uncertain taxonomical status (Burton,

1963). With the advent of new microscopic techniques and molecular studies, the systematics of the genus *Leucosolenia* has received much attention during the last twenty years. The valid status of some species was reconsidered, *e.g.*, North-eastern Atlantic *Leucosolenia corallorrhiza* (Haeckel, 1872) (Rapp, 2015) and *Leucosolenia somesii* (Bowerbank, 1874) (van Soest *et al.*, 2007). Also, several new species were described based on studies using scanning electron microscopy that allowed the identification of fine spines on spicules (van Soest, 2017; Chu *et al.*, 2020). Recent molecular phylogenetic analysis of North Atlantic *Leucosolenia* species showed the paraphyly of the genus (Alvizu *et al.*, 2018) and the high rate of hidden biodiversity within it. Nevertheless, no integrative revision has been conducted yet, and the taxonomical status of most North-Atlantic species remains unverified.

The main goal of our study is to revise the diversity and taxonomy of the genus *Leucosolenia* from the White Sea using an integrative approach, which includes vast molecular, morphological and cytological data. Additionally, the specific aims of the study are to identify phylogenetically significant morphological characters and to propose optimal sets of molecular markers for further taxonomical and phylogenetic research on calcareous sponges.

Material and methods

Material

The representatives of the genus *Leucosolenia* were collected in the White Sea at N.A. Pertsov White Sea Biological Station MSU (66°34′N, 33°08′E) during 2016–2018 at the upper subtidal zone and by SCUBA diving (Table S1). The identification of the specimens was based on external and internal (skeletal) characteristics, such as spicule types and their spatial arrangement in different regions of the sponge body. Additionally, we studied specimens of *Leucosolenia complicata* collected in the English Channel (Roscoff, France) and a specimen of *Leucosolenia somesii* from the collection of the Zoological Museum of Amsterdam (ZMA). Several spicule slides from the collection of the British Museum of Natural History (BMNH) of *L. complicata, L. variabilis* and *L. somesii,* including the type material for the latter two species, were also examined for comparison with species from the White Sea (Table S1). Collection data, voucher numbers and GB accession numbers are summarised in Table S1. All new samples were fixed in 96% ethanol. Voucher specimens are deposited in the collections of the Zoological Museum of Moscow State University, White Sea Branch (WS).

Taxon sampling

Our molecular sampling included 279 individuals from the White Sea, the Netherlands and Roscoff (Table S1). For species delimitation, the 28S C-region was sequenced for all specimens available for study (to make sure that the morphological identification is correct). In several cases, 28S did not give enough resolution to undoubtedly support the genetic distinctness of species; therefore, for a large number of samples from the White Sea, we additionally obtained a novel histone H3 marker (see below for details). Finally, 18S was obtained only for several specimens for the concatenated phylogenetic analysis to test the monophyly of the genus *Leucosolenia*.

Seventeen *Leucosolenia* specimens from the White Sea, Greenland, Norway and the North-East Atlantic (unspecified), for which only GenBank sequences were available, were also included in the analyses (Table S1). The final datasets for each gene included as many specimens from

different localities as possible to improve the resolution of phylogenetic reconstructions. *Plectroninia novaecaledoniense* Vacelet, 1981 and *Clathrina arnesenae* (Rapp, 2006) were chosen as outgroups based on recent papers on the calcaronean phylogeny (Voigt & Wörheide, 2016; Alvizu *et al.*, 2018). To test the identity of high-level taxonomic groups, specimens included in the most recent Calcaronea phylogenetic study (Alvizu *et al.*, 2018) were used in the concatenated analysis (Table S1).

DNA extraction, amplification and sequencing

DNA was extracted from small pieces of tissue using PALL AcroPrep 96-well plates (PALL Corp., USA) (Ivanova *et al.*, 2006) and the Diatom DNA Prep100 kit (Isogen Lab, Russia) according to manufacturer protocol with minor modifications: an increased lysis stage time for better dissolving of tissues and a reduced volume of extraction reagents at the final step for increasing the final DNA concentration. Extracted DNA was used as a template for the amplification of partial 28S rRNA (C-region, LSU) and 18S rRNA (SSU). To support the results obtained with ribosomal markers, we also included the nuclear protein-coding gene histone *H3* (H3) in the analysis. Although this marker is commonly used in systematic and phylogenetic studies in other invertebrate groups, sequences for the calcarean sponges are absent in GenBank. Primers were modified from standard H3 metazoan primers (H3AF: 5'-ATG GCT CGT ACC AAG CAG ACV GC-3' H3AR: 5'-ATA TCC TTR GGC ATR ATR GTG AC-3' see Colgan, 1998), the annotated transcriptome of *S. ciliatum* (Fortunato *et al.*, 2014) was used for a primer design (Table 1). Polymerase chain reactions were carried out in a 25-µL reaction volume, which included 5 µL of 5x Taq Red Buffer (Eurogen Lab, Russia), 0.5 µL of HS-Taq Polymerase (Eurogen Lab, Russia), 0.5 µL of dNTP (50 µM stock), 0.3 µL of each primer (10 µM stock), 1 µL of genomic DNA and 17.7 µL of sterile water. The PCR conditions for the corresponding primers are given in Table 1. Sequencing for both strands proceeded with the Big Dye Terminator v3.1 sequencing kit (Applied Biosystems, USA), the same primers as for PCR were used.

Sequencing reactions were analysed using the ABI 3500 Genetic Analyzer (Applied Biosystems, USA). All new sequences were deposited in GenBank (Table S1).

Phylogenetic reconstruction

Raw reads for each gene were assembled and checked for improper base-calling using GeneiousPro 4.8.5 (Biomatters, New Zealand). Original data and publicly available sequences were aligned with the MUSCLE (Edgar, 2004) algorithm in MEGA7 (Kumar *et al.*, 2016). Protein-coding sequences were translated into amino acids to verify the coding sequences. The resulting alignments were 353 bp for 28S, 1493 bp for 18S and 359 bp for H3. Phylogenetic analyses were conducted for each marker individually and for the concatenated dataset. Sequences were concatenated by a simple biopython script (Chaban *et al.*, 2019). The best-fitting nucleotide evolution model was tested in MEGA7 based on the Bayesian information criterion (BIC) for each partition. The best-fitting model for the 28S partition was HKY+G, for the 18S partition – K2, and for the H3 partition – K2P+G. Phylogenetic reconstruction of the concatenated dataset was performed applying evolutionary models for partitions separately. The Bayesian estimation of posterior probability for all datasets was performed in MrBayes 3.2 (Ronquist & Huelsenbeck, 2003). Markov chains were sampled at intervals of 500 generations. The analysis was started with random starting trees and 10^7 generations. Maximum likelihood-based phylogeny inference for all datasets was performed in the HPC-PTHREADS-AVX version of RaxML (Stamatakis, 2014) with ultrafast bootstrapping (UFBoot approximation approach) (Minh *et al.*, 2013) in 1000 pseudoreplicates under the GTRCAT model of nucleotide evolution. Bootstrap values were placed on the best tree found with SumTrees 3.3.1 from DendroPy Phylogenetic Computing Library Version 3.12.0 (Sukumaran & Holder, 2010). The final phylogenetic tree images were rendered in FigTree 1.4.0.

Species delimitation

Uncorrected inter- and intra-specific *p*-distances were calculated in MEGA7 (Kumar *et al.*, 2016). Assemble Species by Automatic Partitioning (ASAP) (Puillandre *et al.*, 2021), calculation

of uncorrected *p*-distances and single-gene trees were applied to assist in the species delimitation analysis. 28S and H3 sequences of *Leucosolenia* species (excluding outgroups) used in the phylogenetic analysis, were aligned for ASAP analysis with the MUSCLE algorithm (Edgar, 2004) in MEGA7 (Kumar *et al.*, 2016). 18S sequences were not used in the analysis due to low substitution rates. The analysis was run on the online version of the programme (https://bioinfo.mnhn.fr/abi/public/asap/asapweb.html) with the default setting and three proposed models: Jukes-Cantor (JC), Kimura (K80) and Simple distance. Uncorrected *p*-distances were calculated for the same alignments used for ASAP in MEGA7 (Kumar *et al.*, 2016). Single-gene trees were calculated using the Maximum Likelihood approach in HPC-PTHREADS-AVX version of RaxML (Stamatakis, 2014) with ultrafast bootstrapping (UFBoot approximation approach) (Minh et al., 2013) with 1000 pseudoreplicates under the GTRCAT model of nucleotide evolution.

A visualisation of character heterogeneity was assessed using PopART 1.7 (http://popart.otago.ac.nz) (Leigh & Bryant, 2015) with the TCS network algorithm (Clement *et al.*, 2002) and a connection limit of 5%. The resulting networks were edited in Adobe Illustrator CS 2015 to highlight certain features.

Morphological studies

The external morphology of each species was studied under Leica M165FC stereomicroscope (Leica, Germany) equipped with a digital camera Leica DFC420 (Leica, Germany). Extraction of spicules and slide preparation for a total of 34 specimens were made according to standard protocols (Klautau & Valentine, 2008). The general skeleton morphology of both the oscular rim and cormus tubes was studied under Leica M165C stereomicroscope (Leica, Germany). For detailed studies of skeleton morphology, parts of the oscular rim and cormus tubes were treated with Murray's Clear according to the standard protocol to clarify soft tissues (Miller *et al.*, 2005). Slides of dissociated spicules and skeletons were studied under Zeiss Axioplan 2 (Carl Zeiss, Germany) and Leica DM2500 (Leica, Germany) with the digital cameras

AxioCam HRm (Carl Zeiss, Germany) and Leica DFC420C (Leica, Germany), respectively. Scanning electron microscopy (SEM) analysis of the spicules was performed under Carl Zeiss EVO-40 (Carl Zeiss, Germany), Hitachi S-405A (Hitachi, Japan) and CamScan S2 (Clinton Electronics Corp., UK) scanning electron microscopes. For this purpose, isolated spicules in 96% ethanol were transferred to cover slips, which were mounted onto stubs with nail polish, dried and sputter-coated. Figures of spicules under SEM are montages of the most typical spicule morphology obtained from a number of specimens of each studied species.

The measurements of the spicules (length and basal width at the base of the actines) were made for every spicule category on SEM images using ImageJ v. 1.48 software (National Institute of Health, USA). Strait Line tool was used for straight spicules and rays, Segmented Line tool was used for curved and undulating spicules and rays.

Cytological studies

For semithin sections and transmission electron microscopy (TEM), sponges were fixed with 2.5% glutaraldehyde (Ted Pella, USA) on 0.2M Millonig's phosphate buffer (Millonig, 1964), and postfixed with 1% OsO_4 (Spi Supplies, USA) according to standard protocol (Lavrov *et al.*, 2016a, 2018; Lavrov & Ereskovsky, 2022). Specimens were embedded in SPI-Pon 812/Araldite 6005 epoxy embedding media (Spi Supplies, USA) according to the manufacturer's instructions. Semi-thin sections (1 µm in thickness) were cut on a Reichert Jung ultramicrotome (Reichert, USA) equipped with a "Micro Star" 45° diamond knife before being stained with toluidine blue and observed under a WILD M20 microscope (Wild-Leitz, Germany). Digital photographs were taken with a Leica DMLB microscope (Leica Microsystems, Germany) using the Evolution LC colour photo-capture system (Media Cybernetics, USA). Ultrathin sections (60–80 nm) were cut with a Leica UCT6 (Leica, Germany) and PowerTome XL ultramicrotomes equipped with a Drukkert 45° diamond knife. Ultrathin sections, contrasted with uranyl acetate, were observed under Zeiss-1000 TEM (Carl Zeiss, Germany) and Tecnai G2 20 TWIN (FEI Company, USA). The detailed cytological studies were conducted only for *Leucosolenia corallorrhiza*, as it represents the most

common species in the White Sea. For other species, only the general morphology of the cell types was described. Figures of cell types are montages of the most typical cell morphology obtained from a number of specimens of each studied species.

Nomenclatural acts

The electronic edition of this article conforms to the requirements of the amended International Code of Zoological Nomenclature (ICZN), and hence the new name contained herein is available under that Code from the electronic edition of this article. The LSID for this publication is: urn:lsid:zoobank.org:pub:BA13614B-2884-4E02-9D45-0EE44CBD01A5.

Results

Phylogenetic reconstruction

We obtained 486 new sequences of different *Leucosolenia* species (Table S1). The sequence alignment of concatenated 28S, 18S and H3 loci includes 2160 positions. Single-gene trees based on 28S and H3 loci give good resolution at the species level while, 18S single-gene tree is unresolved due to low substitution rates (Data S1).

The topology of the resulting concatenated trees from Bayesian Inference (BI) and Maximum Likelihood (ML) analyses are congruent and well-supported in most cases (Figs 1, S1, S2). The genus *Leucosolenia* is recovered monophyletic with moderate support (posterior probabilities from BI (PP) = 0.9; bootstrap support from Maximum Likelihood (ML) = 92). Within *Leucosolenia* clade three species groups are monophyletic and highly supported: Clade I, including most specimens from the White Sea (*Leucosolenia* sp. 1, *Leucosolenia* sp. 3 and *Leucosolenia* sp. 4) and several specimens from GenBank initially identified as *Leucosolenia* cf. *variabilis, Leucosolenia* cf. *corallorrhiza* and *Leucosolenia* sp. 1 (PP = 1; ML = 99); Clade II with specimens from the White Sea (*Leucosolenias* sp. 2), *Leucosolenia somesii* from Netherlands, *Leucosolenia* sp. from GenBank (accession number AF100945) and *Leucosolenia botryoides* from GenBank (voucher number SA60) (PP = 1; ML = 93); and Clade III, which comprised only *Leucosolenia complicata* specimens from Roscoff (ws11881-11883) and from GenBank (PP = 1; ML = 100). The Clade III (*L. complicata*) is sister to the Clade II (PP = 1; ML = 93). Within the Clade I at least six monophyletic units are found: (1) *Leucosolenia* sp. 1, clustering with *Leucosolenia* cf. *variabilis* FB33 and *Leucosolenia* cf. *variabilis* FB12 from GenBank (PP = 0.99; ML = 96), (2) *Leucosolenia* cf. *variabilis* FB58 and *Leucosolenia* cf. *variabilis* FB60 (PP = 1; ML = 100), (3) *Leucosolenia* sp. 3 and *Leucosolenia* cf. *variabilis* SA62 (PP = 1; ML = 98), (4) *Leucosolenia* sp. 4 and *Leucosolenia* cf. *corallorrhiza* FB14, FB20, SA43 (PP = 0.81; ML = 100), (5) *Leucosolenia* cf. *corallorrhiza* FB59 and SA44 (PP = 1; ML = 100) and (6) *Leucosolenia* sp. 1 FB73 and FB81 from GenBank (PP = 0.61; ML = 100). Representatives of (1), (2), (4), (5) clades form a compact

monophyletic group (PP = 0.99; ML = 96) with very low genetic distances within it (Table 2). *Leucosolenia* sp. 3 is recovered sister to it (PP = 0.92; ML = 98), and *Leucosolenia* sp. 1 from GenBank shows sister relationships to other representatives of Clade I.

Within Clade II, *L. somesii* specimens from the Netherlands form a single clade with *Leucosolenia* sp. from GenBank. *Leucosolenia* sp. 2 also forms a well-supported clade (PP = 1; ML = 93). It represents a monophyletic group with *L. botryoides* and *L. somesii* (PP = 1; ML = 93), but relationships within this clade are unsupported.

Species delimitation

ASAP analysis of 271 LSU sequences recovers a different number of operational taxonomical units (OTUs) depending on the ASAP score (Data S2). The lowest ASAP score is found for threshold distances of 2.16%, 2.29%, 4.30% or 6.68% in this case five OTUs are recovered: four of them correspond to species from Clades II and III (*Leucosolenia complicata, L. botryoides, L. somesii* and *Leucosolenia* sp. 2) and the fifth group includes all specimens of Clade I. A scenario revealing the same 10 species-level units as in the phylogenetic analysis receives a relatively high ASAP score (5.00) with a threshold distance of 0.69%. ASAP analysis of the H3 dataset (170 sequences) contains only five candidate species (*Leucosolenia* sp. 1, *Leucosolenia* sp. 2, *Leucosolenia* sp. 3, *Leucosolenia* sp. 4, *L. complicata*) due to the absence of H3 sequences for calcareous sponges in GenBank. The lowest ASAP score (2.00) receives a scenario with all five candidate species as distinct (the threshold distance is 1.38%). Scenarios with an ASAP score of 2.5–4.0 reveal 2–4 candidate species; the identities of *Leucosolenia* sp. 1, *Leucosolenia* sp. 3, and *Leucosolenia* sp. 4 are not supported in this case.

A visualisation of character heterogeneity using the Medium Parsimony Network (TCS algorithm) reveals similar results in the 28S and H3 datasets (Fig. 2). On the 28S network, each candidate species either forms a distinct group (*Leucosolenia* sp. 1, *Leucosolenia* sp. 2, *Leucosolenia* sp. 3, *L. complicata*) or has a unique genotype (*Leucosolenia* sp. 4, *L. somesii, L. botryoides* and three candidate species from GenBank) (Fig. 2A). These groups, or genotypes,

differ from each other by three substitutions among species of Clade I and by 8–11 substitutions among species of Clade II. The intraspecific differences do not exceed two substitutions. There are 15–22 substitutions between representatives of Clades I, II, III.

The same results are observed in the H3 dataset, but the overall nucleotide diversity is higher (Fig. 2B). There are 1-2 substitutions within each candidate species except *Leucosolenia* sp. 3, where genotypes differ by 1–4 substitutions. Differences of 6–23 substitutions are found between candidate species.

Uncorrected *p*-distance values of 28S and H3 markers are presented in Tables 2–3 (data from GenBank are not included). Overall, intraspecific *p*-distances of 28S within Clade I show an overlapping range with interspecific distances (0–0.4% intraspecific, 0.4–1.3% intraspecific distances). The distances between the three large clades vary from 5.1 to 10.5%. The H3 marker shows a higher diversity: intraspecific distances vary from 0 to 1.7%, while interspecific distances vary from 2.5 to 5% within larger clades and are of 7.9–10.9% between the clades.

Comparison of morphological and molecular data

Three recovered monophyletic lineages corresponding to the genus *Leucosolenia,* have distinct morphological traits. They differ in the external appearance, the general skeleton composition, the spicular set and the cellular composition (Figs 3-24; Table 4-9). Definitions and technical terms used in this study can be found elsewhere (Boury-Esnault & Rützler, 1997; Ereskovsky & Lavrov, 2021; Łukowiak *et al.*, 2022).

Clade III is represented by a single species, *Leucosolenia complicata,* which was found only in European waters (Roscoff and Norway in our material and public data). Although the type material for this species is not known if it ever existed, morphologically our specimens perfectly fit the descriptions made by previous authors with few exceptions (Haeckel, 1872; Minchin, 1904; Rapp, 2015). The main diagnostic traits in spicular characters are (Fig. 4): (1) two populations of diactines, large lanceolate smooth diactines and small trichoxeas with irregular spines; (2)

parasagittal tri- and tetractines, with the unpaired actine is commonly longer than the paired ones; (3) tetractines are commonly found in both the oscular region and the cormus.

The studied representatives of Clade II (*Leucosolenia* sp. 2 and *Leucosolenia somesii*) have an echinate external appearance due to the high number of diactines protruding through the external surface (Fig. 19). Diactines are non-lanceolate, with rows of spines on the outer tip (commonly only two rows are visible, but there are more) or smooth (Fig. 20A, B). In these species, tri- and tetractines are thinner than in representatives of Clade C (see below), and abnormal spicules are common (Fig. 20C-E; Table 8). At the same time, *Leucosolenia* sp. 2 differs from *Leucosolenia somesii* by having only a single population of spined diactines, while *Leucosolenia somesii* possesses a second type of smooth non-lanceolate diactines (Fig. 24A-C).

Species of Clade I have several common traits: all of them have unique cells with inclusions (see below) (Figs 10C-E, 15C, E-F; Table S2); tri- and tetractines are predominantly T-shaped, the angle between paired actines is commonly 130-150º (Figs 8C-D, 12B, D, 18D, F; Table 5-7); lanceolate diactines are always present, with or without spines (Figs 8A-B, 12A, 13, 18A-C).

Within this clade, *Leucosolenia* sp. 1 has the largest angle between the paired actines (mean 140º) and the unpaired actine is much shorter than the paired ones in tri- and tetractines (Fig. 8C-D; Table 5). Also, it has only lanceolate diactines bearing short spines on the lanceolate tip in some cases (Fig. 8A-B). These characters perfectly fit the description and illustrations of *L. corallorrhiza* (Haeckel, 1872), but not *L. variabilis*.

Leucosolenia sp. 3 commonly forms a large voluminous rounded cormus with a very large oscular tube (there may be more than one oscular tube, but one of them is always enlarged) (Fig. 11A). Other representatives of Clade A commonly have cormus spreading along substrate with numerous oscular tubes of more or less equal size (Figs 7A, 17A). In spicular morphology, this species has a unique type of diactines: extremely long and thin trichoxeas, covered with irregularly placed spines (Fig. 13). Lanceolate diactines lack spines (Fig. 12A). The length of unpaired actines in tri- and tetractines is commonly the same as that of paired ones (Fig. 12B-D; Table 6). The

shape and measurements of spicules, as well as overall body shape mostly resemble those states described for *L. variabilis* (Haeckel, 1872).

Leucosolenia sp. 4 is very similar to *Leucosolenia* sp. 1 in external appearance. In spicular characters, this species contains very few tetractines in both the oscular region and the cormus (Fig. 17B-D). Triactines are usually with undulated paired actines (Fig. 18F). We also detected a high amount of abnormal tri- and tetractines (Fig. 18E), while in other species their amount is lower. Although these differences seem to be valuable to support the species distinctness, the limited studied material (only three specimens available) does not allow us to test for possible intraspecific variation. Also, this species demonstrates low genetic divergence from *Leucosolenia* sp. 1.

To sum up, our integrative approach indicates that the species *Leucosolenia complicata* is restricted to European waters, while in the White Sea, the genus *Leucosolenia* is represented by a complex of four species: *Leucosolenia corallorrhiza* (= *Leucosolenia* sp. 1), *Leucosolenia variabilis* (= *Leucosolenia* sp. 3), and two undescribed species. *Leucosolenia* sp. 2 is described herein under the name *Leucosolenia creepae* sp. nov., while in the case of *Leucosolenia* sp. 4 (further named *Leucosolenia* sp. A), more material is needed to confirm or reject its identity as a separate species from the closely related *Leucosolenia corallorrhiza.*

Systematic descriptions

Subclass Calcaronea Bidder, 1898

Order Leucosolenida Hartman, 1958

Family Leucosoleniidae Minchin, 1990

***Leucosolenia* Bowerbank, 1864**

Type species: Spongia botryoides (Ellis & Solander, 1786) (by original designation).

Type locality: Harbour near Emsworth, between Sussex and Hampshire, the English Channel.

Diagnosis (based on Hooper et al., 2002): Leucosoleniidae, in which the skeleton can consist of diactines, triactines and/or tetractines. There is no reinforced external layer on the tubes.

***Leucosolenia complicata* (Montagu, 1814)**

(Figs 3-6; Table 4)

Type material: Not known, probably lost.

Type locality: British Isles, Devon coast (Montagu, 1818).

Material studied: 3 specimens. Molecular data – 3 specimens (WS11661, WS11662, WS11663), external morphology – 3 specimens (WS11661, WS11662, WS11663), skeleton organisation – 1 specimen (WS11662), spicules (SEM) – 3 specimens (WS11661, WS11662, WS11663), cytology (TEM) – 3 specimens (WS11661, WS11662, WS11663) (Table S1).

External morphology: Cormus more or less spherical, bearing multiple erect oscular tubes with short lateral diverticula in basal part (Fig. 3A). Prominent perioscular spicular crown absent (Fig. 3B). Surface minutely hispid. Colouration of living and preserved specimens grayish white (Fig. 3A).

Spicules: Diactines (Fig. 4A-C). Two populations: (1) Curved lanceolate diactines (Fig. 4A), mean length 263.7 µm, mean width 9.5 µm (Table 4). Slightly curved, smooth, with lanceolate outer tip, variable in length. (2) Trichoxeas (Fig. 4B), mean length 127.3 µm, mean width 2.4 µm (Table 4). Thin, straight, narrowing toward outer end, both ends pointed, not lance-shaped. Numerous irregularly distributed spines, number and size of spines decrease toward inner end (Fig. 4C).

Triactines (Fig. 4D). Predominantly parasagittal V-shaped (mean angle 125.7°), with unpaired actine usually longer than paired (mean length: 113.5 µm – unpaired, 94.9 µm – paired) (Table 4), but equal and shorter unpaired actines also occur. Unpaired actine usually slightly slender than paired (mean width: 6.3 µm – unpaired, 6.8 µm – paired) (Table 4). T-shaped sagittal triactines absent.

Tetractines (Fig. 4E). Predominantly parasagittal V-shaped (mean angle 123.5°). Unpaired actine usually longer than paired, rarely equal (mean length: 109.3 µm – unpaired, 93.9 µm – paired, 23.8 µm – apical) (Table 4). Paired and unpaired actines equal in width, apical actine more slender (mean width: 6.7 µm – unpaired, 6.9 µm – paired, 5.3 µm – apical) (Table 4). Apical actine curved and smooth.

Skeleton: Skeleton of both oscular and cormus tubes predominantly formed by tetractines, triactines quite rare (Fig. 3C, D). In oscular tubes spicules constitute organized array with their unpaired actines directed toward cormus and oriented more or less in parallel to proximo-distal axis of oscular tube (Fig. 3C). In cormus tubes spicule array less organized (Fig. 3D). Lanceolate diactines cover tubes surface, orienting in different directions and extending outside by lance-shaped tip. Trichoxeas sparsely distributed on outer surface. No prominent spicular crown on oscular rim (Fig. 3B).

Cytology: Body wall, 6-9 µm thick, three layers: exopinacoderm, loose mesohyl, choanoderm (Fig. 5A, B; Table S2). Flat endopinacocytes located in only distal part of oscular tube (oscular ring) replacing choanocytes. Inhalant pores scattered throughout exopinacoderm, except the oscular ring area.

Exopinacocytes non-flagellated T-shaped, rarely flat (Fig. 5C). External surface covered by glycocalyx. Cell body (height 4.8 µm, width 2.8 µm), containing nucleus (diameter 2.2 µm), submersed in mesohyl (Fig. 5C). Cytoplasm with specific spherical electron-dense inclusions (0.3-0.4 µm diameter) (Fig. 5C).

Endopinacocytes non-flagellated flat cells, size 20-30 µm × 2-2.5 µm (Fig. 5D). External surface covered by glycocalyx. Nucleus (2.4x1.8 µm) oval with or without nucleolus. Cytoplasm without specific inclusions (Fig. 5D).

Choanocytes flagellated trapeziform or prismatic (height 6 µm, width 3.7 µm) (Fig. 5E). Flagellum surrounded by collar of microvilli. Characteristic pyriform nucleus (diameter 2.3 µm) in apical position. Cytoplasm with phagosomes and small vacuoles (Fig. 5E).

Porocytes tubular cylindrical (height 4.5 µm, width 2 µm), connecting external milieu with choanocyte tube (Fig. 5B, F). Nucleus oval to spherical, diameter 1.8 µm, some time with nucleolus. Cytoplasm with phagosomes and small vacuoles (Fig. 5F).

Sclerocytes amoeboid, size 4 µm × 2 µm (Fig. 6A). Nucleus usually oval or pear-shaped (diameter 1.6 µm), containing single nucleolus. Well-developed Golgi apparatus and rough endoplasmic reticulum. Cytoplasm usually with phagosomes and/or lysosomes (Fig. 6A).

Amoebocytes of different shape (from oval to amoeboid) without special inclusions, size 5.8 µm × 3.4 µm (Fig. 6B). Nucleus spherical (diameter 2.2 µm), sometimes with nucleolus.

Two morphotypes of bacterial symbionts in mesohyl. Morphotype 1 most abundant. Bacteria large rod-shaped slightly curved, diameter 0.3 µm, length 2.2 µm (Fig. 6C). Double cell wall, cytoplasm transparent, nucleoid region filamentous.

Morphotype 2 rare. Bacteria rod-shaped, diameter 0.18 µm, length 1.2 µm (Fig. 6D). Double cell wall, cytoplasm transparent, nucleoid region filamentous.

Distribution: Boreal species. Molecular species identity confirmed for specimens from France (Roscoff). Live in low intertidal and subtidal zones up to 20 m depth, on rocks and kelps (Borojevic et al., 1968).

Reproduction: The specimens collected in February 2017 in Roscoff contain oocytes at the early stages of development.

Remarks: Leucosolenia complicata was one of the most undoubted species described in the XIX century. According to our data, it shows stable internal characters and easily diagnosable external features, *i.e.*, erect multiply oscular tubes extending from the small cormus. The species identity and validity of *L. complicata* are strongly supported by our molecular data as well. It represents a distinct monophyletic lineage on all phylogenetic trees, and *p*-distance values to other *Leucosolenia* species are very high (more than 5% in LSU and 3.8% in SSU). Extensively studied morphology allows clarifying the species diagnosis, which varied from author to author (Haeckel, 1872; Minchin, 1904; Jones, 1954; Rapp, 2015): small cormus, erect multiple oscular tubes, two

populations of diactines (curved lanceolate diactines and small trichoxea), parasagittal tri- and tetractines with predominately longer unpaired actines, skeleton of tubes predominately formed by tetractines. *Leucosolenia complicata* is easily differentiated from other *Leucosolenia* species (*Leucosolenia variabilis, L. somesii* and others) in these traits. In addition, the mesohyl cell composition of *L. complicata* is very poor compared to other studied *Leucosolenia* species: the mesohyl contains only sclerocytes and amoebocytes (Table S2). The composition of symbiotic bacteria (two morphotypes of rod-shaped bacteria) differs in *L. complicata* from *L. corallorrhiza* and *L. variabilis* (Table S2).

Although the type material of this species is not available, if it ever existed, we studied spicule slides from Minchin type collections (BMNH 1910.1.1.415a and BNMH 1910.1.1.435.Aa). They are listed as the type material of *L. complicata* in the BMNH collection. These slides contain hand-written information on the corresponding paragraphs in Minchin (1904) work with relevant collection information (slides nos. 1, 2; Minchin, 1904:372). Accordingly, both slides appeared from Canon Normans's Collection. The specimen BMNH 1910.1.1.415a was collected at Scarborough (the North Sea) by Bean and sent to Haeckel for examination. The specimen BNMH 1910.1.1.435.Aa was collected at Guernsey Islands (the English Channel) by J. Bowerbank and likely represents a syntype of *Ascandra contorta* (Bowerbank, 1866). According to Minchin (1904), this slide contains an admixture of *L. complicata* spicules with *A. contorta.* All this indicates that slides BMNH 1910.1.1.415a and BNMH 1910.1.1.435.Aa are not the type material of *L. complicata*, and the label 'type' likely refers to the Minchin's type collection, which contained most typical specimens. Since no type material exists, the designation of neotype is needed once the material from the type locality (British Isles, Devon coast) becomes available for the molecular study.

Ascandra pinus Haeckel, 1872 and *Leucosolenia fabricii* Schmidt, 1869 are regarded herein as minor synonyms. *Ascandra pinus* lacks small trichoxeas, which were most probably overlooked by Haeckel (Minchin, 1904), and in *Leucosolenia fabricii*, the skeleton is formed mostly by

triactines, which was considered intraspecific variation by many authors (Minchin, 1904; Burton, 1963; Rapp, 2015). However, our data shows that these characters may be regarded as diagnostic interspecific features, as shown for the *L. variabilis* species complex (see below); therefore, both of these species names should be taken into account for future research on European *Leucosolenia*.

Our data also suggest the absence of *L. complicata* in the White Sea. In works by Breitfuss (1898a), three *Leucosolenia* species were found at different localities in the White Sea and described under the names *Ascandra variabilis* Haeckel, 1872, *Ascandra contorta* (Bowerbank, 1866) and *Ascandra fabricii* (Schmidt, 1869). Minchin (1904) later considered the latter two species *sensu* Breitfuss (1898a) as minor synonyms of *Leucosolenia complicata* due to external morphological characters, while spicular characters were ignored in most cases. However, *Ascandra contorta sensu* Breitfuss (1898a) possesses tri- and tetractines with short unpaired actines, which is most likely a diagnostic feature for *L. variabilis*. Due to the absence of *L. complicata* in our material from the White Sea and uncertainties in previous research, more material is required from different localities in the White and Barents Seas to clarify the distribution ranges of this species in Arctic waters.

***Leucosolenia corallorrhiza* (Haeckel, 1872)**

(Figs 7-10; Table 5)

=*Ascortis corallorrhiza* Haeckel, 1872

=*Sycorrhiza corallorrhiza,* Haeckel, 1870

=*Auloplegma corallorrhiza* Haeckel, 1872

=*Leucosolenia* cf. *variabilis* (Alvizu *et al.*, 2018; Lavrov *et al.*, 2018).

=*Leucosolenia variabilis* (Lavrov & Ereskovsky, 2022; Lavrov *et al.*, 2022; Melnikov *et al.*, 2022).

=*Leucosolenia complicata* (Ereskovsky *et al.*, 2017a).

Type material: Type material is not known.

Type locality: Haeckel based his description on one specimen from Norway and one from Greenland, without designating the type material (Rapp, 2015).

Material studied: 177 specimens. Molecular data – 177 specimens, external morphology – 177 specimens, skeleton organisation – 2 specimens (WS11650, WS11653), spicules (SEM) – 5 specimens (WS11649, WS116450, WS11653, WS11657, WS11658), cytology (TEM) – 6 specimens (WS11631, WS11632, WS11634, WS11635, WS11636, WS11637) (Table S1).

External morphology: Cormus formed by basal reticulation of tubes, from which erect oscular tubes and long diverticula arising. Sponge bear from one to multiple slightly curved oscular tubes with or without short lateral diverticula in basal part. Oscular tubes gradually narrows to oscular rim, possessing short spicular crown (Fig. 7A, B). Surface minutely hispid or echinate. Colouration of living and preserved specimens grayish white (Fig. 7A).

Spicules: Diactines (Fig. 8A, B). Curved lanceolate diactines, mean length 179 µm, mean width 6 µm (Table 5). Slightly curved with lanceolate outer tip, variable in size, smooth or with few small spines at lanceolate tip (Fig. 8B).

Triactines (Fig. 8D). T-shaped sagittal (mean angle 142.9º), unpaired actine usually shorter than paired (mean length: 70.5 µm – unpaired, 82.7 µm – paired) (Table 5), rarely equal. Actines equal in width (mean width: 6.5 µm – unpaired, 6.5 µm – paired) (Table 5).

Tetractines (Fig. 8C). T-shaped sagittal (mean angle 151.4 º), unpaired actine shorter than paired or equal (mean length: 68.8 µm – unpaired, 80.7 µm – paired, 22.9 µm – apical) (Table 5). All actines equal in width (mean width: 5.6 µm – unpaired, 5.8 µm – paired, 5.5 µm – apical) (Table 5). Apical actine curved and smooth.

Skeleton: Skeleton of oscular tubes predominantly formed by both tri- and tetractines, while in cormus tubes tetractines rare (Fig. 7C, D). In oscular tubes, spicules constitute organized array with their unpaired actines directed toward cormus and oriented more or less in parallel to proximo-distal axis of oscular tube (Fig. 7C). In cormus tubes, spicule network appears completely disordered (Fig. 7D). Both populations of diactines forming small oscular crown up to 60 µm and

cover tubes surface, orienting in different directions and extending outside by lance-shaped tip (Fig. 7B).

Cytology: Body wall, 8.4-12 μm thick, three layers: exopinacoderm, loose mesohyl, choanoderm (Fig. 9A, B; Table S2). Flat endopinacocytes located only in the distal part of oscular tube (oscular ring) replacing choanocytes. Inhalant pores scattered throughout exopinacoderm, except the oscular ring area.

Exopinacocytes non-flagellated T-shaped, rarely flat (Fig. 9C). External surface covered by glycocalyx. Cell body (height 7-10.5 μm, width 4.3-5.5 μm), containing spherical to oval nucleus (diameter 3.1 μm), submersed in mesohyl. Cytoplasm with specific spherical electron-dense inclusions (0.2-0.4 μm diameter) (Fig. 9C).

Endopinacocytes non-flagellated flat cells, size 16.8 μm × 2.2 μm (Fig. 9D). External surface covered by glycocalyx. Nucleus (2.1 μm × 1.6 μm) spherical to oval with nucleolus. Cytoplasm with specific spherical electron-dense inclusions (0.2-0.5 μm diameter) (Fig. 9D).

Choanocytes flagellated trapeziform or prismatic (height 8.2 μm, width 4.1 μm) (Fig. 9E). Flagellum surrounded by collar of microvilli. Characteristic pyriform nucleus (2.6 μm × 4.1 μm) in apical position. Cytoplasm with phagosomes and small vacuoles. Choanocytes united by specialized intercellular contacts similar to septate junctions, but has no basal membrane (Fig. 9E).

Porocytes tubular cylindrical (height 5.5 μm, width 4.2 μm), connecting external milieu with choanocyte tube (Fig. 9F). Nucleus pyriform (diameter 3.1 μm), containing nucleolus. Cytoplasm with phagosomes, small vacuoles and spherical electron-dense inclusions identical with inclusions of exopinacocytes.

Sclerocytes amoeboid, size 8.7 μm × 3.5 μm (Fig. 10A). Nucleus usually oval or pear-shaped (diameter 2.5 μm), containing single nucleolus. Well-developed Golgi apparatus and rough endoplasmic reticulum. Cytoplasm usually with phagosomes and/or lysosomes. During spicules secretion, sclerocytes form groups of three to six cells, connected by septate junctions (Fig. 10A).

Amoebocytes of different shape (from oval to amoeboid) without special inclusions, size 5.7

µm × 4.7 µm (Fig. 10B). Nucleus spherical (diameter 2.9 µm), sometimes with nucleolus.

Granular cells oval, size 9 µm × 5.5 µm. Regularly distributed numerous cells, usually located under choanocytes (Fig. 10C-E). Nucleus in peripheral position, spherical (diameter 2.5 µm). Cytoplasm with oval electron dense inclusions (size 0.9-2.7 µm × 1.1-3.7 µm) (Fig. 10E). Inclusion content homogenous or granulated. Often found in stage of degradation, cytoplasm completely filled with 2-4 large oval inclusions with highly osmiophilic granulated content (Fig. 10F).

Myocytes are fusiform cells, size 22 µm × 2.7 µm; distributes in the mesohyl mostly in the oscular ring. Nucleus usually oval (2.9 µm × 1.6 µm), without nucleolus (Fig. 10G). Cytoplasm includes mitochondria, ribosomes, small vesicles and, most importantly, the presence of cytoplasmic myofilaments of 19-12 nm in diameter (Fig. 10G). Myofilaments form bundles (0.37-0.16 µm diameter) that located along the long axis of the cell.

One morphotype of bacterial symbionts in mesohyl. Bacteria numerous, rod-shaped with double cell wall, diameter 0.3-0.33 µm, length 3.0-5.6 µm (Fig. 10H). Nucleoid region electron-dense with irregular network of filaments.

Distribution: Boreal-Arctic species. Molecular identity confirmed for Greenland and the White Sea (Alvizu *et al.*, 2018). In the White Sea it is the most abundant species, inhabiting kelps and hard substrates in low intertidal and subtidal zones up to 15-20 m depth.

Reproduction: In the White Sea specimens collected in late October contained early oocytes, specimens collected in January-February contained fully-developed larvae.

Remarks: In the White Sea, this species was initially identified as *Leucosolenia variabilis,* based on its external morphology (Lavrov *et al.*, 2018). In addition, most of our sequences for this species were identical to LSU and SSU sequences downloaded from the GenBank under the name *L. variabilis*. Regarding morphology, the spicular characters of our specimens were different from the original description of *L. variabilis* (Haeckel, 1872), but partly fit the description given in Minchin (1904). The main differences relate to diactine morphology: in our specimens, there is a

single type of curved lanceolate diactines. In *L. variabilis sensu* Haeckel (1872), two diactine populations were found: the first is small strait trichoxea, and the second is normal curved lanceolate diactines. Minchin (1904) found connectivity in size among small and long diactines and suggested they represented a single type of diactines, which was overlooked by Haeckel. Since our specimens possess only a single diactine population, it might support Minchin's conclusions. However, *Leucosolenia variabilis sensu* Minchin (1904) is a species complex since he designated *Leucosolenia somesii* a junior synonym of *L. variabilis,* while morphological and molecular data supported its identity as a distinct species (see below, see also van Soest *et al.*, 2007). Therefore, the diagnosis provided by Minchin (1904) should not be taken into consideration.

To address the possible ontogenetic variation of diactines, we studied the type material *L. variabilis* from the collection of BMNH (syntype BMNH-1910.1.1.421). The spicular characters of this specimen perfectly fit the original description made by Haeckel (1872), with two diactine types, tri- and tetractines of equal abundance and unpaired actine in tri- and tetractines always shorter than paired ones. On the other hand, specimens in our material possess only a single diactine type, and tetractines are rare. Therefore, the species from the White Sea is not *L. variabilis,* despite its molecular similarity to specimens, placed in the GenBank under the name *L. variabilis.*

Another species, that is characterised by a single diactine type and short unpaired actines in tri- and tetractines is *Leucosolenia corallorrhiza,* which was designated a valid species in the most recent morphology-based revision of Greenland calcareous sponges (Rapp, 2015). Haeckel (1872) described this species under the name *Ascortis corallorrhiza*, addressing a small proportion or absence of tetractines, small and thick triactines with short unpaired actine. Diactines are curved lance-shaped (Haeckel, 1872:74). This feature is characteristic of samples from the White Sea, although in our specimens, some diactines bear small spines on their lance-shaped tips. These spines are hardly visible with light microscopy and may be overlooked even during SEM studies. Since we could not study the morphology of specimens whose sequences were obtained from GenBank, and morphological data for those specimens are absent in the respective paper (Alvizu

et al., 2018), we designate our specimens from the White Sea as *Leucosolenia corallorrhiza,* until both morphological and molecular conformation for specimens from the type localities would be available. Also, neotype designation for this species is necessary to establish the type material, specimens for this purpose should be collected in the type locality. It should be mentioned, that our specimens demonstrate minor differences in colouration from the original description (*L. corallorrhiza* is brown according to Haeckel, 1872). Also, actines in tri- and tetractines are thicker in initial description (widths ~ 15 µm in Haeckel, 1872; up to 12.5 µm in our material (Table 5); up to 10.7 µm in Rapp, 2015), but this difference may be associated either with ontogenetic or intraspecific variation, or different measurement procedures and equipment.

From *Leucosolenia variabilis* this species differs by spicular characters: in *L. variabilis*, there are two types of diactine, while there is only one type of diactines in *L. corallorrhiza*. *Leucosolenia corallorrhiza* never forms a large, massive cormus. *Leucosolenia corallorrhiza* also differs from other species in cytological characteristics (Table S2): in contrast to *L. complicata,* the mesohyl of *L. corallorrhiza* includes not only amoeboid cells but also numerous granular cells, regularly distributed in the body wall; in contrast to *L. variabilis*, *L. corallorrhiza* has larger granular cells, no spherulous cells and only one morphotype of rod-shaped symbiotic bacteria.

***Leucosolenia variabilis* Haeckel, 1870**

(Figs 11-16; Table 6)

Type material: Syntype BMNH-1910.1.1.421. Other type material is not known.

Type locality: Norway, Bergen.

Material studied: 40 specimens. Molecular data – 40 specimens, external morphology – 40 specimens, skeleton organisation – 3 specimens (WS11643, WS11708, WS11735), spicules (light microscopy, SEM) – 7 specimens (WS11707, WS11714, WS11731, WS11732, WS14637, WS14671, WS14681), cytology (TEM) – 3 specimens (WS11643, WS11644, WS11645) (Table S1).

External morphology: Length of cormus up to 5 cm. Cormus massive, often spherical, otherwise formed by basal reticulation of tubes. Cormus built as reticulation around one or several largest central tubes. Outline of cormus formed by numerous short diverticula. Largest tubes of cormus always end with oscula. Main oscular tubes large prominent erect, bearing many small diverticula, spreading to 2/3 of tubes length. Oscular tube gradually narrows to oscular rim, possessing short spicular crown (Fig. 11A, B). In addition to main oscula on largest tubes of cormus, smaller oscular tubes usually scattered all over the cormus. Surface minutely hispid. Colouration of living specimens grayish white. Colouration of preserved specimens from grayish white to ochre (Fig. 11A).

Spicules: Diactines (Figs 12A, 13, 16A). Two populations: (1) Curved smooth lanceolate diactines (Fig. 12A), mean length 306.7 µm, mean width 9.8 µm, (Table 6). Slightly curved, smooth, with lanceolate outer tip, variable in length. (2) Trichoxeas (Fig. 13). Thin (mean width 0.9 µm) (Table 6), with numerous irregularly distributed spines (Fig. 13C), long, but usually represented by fragments of variable length (up to 362.4 µm long) (Table 6).

Triactines (Figs 12B, C, 16A). Predominantly T-shaped sagittal (mean angle 138.5°), unpaired actine variable in length: most frequently equal to paired actines, commonly shorter or rarely longer than paired (mean length: 122.3 µm – unpaired, 128.0 µm – paired) (Table 6). Abnormal triactines with one of paired actines undulated also common (Fig. 12C). Actines equal in width (mean width: 8.1 µm – unpaired, 8.5 µm – paired) (Table 6).

Tetractines (Fig. 12D). Predominantly T-shaped sagittal (mean angle 142.2°), unpaired actine variable in size: equal to, shorter or longer than paired actines (mean length: 147.6 µm – unpaired, 143.0 µm – paired, 22.8 µm – apical) (Table 6). Unpaired actine usually slightly slender than paired (mean width: 8.5 µm – unpaired, 9.1 µm – paired) (Table 6). Apical actine curved, smooth and slender (mean width 5.9 µm) (Table 6).

Skeleton: Skeleton of both oscular and cormus tubes formed by dense net of tetractines and triactines (Fig. 11C, D). In oscular tubes spicules constitute organized array with their unpaired

actines directed toward cormus and oriented more or less in parallel to proximo-distal axis of oscular tube (Fig. 11C). In cormus tubes spicule array completely disordered (Fig. 11D). Diactines form small oscular crown up to 100 µm (Fig. 11B) and cover tubes surface, orienting in different directions and extending outside by lance-shaped tip.

Cytology: Body wall, 9-13.8 µm thick, three layers: exopinacoderm, loose mesohyl, choanoderm (Fig. 14A, B; Table S2). Flat endopinacocytes located only in distal part of oscular tube (oscular ring) replacing choanocytes. Inhalant pores scattered throughout exopinacoderm, except the oscular ring area.

Exopinacocytes non-flagellated T-shaped, rarely flat (Fig. 14C). External surface covered by glycocalyx. Cell body (height 6.3 µm, width 3.7 µm), containing spherical to oval nucleus (diameter 2.7 µm), submersed in mesohyl. Cytoplasm with specific spherical electron-dense inclusions (0.2-0.35 µm diameter) (Fig. 14C).

Endopinacocytes non-flagellated flat cells, size 16 µm × 2.8 µm. External surface covered by glycocalyx. Nucleus (3.2 µm × 2.3 µm) spherical to oval with nucleolus. Cytoplasm without specific inclusions (Fig. 14F).

Choanocytes flagellated trapeziform or prismatic (height 10.7 µm, width 4.1 µm) (Fig. 14D). Flagellum surrounded by collar of microvilli. Characteristic pyriform nucleus (diameter 2.5 µm) in apical position. Cytoplasm with phagosomes and small vacuoles (Fig. 14D).

Porocytes tubular cylindrical (height 2.5-4.7 µm, width 4.3-5 µm), connecting external milieu with choanocyte tube (Fig. 14E). Nucleus spherical (diameter 2.7 µm), containing nucleolus. Cytoplasm with spherical electron-dense inclusions identical with inclusions of exopinacocytes (Fig. 14E).

Sclerocytes amoeboid, size 6 µm × 3.1 µm (Fig. 15G). Nucleus usually oval or pear-shaped (diameter 2.2 µm), containing single nucleolus. Well-developed Golgi apparatus and rough endoplasmic reticulum. Cytoplasm usually with phagosomes and/or lysosomes (Fig. 15G).

Amoebocytes of different shape (from oval to amoeboid) without special inclusions, size 3

μm × 4-7.5 μm (Fig. 15A). Nucleus spherical (diameter 2.7 μm), sometimes with nucleolus.

Large amoeboid cells of different shape (from elongate to amoeboid), size 20 μm × 4.2 μm (Fig. 15B). Rare cells located under choanoderm. Nucleus oval (size 4.8 μm × 1.7 μm). Cytoplasm with numerous large heterophagosomes (diameter 1.1-3.2 μm), well-developed Golgi apparatus (Fig. 15B).

Granular cells small oval, size 4 μm × 3.3 μm (Fig. 15C). Rare cell type, located under the choanoderm. Nucleus in peripheral position, spherical (diameter 1.7 μm) with large amounts of heterochromatin, associated with nucleus membrane Cytoplasm with electron dense oval inclusions (size 0.7-6 μm × 0.4-1.1 μm) and rare spherical electron-transparent vacuoles (diameter 1.2 μm) (Fig. 15C).

Spherulous cells with irregular shape from amoeboid to crescent, size 2.7-9.2 μm × 4.7-5.3 μm (Fig. 15E-G). Regularly distributed numerous cells, usually located under choanocytes. Distance between cells 2-9 μm (Fig. 15F). Nucleus deformed (size 2.4 μm × 1.7 μm). Cytoplasm mostly occupied by large crescent or irregular electron-dense homogenous inclusions (diameter 1.8-4.5 μm) and less electron-dense fine-granular inclusions (diameter 0.7-2.6 μm). Granular or foamy material fills cytoplasm spaces between inclusions (Fig. 15E, G).

Myocytes rare fusiform cells, size 18 μm × 2.7 μm, located in mesohyl (Fig. 15D). Nucleus oval (3.5 μm × 2.7 μm), with nucleolus. Cytoplasm with mitochondria, ribosomes, small vesicles and cytoplasmic myofilaments. Myofilaments grouped in bundles (diameter 0.07-0.2 μm) located along long axis of myocyte (Fig. 15D).

Three morphotypes of bacterial symbionts in mesohyl (Fig. 15H-J). Morphotype 1 numerous (Fig. 15H). Bacteria large spiral-shaped, diameter 0.2 μm, length 2.5-3.9 μm. Spiral turns regular and compact. Single membrane cell wall, cytoplasm granular, nucleoid region tubular (Fig. 15H).

Morphotype 2 rare (Fig. 15I). Bacteria small spiral-shaped, diameter 0.3 μm, length 1.5-1.8 μm. Spiral turns irregular and sparse. Cytoplasm transparent, nucleoid region tubular (Fig. 15I).

Morphotype 3 rare (Fig. 15J). Bacteria small rod-shaped bacteria, diameter 0.23 μm, length

0.8 µm. Double membrane cell wall, cytoplasm with dark filamentous materials, no distinction between cytoplasm and nucleoid region (Fig. 15J).

Distribution: Boreal-Arctic species, described from Norway. Molecular identity confirmed for the White Sea and Greenland (Alvizu *et al.*, 2018). In the White Sea occurs in low intertidal and subtidal zones up to 40-45 m depth, on rocks and kelps.

Reproduction: No data about reproduction time for this species.

Remarks: We studied three type specimens (slides with spicules) of *Leucosolenia variabilis* from the British Museum of Natural History (BMNH): BMNH-1910.1.1.421, BMNH-1906.12.1.40 and BMNH-1906.12.1.50. Spicules are similar morphologically across these specimens (Fig. 16B-D), which supports the idea that they belong to the same species. At the same time, their type status should be reconsidered due to the data represented in the revision by Minchin (1904). Slide labels contain specific information (exact page and number), allowing an unambiguous comparison with the collection data of these samples given in Minchin (1904). Accordingly, BMNH-1906.12.1.50 was collected from Bantry Bay, Ireland, by C. Norman and identified by him as *Leucosolenia botryoides*; this label was endorsed by Haeckel '*Ascandra variabilis*' (slide no. 1; Minchin, 1904:385). BMNH-1906.12.1.40 was received by Haeckel for reexamination from Bowerbank and collected from Guernsey (slide no. 4; Minchin, 1904:385). Finally, BMNH-1910.1.1.421 was collected by Haeckel in Bergen, Norway, the type locality of this species, and contained a printed label '*Ascandra variabilis* H.' (slide no. 3; Minchin, 1904:385). Therefore, the slide BMNH-1910.1.1.421 could be designated as a syntype.

The analysis of *L. variabilis* syntype BMNH-1910.1.1.421 indicated two diactine types (lanceolate diactines and trichoxeas), and V- and T-shaped tri- and tetractines with shorter unpaired actines (Fig. 16D). Although Haeckel's description lacks long trichoxeas, it should be mentioned that such spicules are easily broken during preparation. It may also be suggested that the second type of diactines without lanceolate tips described by Haeckel (1872) is in fact broken

long trichoxeas. Direct comparison of spicule slides of specimens from the White Sea with *L. variabilis* syntype BMNH-1910.1.1.421 shows strong correspondence between them.

Leucosolenia variabilis has a large, massive, sometimes spherical cormus, which could be a good distinctive trait, since all other sympatrically living species (*Leucosolenia complicata, L. corallorrhiza, Leucosolenia* sp. A) are represented by basal reticulation of tubes with extended oscular tubes. In spicular characters, *L. variabilis* differs from *L. somesii* by the presence of lanceolate spined diactines; and from *L. complicata* and *Leucosolenia* sp. A by the presence of extremely long and highly spined trichoxeas. *Leucosolenia variabilis* also has the highest diversity of mesohyl cells and symbiotic bacteria among the studied *Leucosolenia* species (Table S2). In addition to the usual amoebocytes, *L. variabilis* also has rare large amoebocytes and small granular cells, as well as numerous unusual spherulous cells of different shapes regularly distributed in the body wall. The composition of symbiotic bacteria of *L. variabilis* includes three morphotypes: one typical rod-shaped and two unusual spiral-shaped.

***Leucosolenia* sp. A**

(Figs 17-18; Table 7)

Material studied: Three specimens. Molecular data – 3 specimens (WS11692, WS11752, WS11770), external morphology – 3 specimens (WS11692, WS11752, WS11770), skeleton organisation – 2 specimens (WS11752, WS11770), spicules (SEM) – 2 specimens (WS11692, WS11770) (Table S1).

External morphology: Studied specimens small. Length of cormus up to 1 cm. Cormus represented by compact reticulation of tubes, from which several oscular tubes arising. Oscular tubes erect and almost straight. Surface minutely hispid. Colouration of living and preserved specimens grayish white (Fig. 17A).

Spicules: Diactines (Fig. 18A-C). Two populations: (1) Curved spiny lanceolate diactines (Fig. 18B), mean length 189.1 µm, mean width 7.2 µm (Table 7). Small, from almost straight to slightly

curved and undulating, with lanceolate and spiny outer tip, spines in distinct rows (Fig. 18C). (2) Curved smooth diactines (Fig. 18A), mean length 515.0 µm, mean width 11.6 µm (Table 7). Rare, long, slightly curved, without spines and lanceolate tips (Fig. 18C).

Triactines (Fig. 18D, E). Predominantly T-shaped sagittal (mean angle 146.5°) (Table 7). Unpaired actine variable in size: equal to, shorter or longer than paired actines, but shorter unpaired actine most common (mean length: 118.5 µm – unpaired, 125.1 µm – paired) (Table 7). Both straight and bent paired actines common. Abnormal triactines in high number (Fig. 18E), sometimes with undulated actines. Unpaired actine usually slightly slender than paired (mean width: 11.1 µm – unpaired, 11.6 µm – paired) (Table 7).

Tetractines (Fig. 18F). Quite rare. Predominantly T-shaped (mean angle 140.8°) (Table 7), variable in size. Unpaired actine equal to paired ones (mean length: 114.3 µm – unpaired, 113.2 µm – paired, 30.0 µm – apical) (Table 7). Unpaired actine straight, paired actines straight or undulating, apical actine curved or undulating, smooth. Paired and unpaired actines equal in width, apical actine more slender (mean width: 8.6 µm – unpaired, 8.5 µm – paired, 7.1 µm – apical) (Table 7).

Skeleton: Skeleton of both oscular rim and cormus tubes predominantly formed by triactines, tetractines rare (Fig. 17C, D). In oscular tubes spicules constitute organized array with their unpaired actines directed toward cormus and oriented more or less in parallel to proximo-distal axis of oscular tube (Fig. 17C). In cormus tubes spicule array completely disordered (Fig. 17D). Prominent oscular crown absent (Fig. 17B). Both populations of diactines cover tubes surface, orienting in different directions and extending outside.

Cytology: No material was available for cytological studies.

Distribution: Arctic species. Molecular identity confirmed only for the White Sea and Greenland. Found subtidal up to 15 m on rocks and red algae.

Reproduction: No data about reproduction time for this species.

Remarks: Although both our species delimitation analysis based on the H3 dataset and morphological data suggest that this species represents a distinct species-level unit, we avoid describing a new species as this case requires additional studies for several reasons. *Leucosolenia* sp. shares some features with *Leucosolenia corallorrhiza*: (1) the external appearance is similar, (2) the angle between unpaired actines in tri- and tetractines is similar (the mean angle is 142.9° in *L. corallorrhiza* and 146.5° in *Leucosolenia* sp. A), (3) the unpaired actine in tri- and tetractines is commonly shorter than the unpaired ones. However, these two species show several differences. Firstly, *Leucosolenia* sp. A has two populations of diactines, the smaller with lanceolate tips and the rare large curved smooth non-lanceolate diactines, whereas in *L. corallorrhiza* only the first type is present. Also, the tetractines are rare in both the cormus and oscular regions of *Leucosolenia* sp. A, while they are commonly present in the osculum of *L. corallorrhiza*. *Leucosolenia* sp. A commonly has triactines with bent unpaired actines, which are straight in *L. corallorrhiza.* Finally, the mean length of actines in tri- and tetractines of *L. corallorrhiza* is shorter than those of *Leucosolenia* sp. A (*L. corallorrhiza:* 70.5 µm – unpaired actine mean length, 82.7 µm – paired actine mean length; *Leucosolenia* sp. A: 118.5 µm – unpaired mean length, 125.1 µm – paired mean length). At the same time, the limited material of *Leucosolenia* sp. A (only three specimens were collected and studied) does not allow us to study the possible interspecific variation and ontogenetic variation. Therefore, we avoid the designation of this species as a distinct one, until more material would be available for study.

***Leucosolenia creepae* sp. nov.**

(Figs 19-22; Table 8)

ZooBank LSID: urn:lsid:zoobank.org:act:D60461BE-F215-4BE2-AFB5-25AF542FC4B9

Type material: Holotype: WS11702, White Sea, Kandalaksha Bay, Velikaya Salma Strait, vicinity of the N.A. Pertsov White Sea Biological Station, 0-2 m depth, 28.viii.2018, coll. A.I. Lavrov. *Paratypes:* WS11703, 1 specimen, White Sea, Kandalaksha Bay, Velikaya Salma Strait, vicinity

of the N.A. Pertsov White Sea Biological Station, 0-2 m depth, 28.viii.2018, coll. A.I. Lavrov. WS11728 paratype agrees in locality, date and collector with holotype WS11702 and paratype WS11703. WS11655 was collected in 30.viii.2017, and WS11725, WS11726, WS11771 were collected in 24.viii.2018, but all agree in locality and collector with holotype WS11702 and paratype WS11703

Type locality: White Sea, Kandalaksha Bay, Velikaya Salma Strait, vicinity of the N.A. Pertsov White Sea Biological Station (66°34′N, 33°08′E).

Material studied: 54 specimens. Molecular data – 54 specimens, external morphology – 54 specimens, skeleton organisation – 3 specimens (WS11655, WS11728, WS11762), spicules (SEM) – 5 specimens (WS11579, WS11605, WS11704, WS11729, WS11775), cytology (TEM) – 3 specimens (WS11579, WS11600, WS11698) (Table S1).

Etymology: From English "creep", referring to specific decumbent cormus and unusual growth form of this species in contrast to sympatrically living *Leucosolenia corallorrhiza.*

External morphology: Length of cormus up to 5 cm. Cormus formed by basal reticulations of creepy tubes with one or several oscular tubes (Fig. 19A). Tubes brittle. Oscular tubes creepy slightly curved and erect at distal end, sometimes with few diverticula. Oscular rim gradually narrows, possessing prominent spicular crown (Fig. 19A). Surface echinate. Colouration of living and preserved specimens grayish white (Fig. 19A).

Spicules: Diactines (Fig. 20A, B). Spiny diactines, mean length 194.9 µm, mean width 5.1 µm (Table 8). Extremely variable in length, without lanceolate tips, spiny. Largest diactines slightly curved, intermediate and short diactines straight. Spines in distinct rows at one end of diactines, more or less reduced in large ones (Fig. 20B).

Triactines (Fig. 20C, D). Sagittal, T-shaped and V-shaped (mean angle 131.1°) (Table 8), usually recurved, unpaired actine variable in length: most frequently shorter then paired actines, but equal and longer unpaired actines rarely occur (mean length: 80.7 µm – unpaired, 94.9 µm – paired) (Table 8). Aberrant T- and V-shaped triactines present, sometimes with undulated rays

(Fig. 20D). Unpaired actine often more slender than paired actines (mean width: 5.4 μm – unpaired, 5.9 μm – paired) (Table 8).

Tetractines (Fig. 20E). Quite rare. Sagittal, T-shaped and V-shaped (mean angle 139.5°) (Table 8), variable in size and proportions. Unpaired actine variable in length: longer, shorter and equal to unpaired actines (mean length: 85.1 μm – unpaired, 95.3 μm – paired, 25.6 μm – apical) (Table 8). Paired and unpaired actines equal in width (mean width: 6.2 μm – unpaired, 6.3 μm – paired) (Table 8). Apical actine curved, smooth and slender (mean width 5.2 μm) (Table 8).

Skeleton: Skeleton of oscular rim predominantly formed by both tri- and tetractines, while in other body parts tetractines absent (Fig. 19C, D). In oscular tubes spicules constitute organized array with their unpaired actines directed toward cormus and oriented more or less in parallel to proximo-distal axis of oscular tube (Fig. 19C). In cormus tubes spicule array completely disordered (Fig. 19D). Diactines forms extending oscular crown up to 500 μm (Fig. 19B) and cover tubes surface in large number, orienting in different directions and making it hispid.

Cytology: Body wall, 9-14 μm thick, three layers: exopinacoderm, loose mesohyl, choanoderm (Fig. 21A, B; Table S2). Flat endopinacocytes located only in distal part of oscular tube (oscular ring) replacing choanocytes. Inhalant pores scattered throughout exopinacoderm, except the oscular ring area.

Exopinacocytes non-flagellated T-shaped, rarely flat (Fig. 21C). External surface covered by glycocalyx. Cell body (height 5.8 μm, width 2.8 μm), containing spherical to oval nucleus (diameter 2.7 μm), submersed in mesohyl. Cytoplasm with specific spherical electron-dense inclusions (0.25-0.35 μm diameter) (Fig. 21C).

Endopinacocytes non-flagellated flat cells, size 16.2 μm × 2.7 μm (Fig. 21D). External surface covered by glycocalyx. Nucleus (diameter 2.7 μm) spherical without nucleolus. Cytoplasm without specific inclusions (Fig. 21D).

Choanocytes flagellated trapeziform or prismatic (height 11.4 μm, width 3.6 μm) (Fig. 21E). Flagellum surrounded by collar of microvilli. Characteristic pyriform nucleus (diameter 2.3 μm)

in apical position. Cytoplasm with phagosomes and small vacuoles (Fig. 21E).

Porocytes tubular cylindrical (height 4.6-8.9 μm, width 2.8-2.9 μm), connecting external milieu with choanocyte tube (Fig. 21F). Nucleus oval to spherical (diameter 2.5 μm), sometime with nucleolus. Cytoplasm with spherical electron-dense inclusions identical with inclusions of exopinacocytes, phagosomes and small vacuoles (Fig. 21F).

Sclerocytes amoeboid, size 7.6 μm × 2.9 μm (Fig. 22A). Nucleus usually oval or pear-shaped (diameter 2.3 μm), sometimes with single nucleolus. Well-developed Golgi apparatus and rough endoplasmic reticulum. Cytoplasm usually with phagosomes and/or lysosomes (Fig. 22A).

Amoebocytes of different shape (from oval to amoeboid) without special inclusions, size 5.7 μm × 2.6 μm (Fig. 22B). Nucleus spherical (diameter 2.5 μm), sometimes with nucleolus.

Myocytes fusiform cells, size 16.5 μm × 3.3 μm, located in mesohyl. Nucleus oval (2.4 μm × 1.9 μm), without nucleolus (Fig. 21D). Cytoplasm with mitochondria, ribosomes, small vesicles and cytoplasmic myofilaments. Myofilaments grouped in bundles (diameter 0.25–0.32 μm) that are located along the long axis of the cell (Fig. 21D).

Two morphotypes of bacterial symbionts in mesohyl. Morphotype 1 numerous (Fig. 22C, D). Bacteria large rod-shaped slightly curved, diameter 0.4-0.5 μm, length 2.7 μm. Cell is double, smooth and covered with fibers, cytoplasm transparent with vacuolar inclusions, nucleoid region filamentous (Fig. 22C, D).

Morphotype 2 abundant (Fig. 22E, F). Bacteria small rod-shaped bacteria, diameter 0.19 μm, length 1.9-2.1 μm. Cell wall smooth, cytoplasm transparent, nucleoid region filamentous (Fig. 22E, F).

Distribution: Arctic species. In the White Sea quite rare, found in low intertidal and upper subtidal zones up to 5-10 m depth, on kelps and rocks.

Reproduction: In White Sea specimens, collected in mid-June to the end of the August contained oocytes at different stages (mostly, early) of development (Figs 21B, 22G).

Remarks: Leucosolenia creepae sp. nov. well differs from other *Leucosolenia* species in both external characters and the morphology of spicules. In *L. somesii*, diactines are of two types: (1) smooth diactines, which are variable in length and (2) short and highly spined ones. In *Leucosolenia creepae* sp. nov., we identified only one type of diactines, which have spines on the outer tip and are variable in length. However, in *Leucosolenia creepae* sp. nov., spines are more expressed in small and medium-size diactines but become hardly visible in longer diactines of ~250-300 µm in length. In *L. somesii*, all medium-size diactines have smooth tips (Fig. 24B). *Leucosolenia creepae* sp. nov. forms a sparse basal reticulation with few oscular tubes, while the cormus of *L. somesii* is formed by a dense reticulation of extremely branched winding tubes. From all other North Atlantic and Arctic *Leucosolenia* species, *Leucosolenia creepae* sp. nov. differs by the absence of lanceolate diactines. The mesohyl cell composition of *Leucosolenia creepae* sp. nov. includes only amoebocytes, myocytes and sclerocytes, differing this species from sympatrically living *L. corallorrhiza* and *L. variabilis* (Table S2).

***Leucosolenia somesii* (Bowerbank, 1874)**

(Figs 23-24; Table 9)

Type material: Lectotype BMNH 1925.11.2.24, paralectotype BMNH 1925.11.2.25, slides of the same: BMNH 1956.4.26.35.

Type locality: Brighton Aquarium.

Material studied: 1 specimen, ZMA Por. 17572 (external morphology, skeleton organisation, spicules) (Table S1).

External morphology: Length up to 12 cm. Cormus formed by dense reticulation of extremely branched winding tubes (Fig. 23A). Surface hispid. Colouration of living and preserved specimens grayish white. Examined specimen lacks oscular tubes. According to the original description (Bowerbank, 1874), sponge have numerous small and large oscular tubes, bearing spicular crown. Oscular tubes erect and slightly curved, gradually narrowing to oscular rim.

Spicules: Diactines (Fig. 24A-C). Two populations of diactines: (1) Curved smooth diactines (Fig. 24A, C), mean length 425.5 µm, mean width 9.9 µm (Table 9). Slightly curved, smooth, variable in length, lacking lanceolate tips, with undulated tip. (2) Straight spiny diactines (Fig. 24B, C), mean length 90.0 µm, mean width 3.3 µm (Table 9). Short, strait, lacking lanceolate tips, with numerous spines in distinct rows (Fig. 24B).

Triactines (Fig. 24D, E). Sagittal, mostly T-shaped, but V-shaped also occurs (mean angle 131.7°) (Table 9), unpaired actine usually shorter then paired actines, but longer unpaired actines rarely occur (mean length: 127.4 µm – unpaired, 155.2 µm – paired) (Table 9). Paired and unpaired actines equal in width (mean width: 8.2 µm – unpaired, 8.0 µm – paired) (Table 9). Abnormal triactines in common, sometimes with undulated rays (Fig. 24E).

Tetractines (Fig. 24F). Quite rare. Sagittal, mostly T-shaped, but V-shaped also occurs (mean angle 139.3°) (Table 9), unpaired actine usually shorter then paired actines, but longer unpaired actines rarely occur (mean length: 156.0 µm – unpaired, 178.7 µm – paired, 21.5 µm – apical) (Table 9). Apical actine curved and smooth. All actines more or less equal in width (mean width: 9.1 µm – unpaired, 9.5 µm – paired, 10.0 µm – apical) (Table 9).

Skeleton: Very dense net predominantly formed by triactines, oriented in different directions, tetractines rare (Fig. 23B). Both trichoxea populations cover tubes surface in large number, orienting in different directions and making it hispid. Skeleton of osculum was not studied.

Cytology: No material was available for cytological studies.

Distribution: Boreal species. Described from Brighton Aquarium with confirmed reports from Netherlands (van Soest *et al.*, 2007). Probably it has wider distribution in North-East Atlantic.

Reproduction: No data on reproduction time are available.

Remarks: Leucosolenia somesii was considered a minor synonym of *L. variabilis* until a recent study by van Soest *et al.* (2007) was published. They showed valuable differences between these two species, based on a large number of specimens, including the type material. Here we provide its first molecular data and an updated morphological description. Our novel data confirms that *L.*

somesii represents a distinct species, based on both morphological and molecular analyses. The reexamination of spicules of specimen ZMA Por. 17572 studied by van Soest *et al.* (2007) confirms the strong correspondence of its specular characteristics to the paralectotype BMNH 1956.4.26.35 (Fig. 23C, D). According to our phylogenetic reconstruction, the most closely related species is Arctic *Leucosolenia creepae* sp. nov., with which *Leucosolenia somesii* shares some specific morphological features: echinate external appearance due to the high number of non-lanceolate diactines protruding to the external surface, dimensions of tri- and tetractines. The discussion of their differences is given above under *Leucosolenia creepae* sp. nov. description. From all other North Atlantic and Arctic *Leucosolenia* species, *L. somesii* differs by the absence of lanceolate diactines.

Discussion

Leucosolenia taxonomy

The calcarean biodiversity in the Arctic region remains poorly studied. In the beginning of the XX century, only three asconoid species were detected in the White and Barents Seas (Breitfuss, 1898a): *Ascandra variabilis, A. contorta* and *A. fabricii.* This view was even more simplified in subsequent works, designating that only *Leucosolenia complicata* occurs in these seas (Koltun, 1952). The present study demonstrates that *L. complicata* is restricted to the North-East Atlantic, while in the Arctic, the *Leucosolenia* diversity is represented by at least four species: *Leucosolenia corallorrhiza, L. variabilis, Leucosolenia creepae* sp. nov. and yet undescribed *Leucosolenia* sp. A. These species represent different clades in the present phylogenetic analysis (Fig. 1): (1) Clade I, which includes the nominative species, *L. corallorrhiza, Leucosolenia* sp. A and several phylogenetically distinct lineages formed by Norway and Greenland specimens (*Leucosolenia* sp. B–D), (2) Clade II with the closely related North-Atlantic *L. somesii* and *Leucosolenia creepae* sp. nov. restricted to the White Sea. *Leucosolenia botryoides,* the type species of the genus, shows sister relationships with the latter group, and *L. complicata* is sister to this clade. The phylogenetic signal from different molecular markers gave a similar result (Data S1), supporting the chosen species hypothesis from the concatenated phylogenetic dataset (Figs 1, S1, S2), and the lack of heterozygous sites in the studied markers indicates the absence of hybridization between different species and supports well-established species boundaries.

Overall, species within each group show several common characters, which correlate with the level of molecular divergence. Most of the traits traditionally used in calcarean systematics (the general skeleton composition, the spicular set and their fine morphology) supported the species hypothesis obtained from the molecular phylogenetic analysis. Spicular set is the most useful character to delimit species, and general spicular composition and proportions of spicules may also have a certain phylogenetic signal: (i) Lanceolate diactines with or without spines are found within the Clade I (Fig. 1) and in *L. complicata;* (ii) T-shaped tri- and tetractines with shorter

unpaired actines are common only in species from the Clade I; (iii) sister species *L. somesii* and *L. creepae* sp. nov. bear generally thinner spicules than other species of the genus; these species also have an echinate appearance due to the high number of long diactines protruding through the surface.

Here we also show that modern techniques like scanning electron microscopy may give a new insight into understanding actual biodiversity, as in closely related species, similar spicular types differ by fine features like the presence or absence of spines. This micromorphological approach has been successfully applied in the taxonomy of calcareous sponges from subclass the Calcinea (Azevedo *et al.*, 2009, 2015; Klautau *et al.*, 2016). For example, although both *Leucosolenia creepae* sp. nov. and *L. somesii* have similar specular sets, the latter species has two populations of non-lanceolate diactines (spined and smooth), while only a single population of spined diactines with a continuous reduction of spines in larger diactines is found in *Leucosolenia creepae* sp. nov. The same was shown for *L. variabilis* and *L. corallorrhiza*: both species have lanceolate and sometimes spined diactines, but in *L. variabilis* we also detected thin long and highly spined trichoxeas. These differences in diactine types are obvious with the help of SEM techniques but may be overlooked during investigation using light microscopy alone.

The proportion of spicular types in different parts of cormus and the form of actines in tri- and tetractines (straight *vs.* bent) may also be important taxonomical characters. Haeckel (1872) recognised several species as distinct based on these differences. For example, *Ascandra fabricii* differs from *L. complicata* by the absence of tetractines, and *Asculmis armata* Haeckel, 1870 – by a low amount of triactines. Furthermore, Haeckel described two varieties of *L. complicata*: *L. complicata* var. *hispida* with straight paired actines and *L. complicata* var. *ameboides* in which paired actines are bent. Also, some varieties – *cervicornis, confervicola, arachnoides, hispidissima* – were distinguished for *L. variabilis* (Haeckel, 1872). Although these names are currently accepted as valid species within *Leucosolenia* (de Voogd *et al.*, 2023), these forms were for a long time designated as morphotypes of either *L. complicata* or *L. variabilis* (Minchin, 1904; Burton,

1963) and no integrative study of Norway species has been conducted yet to support or reject their validity. At the same time, our results show that *Leucosolenia* sp. A differs from *L. corallorrhiza* by the low amount of tetractines and by bent paired actines in triactines. Since we suspect that *Leucosolenia* sp. A also represents a distinct species, all the above-mentioned characters should be taken into account for further taxonomical revisions of the North Atlantic and Arctic *Leucosolenia.*

In addition to the proportion of spicules in different parts of a skeleton, we identified several differences in the spiculation of the oscular crown among different species. The oscular rim bears numerous diactines protruding through the surface and forming a crown. The crown may be short (max length 50-100 µm, in most species) or extremely long (up to 500 µm, in *Leucosolenia creepae* sp. nov.). This character was not tracked in previous works on *Leucosolenia* systematics, as researchers commonly pointed at the smooth or echinate surface of the oscular tube without considering the spiculation of the oscular rim. The only exception is a recent description of *Leucosolenia salpinx* van Soest, 2017 as in this species the extended, long oscular crown is a notable diagnostic trait (van Soest, 2017). At the same time, forms with more or less echinate surface may be found in *L. corallorrhiza* in the White Sea, making its external appearance similar to that of sympatrically occurring *Leucosolenia creepae* sp. nov. In this case, the oscular rim spiculation is more useful for accurate identification of these species in the field. However, the phylogenetic value of this character is a subject for further studies, as the current results lack data on *L. somesii, L. botryoides* and *Leucosolenia* sp. A.

Another source of species-specific traits is the cytological structure of the studied *Leucosolenia* species. It is well known that cytological characters, such as the cell types with inclusions, are very important for Demospongiae and Homoscleromorpha species without skeleton identification (*e.g.*, Muricy *et al.*, 1996; Ereskovsky *et al.*, 2011, 2017b; Gazave *et al.*, 2013; Willenz *et al.*, 2016). Despite the fact, that the set of cell types is generally similar among studied *Leucosolenia* species, some species have characteristic cytological features. Both *L. corallorrhiza*

and *L. variabilis* have unique types of mesohyl cells - cells with inclusions (granular and/or spherulous) (Table S2), while *L. complicata* and *Leucosolenia creepae* sp. nov. lack such cells. There are no cytological data for *L. somesii* and *Leucosolenia* sp. A., but it is reasonable to assume that considering the phylogenetic position of these species, *Leucosolenia* sp. A. should have cells with inclusions and *L. somesii* should not. We have for the first time clearly shown the presence of myocytes in all species studied, as well as the presence of endopinacocytes in the oscular ring. However, further broad studies of cytology in the genus *Leucosolenia* are required to evaluate the phylogenetic value of these characters.

The composition of symbiotic bacteria also shows variation among studied species, both in the number of bacterial morphotypes and their morphology (Table S2). The differences in composition of symbiotic bacteria are obvious even in the case of closely related sympatric species, *e.g.*, *L. corallorrhiza* and *L. variabilis*. Considering the stability of the core microbiome for a particular sponge species across various localities and different environmental conditions (Webster & Thomas, 2016), it could become a useful character for delimiting calcareous sponge species. Species-specific traits in microbiome composition could already be revealed by cytological studies, but the metabarcoding approach enables much more detailed analysis and precise comparison of microbiome composition (Ribeiro *et al.*, 2023), and should be preferred when possible.

Integrative taxonomy of Calcaronea

The systematics of subclass Calcaronea is currently facing many challenges due to the broad implementation of molecular methods in taxonomical studies. Traditional taxonomical schemes were primary typologic (Borojevic *et al.*, 1990, 2000) and the high level of morphological homoplasy obscured the actual evolutionary relationships of high-level taxa within Calcarea (Manuel *et al.*, 2003). As a result, contemporary studies have partially shown the broad incongruence of morphology-based classification with newly reconstructed molecular phylogenies (Dohrmann *et al.*, 2006; Voigt *et al.*, 2012; Voigt & Wörheide, 2016; Alvizu *et al.*, 2018).

However, these analyses strongly supported the monophyly of both subclasses, Calcinea and Calcaronea. In the most recent molecular phylogeny of Calcaronea based on broad taxon sampling and two ribosomal markers, the para- and polyphyly of most families and genera were shown, along with the high hidden diversity (Alvizu *et al.*, 2018). The phylogenetic studies within Calcaronea are also complicated by the unusual architecture of the mitochondrial genome in this group, which is organised in individual linear chromosomes and has a unique genetic code and accelerated rates of sequence evolution (Lavrov *et al.*, 2013, 2016b). This hampers using of the mitochondrial markers, in particular the standard barcode cytochrome c oxidase subunit I (COI). Accordingly, the phylogenetic and taxonomical studies were primarily based on the nuclear ribosomal genes and internal transcribed spacers (ITS1, ITS2) (Voigt *et al.*, 2012; Klautau *et al.*, 2013, 2020, 2021; Azevedo *et al.*, 2015, 2017; Sanamyan *et al.*, 2022). Among ribosomal markers, the C-region of 28S was suggested as a barcode marker for delimitation of taxa on species- and generic levels (Voigt & Wörheide, 2016) and was successfully applied in subsequent integrative studies (Alvizu *et al.*, 2019; Cóndor-Luján *et al.*, 2019; Klautau *et al.*, 2020, 2021). In the present study, this marker was used for species delimitation as well, but it gave doubtful results at the lowest taxonomical level. There was an obvious genetic break between some closely related species, *e.g.*, *L. somesii* and *Leucosolenia creepae* sp. nov., but in the case of *Leucosolenia* species from Clade I, the interspecific differences may be equal to intraspecific values, like in *L. corallorrhiza, L. variabilis* and *Leucosolenia* sp. A (Table 2, Fig. 2). As a result, automatic species delimitation approaches like ASAP failed to find a barcode gap and delimit species within this group, suggesting either oversplitting or overlamping scenarios. Therefore, while the C-region gives a good resolution at the species-level and is useful for detection of the genetic breaks among species, it cannot be considered equivalent to standard mitochondrial COI. The same challenges in detecting of a barcode gap in the C-region dataset were previously shown in the larger taxon sampling of Calcaronea (Alvizu *et al.*, 2018). At the same time, SSU data do not provide sufficient divergence rates to test the automatic species delimitation methods (Data S1, S2, see also Alvizu

et al., 2018). Another part of the nuclear ribosomal operon, ITS1 and ITS2, often contain numerous allele indels in Calcaronea, which complicate the PCR and sequencing processes (Wörheide *et al.*, 2004; Voigt & Wörheide, 2016) and therefore are not useful for testing the large taxon sampling. In this study, the first molecular analysis of calcareous sponges using the nuclear histone H3 marker was performed. Within *Leucosolenia*, the H3 showed higher substitution rates at both intra- and interspecific levels than ribosomal markers (Tables 2, 3; Fig. 2), and topologies of the H3-based and ribosomal trees were congruent. High substitution rates enable the usage of ASAP, and its results fully confirmed the phylogenetic species hypothesis even within Clade I (Data S2). This suggests the H3 marker may be a powerful tool for taxonomical studies within calcaronean sponges in addition to the widely used LSU, and is more useful for delimitation of closely related species. Also, histone H3 is a protein-coding gene with a conservative protein sequence, which eases a verification of possible incorrect base-calling during sequencing. The congruent topologies of single-gene trees based on LSU and H3 markers also indicate that the latter may further improve the resolution and support of multi-locus phylogenetic trees within Calcaronea.

Patterns of biodiversity and biogeography

The obtained results indicate that there is an obvious connectivity between the calcaronean fauna of the White Sea and Greenland, since specimens of *L. corallorrhiza* and *Leucosolenia* sp. from these localities are conspecific in the molecular phylogenetic analysis. Although both localities are parts of the Arctic regions, this is an unexpected result in the case of the genus *Leucosolenia.* Members of this genus have short-living larvae, which are not capable of dispersal to a great distance (Anakina, 1981) so such wide distribution ranges accommodated by long-distance deposition of larvae via existing marine currents seem very unlikely. The connectivity of adult forms is also prevented by the deep and wide Fram Straight (max depth 2545 m) between Greenland and Svalbard, hampering the migration of shallow water forms with short-living larvae or direct development via the North Atlantic route (Meyer-Kaiser *et al.*, 2022). We may suggest two possible explanations for such connectivity. Likely both *Leucosolenia corallorrhiza* and

Leucosolenia sp. A have a circumpolar distribution and may be found in other regions across the Arctic. Another explanation is that the connectivity of distant populations is achieved by transportation via ballast waters or on ship bottoms as a common part of the Arctic fouling communities. Unfortunately, the exact mechanism cannot be evaluated based on the molecular data presented in this study, as the population structure is not evident from the conservative nuclear markers used.

For now, possible calcarean faunal connections between the Arctic and the Boreal North-East Atlantic waters cannot be evaluated due to the low number of sequenced specimens from these regions. *Leucosolenia* diversity in Norwegian waters estimates 10 species (de Voogd *et al.*, 2023), among which at least *Leucosolenia variabilis* and *L. corallorrhiza* inhabit the Arctic. At the same time, neither *L. complicata* nor *L. botryoides* were found in the White Sea, and *Leucosolenia creepae* sp. nov. and *L. somesii* represent two closely related and morphologically similar but distinct species, suggesting the temperate Atlantic fauna is distinct. The integrative studies of the Barents Sea biodiversity are therefore of crucial importance for a precise account of possible faunal links.

Acknowledgments

We thank SCUBA divers from N.A. Pertsov White Sea Biological Station of Lomonosov Moscow State University, especially Fyodor Bolshakov, Tatiana Antokhina and Alexander Semenov, for help with the material collection. We are very grateful to Nikolai Neretin for his help with deposition of material to Zoological Museum of Moscow State University, White Sea Branch (ZMMU WS), to Rob van Soest, Nicole de Voogd and Tom White for sending us material from the collections of Zoological Museum of Amsterdam (ZMA) and Britain Museum of Natural History (BMNH), to Valentina Tambovtseva and Maria Stanovova for assistance in Sanger sequencing and to Daria Tokina and Morphology Service of IMBE, Marseille, France for technical support in specimen preparation for TEM. We thank our colleagues, Fernanda Azevedo, Adriana Alvizu Gomez, Denis Lavrov and Oliver Voigt, for useful discussions. The light microscopy studies were conducted using equipment of the Center of Microscopy WSBS MSU, the electron microscopy studies – using equipment of the Electron Microscopy Laboratory of the Shared Facilities Center of Lomonosov Moscow State University sponsored by the RF Ministry of Education and Science, the Microscopy Core Facility of IMM, Marseille, France and Cooperative Far Eastern Center of Electron Microscopy. Sanger sequencing was conducted using equipment of the Core Centrum of the Institute of Developmental Biology RAS. The authors are very grateful to four anonymous reviewers, whose helpful comments and suggestions have considerably improved the manuscript. The study was supported by the Russian Science Foundation grant no. 17-14-01089.

Statements and Declarations

Competing Interests

Authors declare no competing interests.

Data Availability Statement

All new sequences obtained in the study were deposited in GenBank, GenBank accession numbers are listed in Table S1. Unedited Maximum Likelihood single-gene trees (LSU, H3, 18S and concatenated datasets) are available in the Supplementary materials. Generated raw data on the external morphology, skeleton organisation, spicule types and cytology of studied specimens are available in the Mendeley Data repository (10.17632/4pkf7x4jb9.1 and 10.17632/r7f8zmdh2n.1).

References

Alvizu A, Eilertsen MH, Xavier JR, Rapp HT. 2018. Increased taxon sampling provides new insights into the phylogeny and evolution of the subclass Calcaronea (Porifera, Calcarea). *Organisms Diversity & Evolution* **18:** 279-290.

Alvizu A, Xavier JR, Rapp HT. 2019. Description of new chiactine-bearing sponges provides insights into the higher classification of Calcaronea (Porifera: Calcarea). *Zootaxa* **4615:** 201-251.

Anakina RP. 1981. The embryological development of Barents Sea sponge *Leucosolenia complicata* Mont. (Calcarea). In: Korotkova GP, ed. *Morphogenesis in sponges*. Leningrad: Leningrad University Press. 52-58.

Anakina RP. 1997. The Cleavage specifity in embryoes of the Barents Sea sponge *Leucosolenia complicata* Montagu (Calcispongiae, Calcaronea). In: Ereskovsky AV, Keupp H and Kohring R, eds. *Modern Problems of Poriferan Biology*. Berliner Geowissenschaftliche Abhandlungen. 45-53.

Anakina RP, Korokhov NP. 1989. Spermatogenesis in *Leucosolenia complicata* Mont. from the Barents Sea. *Ontogenez* **20:** 77-86.

Anakina RP, Drozdov AL. 2000. Characteristics of oogenesis in the Barents Sea sponge *Leucosolenia complicata*. *Tsitologiia* **42:** 128-135.

Anakina RP, Drozdov AL. 2001. Gamete Structure and Fertilization in the Barents Sea Sponge *Leucosolenia complicata*. *Russian Journal of Marine Biology* **27:** 143-150.

Azevedo F, Hajdu E, Willenz P, Klautau M. 2009. New records of Calcareous sponges (Porifera, Calcarea) from the Chilean coast. *Zootaxa* **2072:** 1-30.

Azevedo F, Cóndor-Luján B, Willenz P, Hajdu E, Hooker Y, Klautau M. 2015. Integrative taxonomy of calcareous sponges (subclass Calcinea) from the Peruvian coast: Morphology, molecules, and biogeography. *Zoological Journal of the Linnean Society* **173:** 787-817.

Azevedo F, Padua A, Moraes FC, Rossi AL, Muricy G, Klautau M. 2017. Taxonomy and phylogeny of calcareous sponges (Porifera: Calcarea: Calcinea) from Brazilian mid-shelf and oceanic islands. *Zootaxa* **4311:** 301-344.

Borojevic R, Boury-Esnault N, Vacelet J. 1990. A revision of the supraspecific classification of the subclass Calcinea (Porifera, class Calcarea). *Bulletin du Museum National d'Histoire Naturelle, Section A, Zoologie Biologie et Ecologie Animales* **12:** 243-276.

Borojevic R, Boury-Esnault N, Vacelet J. 2000. A revision of the supraspecific classification of the subclass Calcaronea (Porifera, class Calcarea). *Zoosystema* **22:** 203-264.

Boury-Esnault N, Rützler K. 1997. *Thesaurus of sponge morphology*. Smithsonian Institution Press: Washington, D.C.

Breitfuss LL. 1898a. Kalkschwammfauna des weissen Meeres und der Eismeerkusten des europaischen Russlands. *Mémoires de l'Académie Impériale des sciences de St. Pétersbourg* (VIII) **6:** 1-40.

Breitfuss LL. 1898b. Die Kalkschwammfauna von Spitzbergen. Nach den Sammlungen der Bremer-Expedition nach Ost-Spitzbergen. *Zoologische Jahresbericht* **11**: 103-120.

Breitfuss LL. 1898c. *Die arctische Kalkschwammfauna*. Doctoral dissertation, Universität Zürich

Burton M. 1963. *A revision of the Classification of the Calcareous Sponges. With a Catalogue of the specimens in the British Museum (Natural History)*. W. Clowes and Sons Ltd.: London.

Cavalcanti FF, Menegola C, Lanna E. 2014. Three new species of the genus *Paraleucilla* Dendy, 1892 (Porifera, Calcarea) from the coast of Bahia State, Northeastern Brazil. *Zootaxa* **3764:** 537-554.

Chaban EM, Ekimova IA, Schepetov DM, Chernyshev AV. 2019. *Meloscaphander grandis* (Heterobranchia: Cephalaspidea), a deep-water species from the North Pacific: Redescription and taxonomic remarks. *Zootaxa* **4646**: zootaxa-4646.

Chombard C, Boury-Esnault N, Tillier S. 1998. Reassessment of homology of morphological characters in Tetractinellid sponges based on molecular data. *Systematic Biology* **47:** 351–366.

Clement M, Snell Q, Walker P, Posada D, Crandall K. 2002. TCS: estimating gene genealogies. *Parallel and Distributed Processing Symposium, International Proceedings* **2**: 184.

Cóndor-Luján B, Azevedo F, Hajdu E, Hooker Y, Willenz P, Klautau M. 2019. Tropical Eastern Pacific Amphoriscidae Dendy, 1892 (Porifera: Calcarea: Calcaronea: Leucosolenida) from the Peruvian coast. *Marine Biodiversity* **49:** 1813-1830.

Chu YL, Gong L, Li XZ. 2020. *Leucosolenia qingdaoensis* sp. nov. (Porifera, Calcarea, Calcaronea, Leucosolenida, Leucosoleniidae), a new species from China. *Zookeys* **906:** 1-11.

Dayrat B. 2005. Towards integrative taxonomy. *Biological Journal of the Linnean Society* **85:** 407-417.

Dohrmann M, Voigt O, Erpenbeck D, Wörheide G. 2006. Non-monophyly of most supraspecific taxa of calcareous sponges (Porifera, Calcarea) revealed by increased taxon sampling and partitioned Bayesian analysis of ribosomal DNA. *Molecular phylogenetics and evolution* **40:** 830-843.

Edgar RC. 2004. MUSCLE: multiple sequence alignment with high accuracy and high throughput. *Nucleic Acids Research* **32**: 1792–1797.

Ereskovsky, A.V. 1994a. Materials to the faunistic study of the White Sea and Barents Sea sponges. 2. Biogeographical and comparative-faunistic analysis. *Vestnik Leningradskogo Universiteta Seria 3 Biologia*, **3**: 13-26.

Ereskovsky, A.V. 1994b. Materials to the faunistic study of the White Sea and Barents Sea sponges. 3. Dependence of sponge distribution on temperature and salinity. *Vestnik Leningradskogo Universiteta Seria 3 Biologia,* **3**: 3-10.

Ereskovsky, A.V. 1994c. Habitat conditions and distribution of sponges in the littoral zone of eastern Murman. *Zool. Journal.* **73**: 5-17.

Ereskovsky, A.V. 1995a. Materials to the faunistic study of the White Sea and Barents Sea sponges. 4. Vertical distribution. *Vestnik Leningradskogo Universiteta Seria 3 Biologia*, **3**: 3-10.

Ereskovsky, A.V. **1995b**. Materials to the faunistic study of the White and Barents seas sponges. 5. Quantitative distribution. Berliner Geowissenschaftliche Abhandlungen **16**: 709-714.

Ereskovsky AV, Lavrov DV, Boury-Esnault N, Vacelet J. 2011. Molecular and morphological description of a new species of *Halisarca* (Demospongiae: Halisarcida) from Mediterranean Sea and a redescription of the type species *Halisarca dujardini*. *Zootaxa* **2768**: 5-31.

Ereskovsky AV, Lavrov AI, Bolshakov FV, Tokina DB. 2017a. Regeneration in White Sea sponge *Leucosolenia complicata* (Porifera, Calcarea). *Invertebrate Zoology* **14:** 108-113.

Ereskovsky AV, Richter DJ, Lavrov DV, Schippers KJ, Nichols SA. 2017b. Transcriptome sequencing and delimitation of sympatric *Oscarella* species (*O. carmela* and *O. pearsei* sp. nov) from California, USA. *PLoS One* **12:** e0183002.

Ereskovsky AV, Lavrov AI. 2021. Porifera. In: LaDouceur EB, ed. *Invertebrate Histology*: Wiley. 19-54.

Fortunato SAV, Adamski M, Ramos OM, Leininger S, Liu J, Ferrier DEK, Adamska M. 2014. Calcisponges have a ParaHox gene and dynamic expression of dispersed NK homeobox genes *Nature* **514:** 620-623.

Fortunato SAV, Adamski M, Adamska M. 2015. Comparative analyses of developmental transcription factor repertoires in sponges reveal unexpected complexity of the earliest animals *Marine Genomics* **24**: 121-129.

Fortunato SAV, Vervoort M, Adamski M, Adamska M. 2016. Conservation and divergence of bHLH genes in the calcisponge *Sycon ciliatum*. *Evodevo* **7**: 23.

Fontana T, Cóndor-Luján B, Azevedo F, Perez T, Klautau M. **2018.** Diversity and distribution patterns of Calcareous sponges (subclass Calcinea) from Martinique. *Zootaxa* **4410**: 331-369.

Gazave E, Lavrov DV, Cabrol J, Renard E, Rocher C, Vacelet J, Adamska M, Borchiellini C, Ereskovsky AV. 2013. Systematics and molecular phylogeny of the family Oscarellidae (Homoscleromorpha) with description of two new *Oscarella* species. *PLoS One* **8:** e63976.

Goulding TC, Dayrat B. 2016. Integrative taxonomy: ten years of practice and looking into the future. *Archives of Zoological Museum of Lomonosov Moscow State University* **54:** 116-133.

Haeckel E. 1872. *Die Kalkschwämme, eine Monographie*. G.Reimer: Berlin.

Hooper JNA, Van Soest RWM, Willenz P. 2002. *Systema Porifera*. Kluwer Academic/Plenum Publishers: New York.

Ivanova NV, Dewaard JR, Hebert PD. 2006. An inexpensive, automation-friendly protocol for recovering high-quality DNA. *Molecular ecology notes* **6**: 998-1002.

Jones WC. 1954. Spicule Form in *Leucosolenia complicata*. *Journal of Cell Science* **3:** 191-203.

Klautau M, Valentine C. 2008. Revision of the genus *Clathrina* (Porifera, Calcarea). *Zoological Journal of the Linnean Society* **139:** 1-62.

Klautau M, Azevedo F, Cóndor-Luján B, Rapp HT, Collins A, de Moraes Russo CA. 2013. A molecular phylogeny for the order *Clathrinida rekindles* and refines Haeckel's taxonomic proposal for calcareous sponges. *Integrative and comparative biology* **53**: 447-461.

Klautau M, Imešek M, Azevedo F, Pleše B, Nikolić V, Ćetković H. 2016. Adriatic calcarean sponges (Porifera, Calcarea), with the description of six new species and a richness analysis *European Journal of Taxonomy* **178**: 1-52.

Klautau M, Lopes MV, Guarabyra B, Folcher E, Ekins M, Debitus C. 2020. Calcareous sponges from the French Polynesia (Porifera: Calcarea). *Zootaxa* **4748:** 261-295.

Klautau M, Lopes MV, Tavares G, Pérez T. 2021. Integrative taxonomy of calcareous sponges (Porifera: Calcarea) from Réunion Island, Indian Ocean. *Zoological Journal of the Linnean Society* **194:** 671-725.

Koltun VM. 1952. New sponges from the northern seas. *Uchenÿe Zapiski Leningradskogo Ordena Lenina Gosudarstvennogo Universiteta* **31**: 125-129.

Kumar S, Stecher G, Tamura K. 2016. MEGA7: molecular evolutionary genetics analysis v.7.0 for bigger datasets. *Molecular Biology and Evolution* **33**: 1870–1874.

Lavrov DV, Pett W, Voigt O, Wörheide G, Forget L, Lang BF, Kayal E. 2013. Mitochondrial DNA of *Clathrina clathrus* (Calcarea, Calcinea): Six linear chromosomes, fragmented rRNAs, tRNA editing, and a novel genetic code *Molecular biology and evolution* **30:** 865-880.

Lavrov AI, Kosevich IA. 2016a. Sponge cell reaggregation: Cellular structure and morphogenetic potencies of multicellular aggregates. *Journal of Experimental Zoology Part A: Ecological Genetics and Physiology* **325:** 158-177.

Lavrov DV, Adamski M, Chevaldonné P, Adamska M. 2016b. Extensive mitochondrial mRNA editing and unusual mitochondrial genome organisation in calcaronean sponges *Current Biology* **26:** 86-92.

Lavrov AI, Bolshakov FV, Tokina DB, Ereskovsky AV. 2018. Sewing up the wounds: The epithelial morphogenesis as a central mechanism of calcaronean sponge regeneration. *Journal of Experimental Zoology Part B: Molecular and Developmental Evolution* **330:** 351-371.

Lavrov AI, Ereskovsky AV. 2022. Studying Porifera WBR using the calcareous sponges *Leucosolenia*. In: Galliot B and Blanchoud S, eds. *Whole-body regeneration*.

Lavrov AI, Bolshakov FV, Tokina DB, Ereskovsky AV. 2022. Fine details of the choanocyte filter apparatus in asconoid calcareous sponges (Porifera: Calcarea) revealed by ruthenium red fixation. *Zoology* **150:** 125984.

Leigh JW, Bryant D. 2015. POPART: full-feature software for haplotype network construction. *Methods in ecology and evolution* **6**: 1110-1116.

Leininger S, Adamski M, Bergum B, Guder C, Liu J, Laplante M, Bråte J, Hoffmann F, Fortunato SAV, Jordal S, Rapp HT, Adamska M. 2014. Developmental gene expression provides clues to relationships between sponge and eumetazoan body plans. *Nature Communications* **5:** 3905.

Łukowiak M, Van Soest R, Klautau M, Pérez T, Pisera A, Tabachnick K. 2022. The terminology of sponge spicules. *Journal of Morphology* **283**: 1517-1545.

Manuel M, Borchiellini C, Alivon E, Le Parco Y, Boury-Esnault N, Vacelet J. 2003. Phylogeny and evolution of calcareous sponges: monophyly of Calcinea and Calcaronea, high level of morphological homoplasy, and the primitive nature of axial symmetry. *Systematic Biology* **52:** 311-333.

Manuel M, Borchiellini C, Alivon E, Boury-Esnault N. 2004. Molecular phylogeny of calcareous sponges using 18S rRNA and 28S rRNA sequences. *Bollettino dei musei e degli istituti biologici dell'Universita di Genova* **68:** 449-461.

Melnikov NP, Bolshakov FV, Frolova VS, Skorentseva KV, Ereskovsky AV, Saidova AA, Lavrov AI. 2022. Tissue homeostasis in sponges: Quantitative analysis of cell proliferation and apoptosis. *Journal of Experimental Zoology Part B: Molecular and Developmental Evolution* **338:** 360-381.

Meyer-Kaiser KS, Schrage KR, von Appen W-J, Hoppmann M, Lochthofen N, Sundfjord A, Soltwedel T. 2022. Larval dispersal and recruitment of benthic invertebrates in the Arctic Ocean. *Progress in Oceanography* **203:** 102776.

Miller CE, Thompson RP, Bigelow MR, Gittinger G, Trusk TC, Sedmera D. 2005. Confocal imaging of the embryonic heart: how deep? *Microscopy and Microanalysis* **11:** 216-223.

Millonig G. 1964. Study on the factors which influence preservation of fine structure. *Symposium on electron microscopy*. Rome: Consiglio Nazionale delle Ricerche. 347-347.

Minchin EA. 1904. The characters and synonymy of the British species of sponges of the genus *Leucosolenia*. *Proceedings of the Zoological Society of London* **74**: 349-396.

Minchin EA. 1905. On the sponge *Leucosolenia contorta* Bowerbank, *Ascandra contorta* Haeckel, and *Ascetta spinosa* Lendenfeld. *Proceedings of the Zoological Society of London* **1905**: 3-20

Minh BQ, Nguyen MA, Von Haeseler A. 2013. Ultrafast approximation for phylogenetic bootstrap. *Molecular biology and evolution* **30**: 1188-1195.

Montagu G. 1818. An essay on sponges, with descriptions of all the species that have been discovered on the coast of Great Britain. *Memoirs of the Wernerian Natural History Society* **2:** 67-122.

Padial JM, Miralles A, De la Riva I, Vences M. 2010. The integrative future of taxonomy. *Frontiers in zoology* **7**:1-14

Muricy G, Boury-Esnault N, Bézac C, Vacelet J. 1996. Cytological evidence for cryptic speciation in Mediterranean *Oscarella* species (Porifera, Homoscleromorpha). *Canadian Journal of Zoology* **74:** 881-896.

Puillandre N, Lambert A, Brouillet S, Achaz G. 2012. ABGD, Automatic Barcode Gap Discovery for primary species delimitation. *Molecular Ecology* **21**: 1864-1877.

Rapp HT. 2006. Calcareous sponges of the genera *Clathrina* and *Guancha* (Calcinea, Calcarea, Porifera) of Norway (north-east Atlantic) with the description of five new species *Zoological Journal of the Linnean Society* **147:** 331-365.

Rapp HT. 2015. A monograph of the calcareous sponges (Porifera, Calcarea) of Greenland *Journal of the Marine Biological Association of the United Kingdom* **95:** 1395-1459.

Rapp HT, Klautau M, Valentine C. 2001. Two new species of *Clathrina* (Porifera, Calcarea) from the Norwegian coast. *Sarsia* **86**: 69-74.

Ribeiro B, Padua A, De Oliveira BFR, Puccinelli G, Da Costa Fernandes F, Laport MS, Klautau M. 2023. Uncovering the microbial diversity of two exotic calcareous sponges. *Microbial Ecology* **85**: 737–746.

Riesgo A, Cavalcanti FF, Kenny NJ, Ríos P, Cristobo J, Lanna E. 2018. Integrative systematics of clathrinid sponges: morphological, reproductive and phylogenetic characterisation of a new species of *Leucetta* from Antarctica (Porifera, Calcarea, Calcinea) with notes on the occurrence of flagellated sperm. *Invertebrate Systematics* **32:** 827.

Ronquist F, Huelsenbeck JP. 2003. MrBayes 3: Bayesian phylogenetic inference under mixed models. *Bioinformatics* **19**: 1572–1574.

Sanamyan K, Sanamyan N, Martynov A, Korshunova T. 2019. A new species of *Ernstia* (Porifera: Calcarea) described from marine aquarium. *Zootaxa* **4603**: 192-200.

Sanamyan KE, Sanamyan NP, Kukhlevskiy AD, Shilov VA. 2022. *Leucotreton kurilense*, a new genus and species of calcareous sponges of the family Sycanthidae (Porifera: Calcarea: Leucosolenida) from the northwestern Pacific Ocean, with contribution to taxonomy and nomenclature of related genera. *Zoosystematica rossica* **31**: 143–153

Sarà M. 1956. Aspetti genetici ed ecologici dell'ibridazione naturale fra differenti specie di *Leucosolenia* (Calcispongie) a Roscoff. *Bolletino di zoologia* **23:** 149-161.

Schlick-Steiner BC, Steiner FM, Seifert B, Stauffer C, Christian E, Crozier, RH. 2010. Integrative taxonomy: a multisource approach to exploring biodiversity. *Annual review of entomology* **55**: 421-438.

Stamatakis A. 2014. RAxML v.8: a tool for phylogenetic analysis and post-analysis of large phylogenies. *Bioinformatics* **30**: 1312–1313.

Sukumaran J, Holder MT. 2010. DendroPy: a Python library for phylogenetic computing. *Bioinformatics* **26**: 1569–1571.

van Soest RWM. 2017. Sponges of the Guyana Shelf. *Zootaxa* **4217**: 1-225.

van Soest RWM, de Kluijver MJ, van Bragt PH, Faasse M, Nijland R, Beglinger EJ, de Weerdt WH, de Voogd NJ. 2007. Sponge invaders in Dutch coastal waters *Journal of the Marine Biological Association of the UK* **87:** 1733-1748.

van Soest RW, de Voogd NJ. 2018. Calcareous sponges of the western Indian Ocean and Red Sea. *Zootaxa* **4426**: 1-60.

Voigt O, Wülfing E, Wörheide G. 2012. Molecular phylogenetic evaluation of classification and scenarios of character evolution in calcareous sponges (Porifera, Class Calcarea). *PLoS One* **7:** e33417.

Voigt O, Wörheide G. 2016. A short LSU rRNA fragment as a standard marker for integrative taxonomy in calcareous sponges (Porifera: Calcarea). *Organisms Diversity and Evolution* **16:** 53-64.

de Voogd NJ, Alvarez B, Boury-Esnault N, Carballo JL, Cárdenas P, Díaz MC, Dohrmann M, Downey R, Hadju E, Hooper JNA, Kelly M, Klautau M, Manconi R, Morrow CC, Pisera AB, Ríos P, Rützler K, Schönberg C, Vacelet J, Van Soest RWM. 2023. World Porifera Database [doi:10.14284/359]

Webster NS, Thomas T. 2016. The sponge hologenome. *mBio* **7:** 1-14.

Willenz P, Ereskovsky AV, Lavrov DV. 2016. Integrative taxonomic re-description of *Halisarca magellanica* and description of a new species of *Halisarca* (Porifera, Demospongiae) from Chilean Patagonia. *Zootaxa* **4208:** 501-533.

Wörheide G, Nichols SA, Goldberg J. 2004. Intragenomic variation of the rDNA internal transcribed spacers in sponges (Phylum Porifera): implications for phylogenetic studies. *Molecular phylogenetics and evolution*, **33**: 816-830.

Tables

Table 1. Amplification and sequencing primers and PCR conditions.

Marker	Primers	PCR conditions	Reference
28S rRNA	**28S-C2F** GAA AAG AAC TTT GRA RAG AGA GT **28S-D2R** TCC GTG TTT CAA GAC GGG	5 min - 94°C, 35x[1 min - 95°C, 45s - 50°C, 1 min - 72°C], 7 min - 72°C	Chombard et al., 1998
18S rRNA	**18S-328F** CCTGGTGATCCTGCCAG **18S-HI + R** CAACTAAGAACGGCCATGCAC **18S-329R** TAA TGA TCC TTC CGC AGG TT **18S-A-F** CAG CMG CCG CGG TAA TWC	5 min - 94°C, 35x[1 min - 94°C, 1 min - 50°C, 2 min - 72°C], 7 min - 72°C	Alvizu et al., 2018
Histone H3	**Por_h3f** ATG GCC CGT ACC AAG CAG ACT GC **Por_h3r** ATA TCC TTG GGC ATG ATG GTG AC	5 min - 94°C, 35x[15 s - 95°C, 30s - 50°C, 45 s - 72°C], 7 min - 72°C	This study

Table 2. Uncorrected intra- and interspecific *p*-distances of 28S marker in the genus *Leucosolenia*. Intraspecific distances are highlighted in bold.

	L. complicata	*L. corallorrhiza*	*Leucosolenia* sp. A	*L. variabilis*	*L. creepae*	*L. somesii*
L. complicata	**0-0.4**					
L. corallorrhiza	6.3-8	**0-1.3**				
Leucosolenia sp. A	6.8-7.6	0.4-1.7	**0**			
L. variabilis	5.1-7.2	0.4-1.3	0.8-1.3	**0-0.4**		
L. creepae	5.1-5.9	8.9-10.5	8.9-9.3	8.9-9.3	**0-0.4**	
L. somesii	5.5-5.9	10.5-11.8	10.1	10.1	2.5-3	-

Table 3. Uncorrected intra- and interspecific *p*-distances of H3 marker in the genus *Leucosolenia*. Intraspecific distances are highlighted in bold.

	L. complicata	*L. corallorrhiza*	*Leucosolenia* sp. A	*L. variabilis*	*L. creepae*
L. complicata	**0-0.4**				
L. corallorrhiza	7.9-8.8	**0-0.8**			
Leucosolenia sp. A	8.4-9.6	2.5-3.3	**0.4-0.8**		
L. variabilis	7.9-9.2	3.3-5	2.9-4.2	**0-1.3**	
L. creepae	3.8-4.6	9.6-10.5	9.6-10.5	9.2-10.9	**0-1.7**

Table 4. Spicule dimensions of *Leucosolenia complicata* (Montagu, 1814)

Spicule	Length (µm)					Width (µm)					Angle (°)				
	Min	**Mean**	**Max**	**SD**	**n**	**Min**	**Mean**	**Max**	**SD**	**n**	**Min**	**Mean**	**Max**	**SD**	**n**
Curved lanceolate diactines	147.1	263.7	389.3	58.8	46	6.6	9.5	14.4	1.4	47	-	-	-	-	-
Trichoxeas	66.0	127.3	248.7	40.3	18	1.5	2.4	3.5	0.6	17	-	-	-	-	-
Triactines															
Unpaired actine	75.3	113.5	149.4	19.4	40	3.7	6.3	10.5	1.3	41	-	-	-	-	-
Paired actines	62.3	94.9	122.0	13.1	81	4.1	6.8	11.8	1.3	81	120.4	125.7	137.9	4.4	28
Tetractines															
Unpaired actine	30.6	109.3	156.7	24.1	56	3.7	6.7	9.7	1.2	57	-	-	-	-	-
Paired actines	14.2	93.7	170.2	20.4	109	3.5	6.9	10.0	1.2	108	115.7	123.5	134.0	4.4	53
Apical actine	8.9	23.8	49.7	11.1	56	2.0	5.3	10.1	1.4	57	-	-	-	-	-

Table 5. Spicule dimensions of *Leucosolenia corallorrhiza* (Haeckel, 1872)

Spicule	Length (µm)					Width (µm)					Angle (°)				
	Min	**Mean**	**Max**	**SD**	**n**	**Min**	**Mean**	**Max**	**SD**	**n**	**Min**	**Mean**	**Max**	**SD**	**n**
Curved lanceolate diactines	73.5	179.0	455.0	74.2	27	2.8	6.0	11.4	1.7	27	-	-	-	-	-
Triactines															
Unpaired actine	37.1	70.5	100.0	14.9	91	3.5	6.5	10.5	1.4	91	-	-	-	-	-
Paired actines	36.1	82.7	133.3	20.4	165	3.1	6.5	12.5	1.5	164	124.6	142.9	151.2	6.0	28
Tetractines															
Unpaired actine	46.8	68.8	98.8	16.0	14	3.5	5.6	7.9	1.2	15	-	-	-	-	-
Paired actines	37.6	80.7	128.1	22.5	23	2.4	5.8	8.4	1.6	25	144.8	151.4	159.3	4.0	14
Apical actine	11.4	22.9	42.9	10.7	16	3.6	5.5	9.2	1.3	16	-	-	-	-	-

Table 6. Spicule dimensions of *Leucosolenia variabilis* Haeckel, 1870

Spicule	Length (µm)					Width (µm)					Angle (°)				
	Min	Mean	Max	SD	n	Min	Mean	Max	SD	n	Min	Mean	Max	SD	n
Curved smooth lanceolate diactines	123.7	306.7	482.4	100.1	27	5.7	9.8	13.9	1.8	27	-	-	-	-	-
Strait spiny lanceolate diactines	111.4	151.4	191.2	28.7	5	2.4	3.1	3.8	0.5	10	-	-	-	-	-
Trichoxeas		fragments, up to 362.4				0.6	0.9	1.3	0.2	17	-	-	-	-	-
Triactines															
Unpaired actine	46.5	122.3	208.6	31.7	63	5.0	8.1	11.6	1.5	63	-	-	-	-	-
Paired actines	39.0	127.9	180.2	29.3	130	4.0	8.5	12.7	1.7	128	122.1	138.5	150.6	4.8	42
Tetractines															
Unpaired actine	101.3	147.6	196.2	28.4	12	6.4	8.5	11.1	1.5	12	-	-	-	-	-
Paired actines	92.5	142.0	172.5	22.3	25	6.0	9.1	11.5	1.5	26	134.0	142.2	155.3	4.6	34
Apical actine	16.5	22.8	31.1	5.2	14	4.7	5.9	8.5	1.4	15	-	-	-	-	-

Table 7. Spicule dimensions of *Leucosolenia* sp. A.

Spicule	Length (µm)					Width (µm)					Angle (°)				
	Min	Mean	Max	SD	n	Min	Mean	Max	SD	n	Min	Mean	Max	SD	n
Curved spiny lanceolate diactines	131.9	189.1	311.0	48.2	15	5.8	7.2	8.8	0.8	15	-	-	-	-	-
Curved smooth diactines	-	515.0	-	83.4	2	-	11.6	-	1.7	2					
Triactines															
Unpaired actine	81.6	118.5	179.7	22.2	42	6.3	8.9	11.1	1.1	43	-	-	-	-	-
Paired actines	80.5	125.1	174.8	22.4	74	6.6	9.1	11.6	1.0	84	132.9	146.5	160.7	5.6	44
Tetractines															
Unpaired actine	82.4	114.3	157.1	27.2	5	7.9	8.6	9.9	0.7	7	-	-	-	-	-
Paired actines	79.3	113.2	132.0	16.0	14	7.0	8.5	10.2	0.9	14	137.4	140.8	146.2	3.3	5
Apical actine	25.7	30.0	34.2	4.2	3	5.8	7.1	8.5	1.2	5	-	-	-	-	-

Table 8. Spicule dimensions of *Leucosolenia creepae* sp. nov.

Spicule	Length (µm)					Width (µm)					Angle (°)				
	Min	Mean	Max	SD	n	Min	Mean	Max	SD	n	Min	Mean	Max	SD	n
Spiny diactines	83.3	194.9	478.8	98.6	81	2.9	5.1	9.6	1.4	81	-	-	-	-	-
Triactines															
Unpaired actine	29.9	80.7	125.8	18.8	87	3.0	5.4	8.8	1.1	89	-	-	-	-	-
Paired actines	37.9	94.2	148.6	20.9	169	2.7	5.9	9.0	1.2	173	118.5	131.1	137.7	4.7	29
Tetractines															
Unpaired actine	31.8	85.1	137.5	25.9	15	4.1	6.2	7.7	1.3	15	-	-	-	-	-
Paired actines	52.9	95.3	136.2	20.6	30	3.7	6.3	8.1	1.2	31	131.0	139.5	146.1	4.5	13
Apical actine	12.7	25.6	43.7	9.8	18	2.9	5.2	8.4	1.3	18	-	-	-	-	-

Table 9. Spicule dimensions of *Leucosolenia somesii* (Bowerbank, 1874)

Spicule	Length (µm)					Width (µm)					Angle (°)				
	Min	Mean	Max	SD	n	Min	Mean	Max	SD	n	Min	Mean	Max	SD	n
Curved smooth diactines	148.0	424.5	649.8	116.0	68	6.5	9.9	12.3	1.3	88	-	-	-	-	-
Straight spiny diactines	68.0	90.0	105.8	8.9	58	2.1	3.3	4.1	0.4	39	-	-	-	-	-
Triactines															
Unpaired actine	58.3	127.4	186.1	27.0	60	6.5	8.2	10.3	1.0	64	-	-	-	-	-
Paired actines	86.2	155.2	226.0	28.4	111	5.9	8.0	10.7	1.0	131	117.1	131.7	139.9	4.2	67
Tetractines															
Unpaired actine	103.5	156.0	206.9	32.9	10	8.4	9.1	10.5	0.6	13	-	-	-	-	-
Paired actines	156.0	178.7	209.2	14.5	23	7.8	9.5	11.1	0.7	24	133.5	139.3	149.1	3.9	14
Apical actine	16.6	21.5	29.3	4.2	8	8.1	10.0	11.2	1.0	7	-	-	-	-	-

Figure captions

Figure 1. The molecular phylogenetic hypothesis of the genus *Leucosolenia* based on the Bayesian analysis of the concatenated dataset (28S, 18S and H3 markers). Initial species names are used on the tips, bold font indicates original specimens used in this study. Each putative species-level clade is coloured according to the revised species hypothesis, the suggested revised species names are provided on the right. All calcaronean species except representatives of the genus *Leucosolenia* are collapsed into a single group, 'Calcaronea rest'. Numbers above branches indicate posterior probabilities from the Bayesian Inference (> 0.9), numbers below branches – bootstrap support from the Maximum Likelihood (>70).

Figure 2. Medium parsimony network analysis (TCS algorithm) of *Leucosolenia* species. The relative size of circles is proportional to the number of sequences of that same genotype. A – 28S alignment. Colours of the circles refer to the geographic origin of each genotype. Coloured backgrounds and species names indicate the revised species hypothesis. B – H3 alignment. Colours of the circles refer to the revised species hypothesis.

Figure 3. *Leucosolenia complicata* (Montagu, 1814). External morphology and skeleton. A – general morphology (WS11661); B – skeleton of oscular rim (WS11662); C – skeleton of oscular tube (WS11662); D – skeleton of cormus (WS11662). c – cormus, d – diverticulum, o – osculum, or – oscular rim, ot – oscular tube.

Figure 4. *Leucosolenia complicata* (Montagu, 1814). Spicule types, scanning electron microscopy. A – curved lanceolate diactines; B, C – trichoxeas; D – triactines; E – tetractine.

Figure 5. *Leucosolenia complicata* (Montagu, 1814). Body wall structure and cell types of bordering tissues. A, B – semi-thin sections of sponge body wall; C – exopinacocyte; D –

endopinacocyte; E – choanocytes; F – porocyte. Scale bars: A – 50 µm, B – 20 µm, C – F – 2 µm. ch – choanocytes, chd – choanoderm, en – endopinacocyte, ex – exopinacocyte, exp – exopinacoderm, f – flagellum, m – mesohyl, mv – microvilli, n – nucleus, po – porocyte.

Figure 6. *Leucosolenia complicata* (Montagu, 1814). Mesohyl cell types and symbiotic bacteria. A – sclerocyte; B – amoebocyte; C – symbiotic bacteria, morphotype 1; D – symbiotic bacteria, morphotype 2. Scale bars: A, B – 2 µm, C, D – 0.5 µm. am – amoebocytes, m – mesohyl, n – nucleus, sp – spicule.

Figure 7. *Leucosolenia corallorrhiza* (Haeckel, 1872). External morphology and skeleton. A – general morphology (WS11642); B – skeleton of oscular rim (WS11653); C – skeleton of oscular tube (WS11653); D – skeleton of cormus (WS11653). c – cormus, d – diverticulum, o – osculum, oc – oscular crown, ot – oscular tube.

Figure 8. *Leucosolenia corallorrhiza* (Haeckel, 1872). Spicule types, scanning electron microscopy. A – curved lanceolate diactines; B – tips of diactines, I and II refer to the zones marked on A, white arrowheads mark spines; C – tetractine; D – triactines.

Figure 9. *Leucosolenia corallorrhiza* (Haeckel, 1872). Body wall structure and cell types of bordering tissues. A, B – semi-thin sections of body wall of sponge; C – exopinacocyte; D – endopinacocyte; E – choanocytes, inset – junctions between choanocytes; F – porocyte. Scale bars: A – 50 µm, B – 20 µm, C - F– 2 µm, inset – 0.2 µm. am – amoebocyte, ch – choanocytes, chd – choanoderm, en – endopinacocyte, exp – exopinacoderm, f – flagellum, m – mesohyl, mv – microvilli, n – nucleus, ph – phagosome, po – porocytes, sb – symbiotic bacteria.

Figure 10. *Leucosolenia corallorrhiza* (Haeckel, 1872). Mesohyl cell types and symbiotic bacteria. A – sclerocytes, inset – septate junctions between sclerocytes; B – amoebocytes; C, D – granular cells in the body wall; E – granular cell; F – degraded granular cell; G – myocytes, inset – bundles of myofilaments; H, I – symbiotic bacteria, morphotype 1. Scale bars: A, B, E, F – 2 µm, C – 50 µm, C – 20 µm, G – 5 µm, H – 0.5 µm, I – 1 µm. ch – choanocytes, chd – choanoderm, ex – exopinacocyte, exp – exopinacoderm, f – flagellum, gc – granular cells gr – granule, m – mesohyl, mf – myofibrils, mv – microvilli, my – myocytes, n – nucleus, po – porocytes, sb – symbiotic bacteria, sp – spicule.

Figure 11. *Leucosolenia variabilis* Haeckel, 1870. External morphology and skeleton. A – general morphology (WS11731); B – skeleton of oscular rim (WS11731); C – skeleton of oscular tube; D – skeleton of cormus (WS11643). c – cormus, d – diverticulum, o – osculum, or – oscular rim, ot – oscular tube.

Figure 12. *Leucosolenia variabilis* Haeckel, 1870. Spicule types, scanning electron microscopy. A – curved smooth lanceolate diactines; B – triactines; C – abnormal triactines; D – tetractine.

Figure 13. *Leucosolenia variabilis* Haeckel, 1870. Trichoxeas. A, B – general view of trichoxea fragments; C – enlarge view of trichoxea, white arrowhead marks spines. tx – trichoxeas.

Figure 14. *Leucosolenia variabilis* Haeckel, 1870. Body wall structure and cell types of bordering tissues. A, B – semi-thin sections of body wall of sponge; C – exopinacocytes; D – choanocytes; E – porocyte; F – endopinacocyte. Scale bars: A – 50 µm, B – 20 µm, C, D – 5 µm, E, F – 2 µm. am – amoeboid cell, ch – choanocytes, chd – choanoderm, ex – exopinacocyte, exp – exopinacoderm, f – flagellum, m – mesohyl, mv – microvilli, n – nucleus, po – porocyte, sb – symbiotic bacteria, sc – spherulous cells.

Figure 15. *Leucosolenia variabilis* Haeckel, 1870. Mesohyl cell types and symbiotic bacteria. A – amoebocytes; B – large amoeboid cell; C – granular cell; D – myocyte, inset – bundles of myofilaments; E – spherulous cell; F – spherulous cells in the body wall; G – sclerocyte; H – symbiotic bacteria, morphotype 1. I – symbiotic bacteria, morphotype 2. J – symbiotic bacteria, morphotype 3. Scale bars: A – 2 µm, B – 5 µm, C-E – 2 µm, F – 50 µm, G – 2 µm, H-J – 1 µm. am – amoebocyte, bam – large amoeboid cell, ch – choanocytes, gc – granular cell, gr – granule, m – mesohyl, mf – myofibrils, n – nucleus, sc – spherulous cells, sp - spicule.

Figure 16. *Leucosolenia variabilis* Haeckel, 1870. Spicule types in the White Sea specimen (A) and in the specimens from the British Natural History Museum collection (B-D). A – spicules from WS11731; B – spicules from BMNH 1906.12.1.40; C – spicules from BMNH 1906.12.1.50; D – spicules from the syntype BMNH 1910.1.1.421.a. d – diactines, tx – trichoxeas.

Figure 17. *Leucosolenia* sp. A. External morphology and skeleton. A – general morphology (WS11752); B – skeleton of oscular rim (WS11770); C – skeleton of oscular tube (WS11770); D – skeleton of cormus (WS11752). c – cormus, d – diverticulum, o – osculum, or – oscular rim, ot – oscular tube.

Figure 18. *Leucosolenia* sp. A. Spicule types, scanning electron microscopy. A – curved smooth diactines; B – curved spiny lanceolate diactines triactines; C – tips of diactines, I and II refer to the zones marked on A and B, white arrowheads mark spines; D – triactines; E – abnormal triactines; F – tetractine.

Figure 19. *Leucosolenia creepae* sp. nov. External morphology and skeleton. A – general morphology (WS11702, holotype); B – skeleton of oscular rim (WS11762); C – skeleton of

oscular tube (WS11728); D – skeleton of cormus (WS11655). c – cormus, d – diverticulum, o – osculum, oc – oscular crown, ot – oscular tube.

Figure 20. *Leucosolenia creepae* sp. nov. Spicule types, scanning electron microscopy. A – spiny diactines; B – tips of diactines, I, II, III and IV refer zones marked on A, white arrowheads mark spines; C – triactines; D – abnormal triactines; E – tetractines.

Figure 21. *Leucosolenia creepae* sp. nov. Body wall structure and cell types of bordering tissues. A, B – semi-thin sections of body wall of sponge; C – exopinacocyte; D – endopinacocyte and myocyte, inset - bundles of myofilaments in the myocyte; E – choanocytes. F – porocyte. Scale bars: A – 50 µm, B – 20 µm, C – 2 µm, D – 5 µm, E, F – 2 µm. am – amoeboid cell, ch – choanocytes, chd – choanoderm, en – endopinacocyte, ex – exopinacocyte, exp – exopinacoderm, f – flagellum, m – mesohyl, mf – myofibrils, mv – microvilli, my – myocytes, n – nucleus, oo – oocyte, ph – phagosome, po – porocyte, sb – symbiotic bacteria.

Figure 22. *Leucosolenia creepae* sp. nov. Mesohyl cell types and symbiotic bacteria. A – sclerocyte; B – amoebocyte; C, D – symbiotic bacteria, morphotype 1; E, F – symbiotic bacteria, morphotype 2; G – young oocyte. Scale bars: A, B – 2 µm, C - F – 0.5 µm, G – 5 µm. am - amoeboid cell, ch – choanocytes, m – mesohyl, n – nucleus, oo – oocyte, sb – symbiotic bacteria, sp – spicule.

Figure 23. *Leucosolenia somesii* (Bowerbank, 1874). External morphology and skeleton. A – general morphology (ZMA Por. 17572); B – skeleton of cormus (ZMA Por. 17572); C, D – spicules from BMNH 1956.4.26.35. c – cormus, d – diverticulum.

Figure 24. *Leucosolenia somesii* (Bowerbank, 1874). ZMA Por. 17572. Spicule types, scanning electron microscopy. A – curved smooth diactines; B – straight spiny diactines; C – tips of diactines, I and II refer to the zones marked on A and B, white arrowheads mark spines; D – triactines; E – abnormal triactines; F – tetractines.

SUPPLEMENTARY MATERIAL

Data S1. Unedited Maximum Likelihood trees (LSU, H3, 18S and concatenated datasets).

Data S2. Results of ASAP analysis based on LSU and H3 datasets.

Table S1. List of *Leucosolenia* specimens used in the study. Voucher numbers, collection dates and localities, and GenBank accession numbers are given.

Table S2. The cell types and symbiotic bacteria of the studied *Leucosolenia* species.

Figure S1. The molecular phylogenetic hypothesis of the genus *Leucosolenia* based on the Bayesian analysis of the concatenated dataset (28S, 18S and H3 markers). Numbers above branches indicate posterior probabilities from the Bayesian Inference (> 0.9), numbers below branches – bootstrap support from the Maximum Likelihood (>70).

Figure S2. The molecular phylogenetic hypothesis of the genus *Leucosolenia* based on the Bayesian analysis of the concatenated dataset (28S and 18S markers). Numbers above branches indicate posterior probabilities from the Bayesian Inference (> 0.9), numbers below branches – bootstrap support from the Maximum Likelihood (>70).

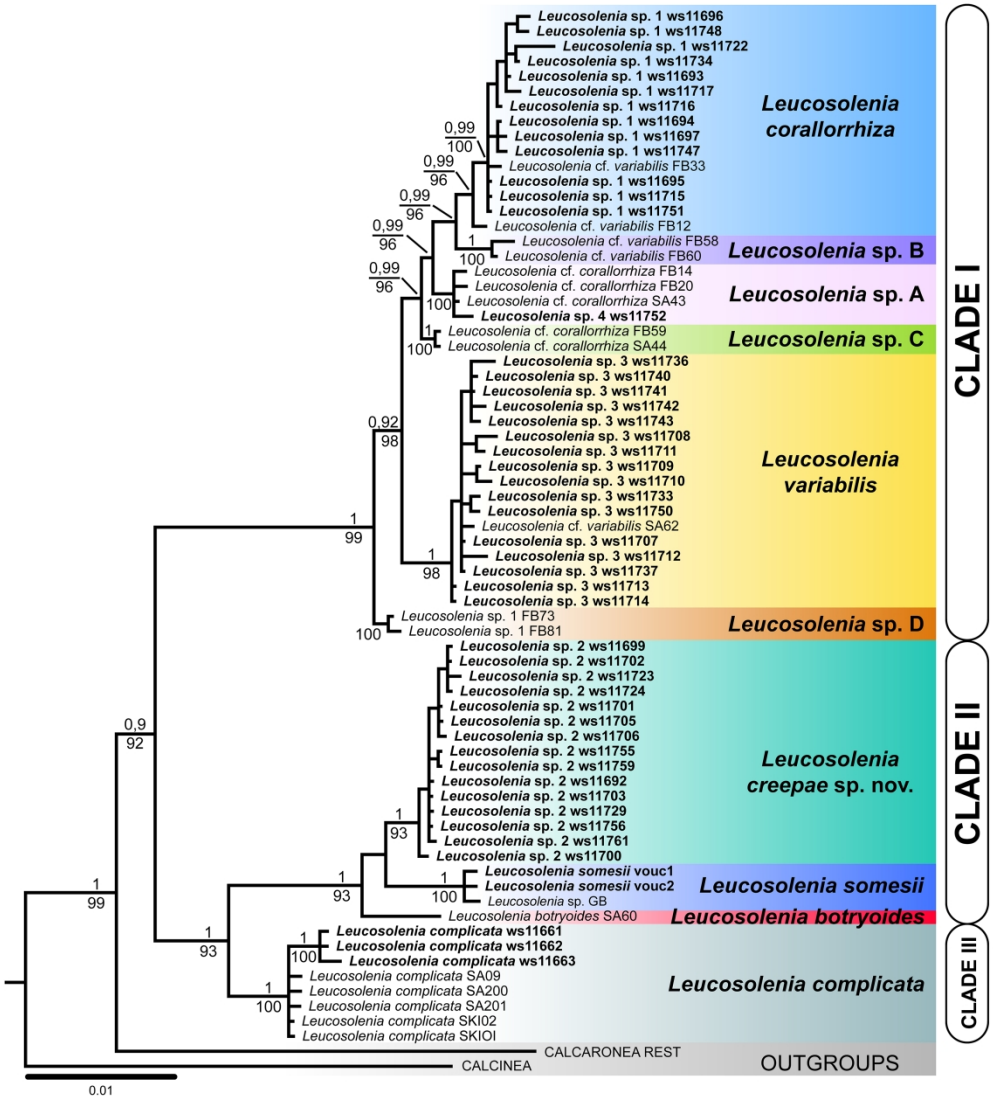

Figure 1. The molecular phylogenetic hypothesis of the genus Leucosolenia based on the Bayesian analysis of the concatenated dataset (28S, 18S and H3 markers). Initial species names are used on the tips, bold font indicates original specimens used in this study. Each putative species-level clade is coloured according to the revised species hypothesis, the suggested revised species names are provided on the right. All calcaronean species except representatives of the genus Leucosolenia are collapsed into a single group, 'Calcaronea rest'. Numbers above branches indicate posterior probabilities from the Bayesian Inference (> 0.9), numbers below branches – bootstrap support from the Maximum Likelihood (>70).

267x296mm (300 x 300 DPI)

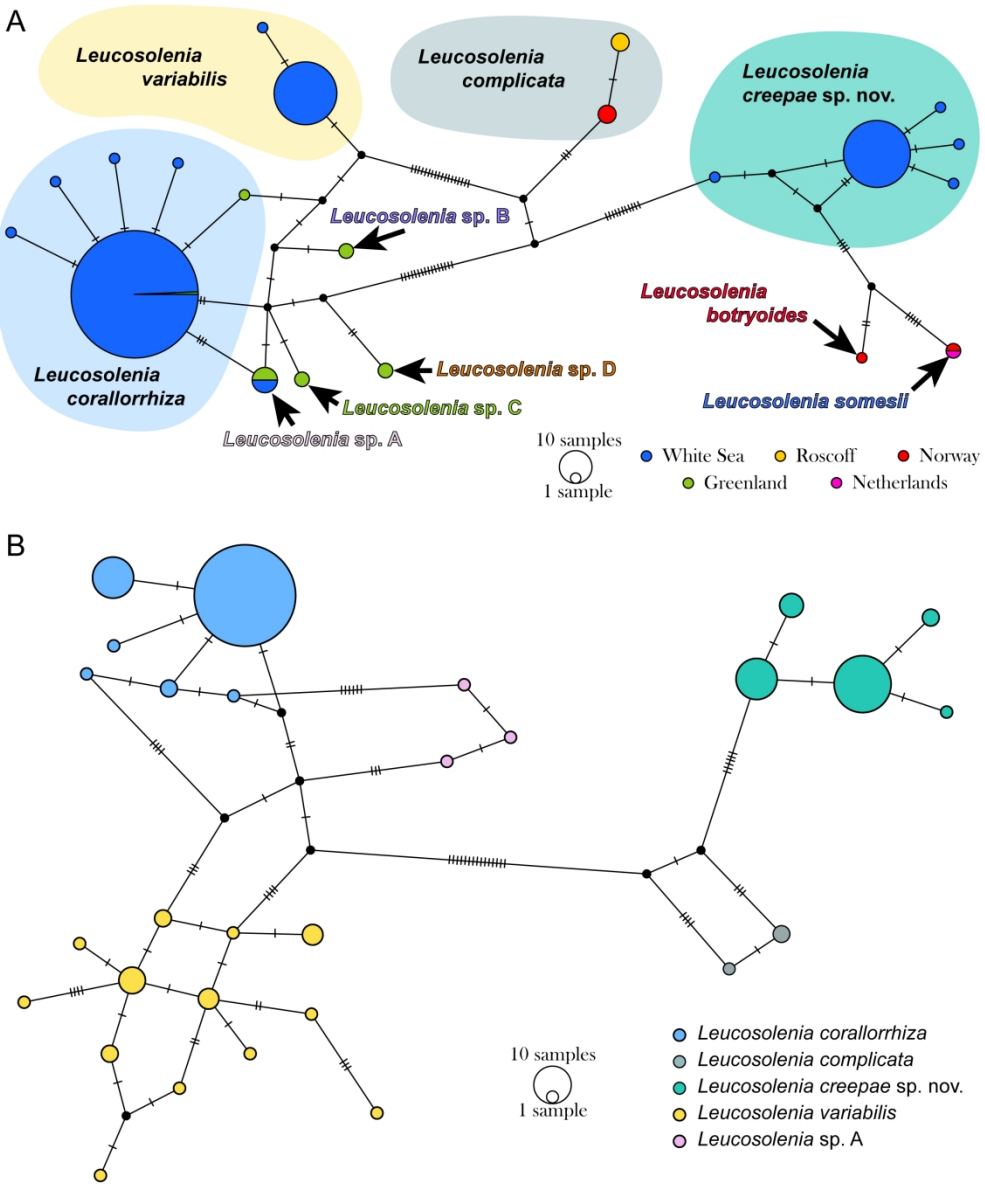

Figure 2. Medium parsimony network analysis (TCS algorithm) of Leucosolenia species. The relative size of circles is proportional to the number of sequences of that same genotype. A – 28S alignment. Colours of the circles refer to the geographic origin of each genotype. Coloured backgrounds and species names indicate the revised species hypothesis. B – H3 alignment. Colours of the circles refer to the revised species hypothesis.

214x256mm (300 x 300 DPI)

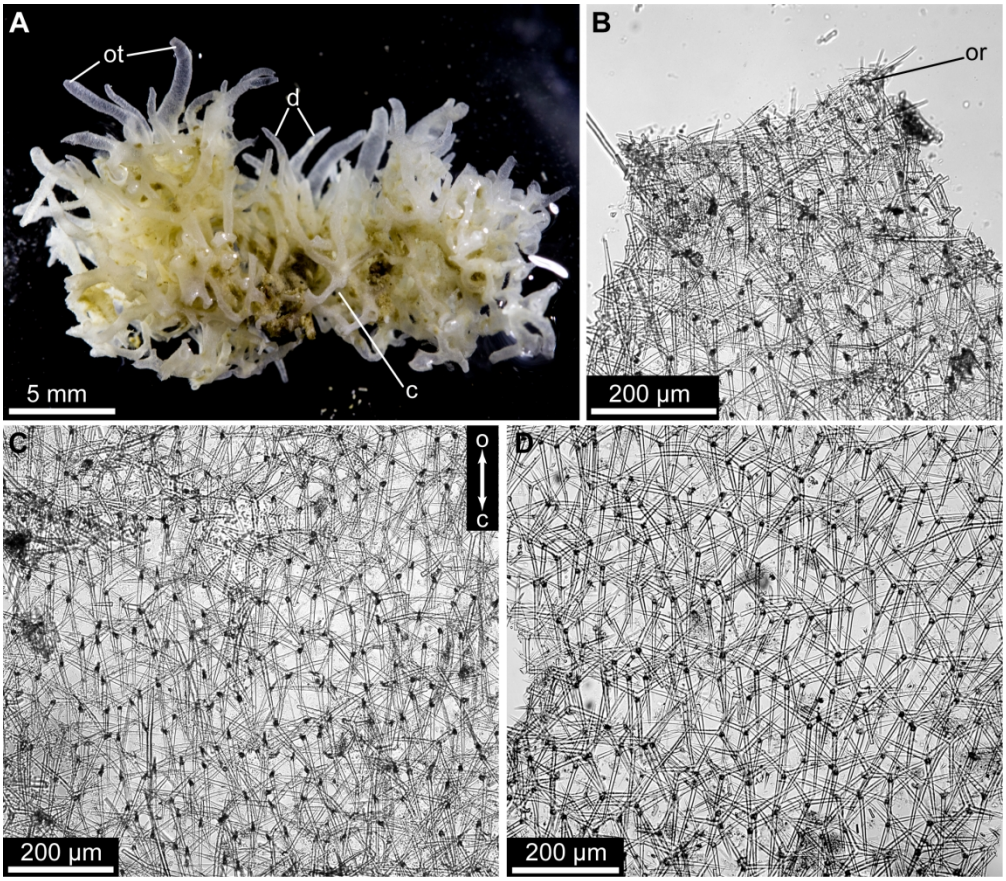

Figure 3. Leucosolenia complicata (Montagu, 1814). External morphology and skeleton. A – general morphology (WS11661); B – skeleton of oscular rim (WS11662); C – skeleton of oscular tube (WS11662); D – skeleton of cormus (WS11662). c – cormus, d – diverticulum, o – osculum, or – oscular rim, ot – oscular tube.

174x151mm (300 x 300 DPI)

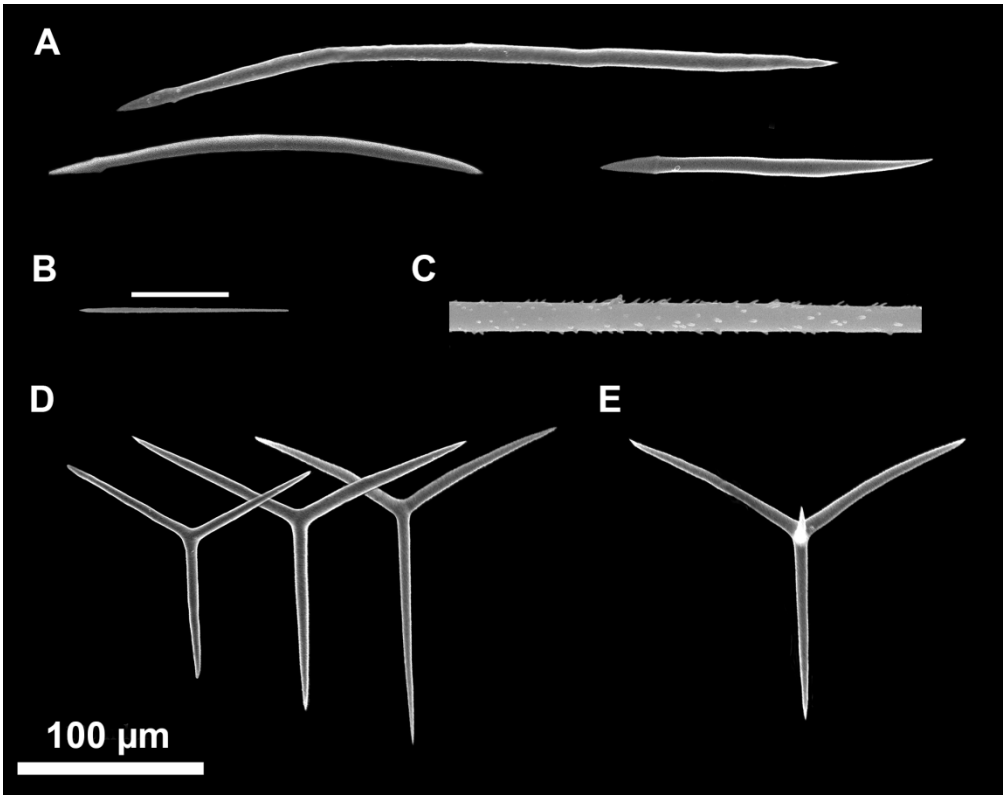

Figure 4. Leucosolenia complicata (Montagu, 1814). Spicule types, scanning electron microscopy. A – curved lanceolate diactines; B, C – trichoxeas; D – triactines; E – tetractine.

173x137mm (300 x 300 DPI)

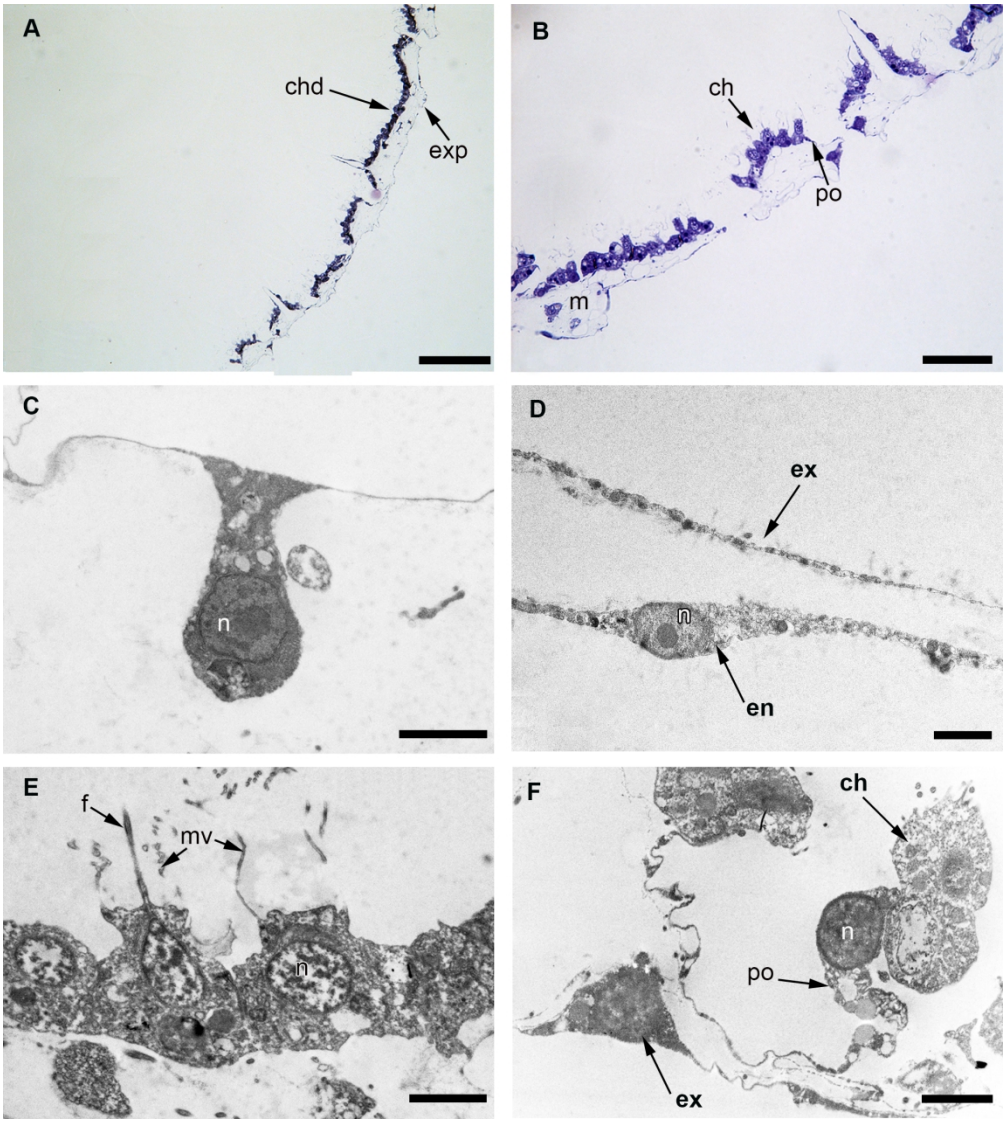

Figure 5. Leucosolenia complicata (Montagu, 1814). Body wall structure and cell types of bordering tissues. A, B – semi-thin sections of sponge body wall; C – exopinacocyte; D – endopinacocyte; E – choanocytes; F – porocyte. Scale bars: A – 50 μm, B – 20 μm, C - F – 2 μm. ch – choanocytes, chd – choanoderm, en – endopinacocyte, ex – exopinacocyte, exp – exopinacoderm, f – flagellum, m – mesohyl, mv – microvilli, n – nucleus, po – porocyte.

173x193mm (300 x 300 DPI)

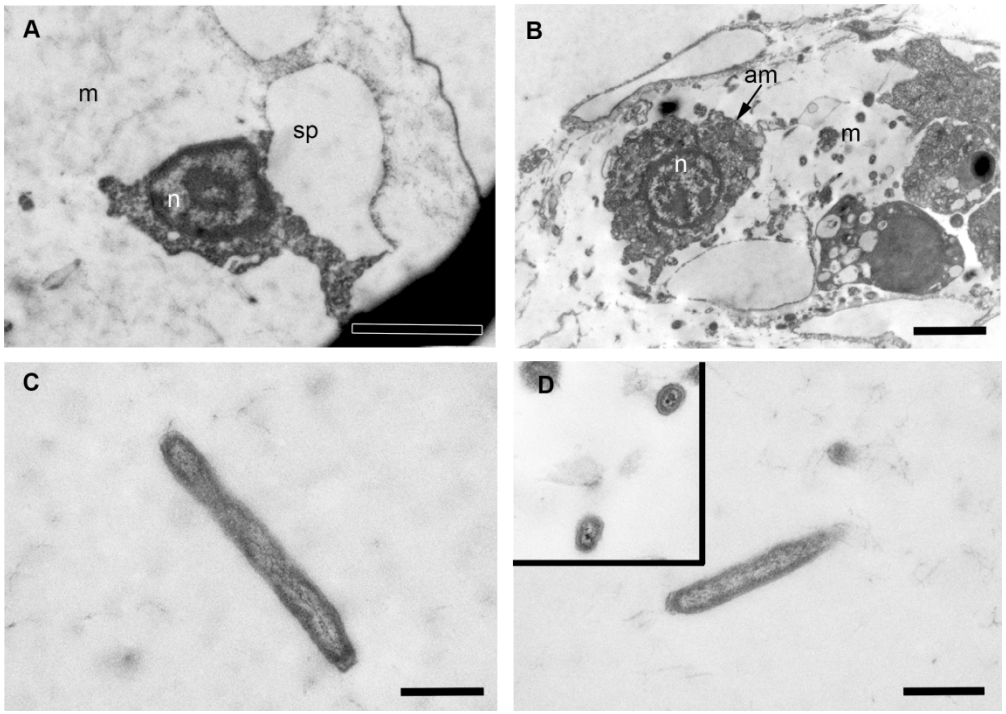

Figure 6. Leucosolenia complicata (Montagu, 1814). Mesohyl cell types and symbiotic bacteria. A – sclerocyte; B – amoebocyte; C – symbiotic bacteria, morphotype 1; D - symbiotic bacteria, morphotype 2. Scale bars: A, B – 2 μm, C, D – 0.5 μm. am – amoebocytes, m – mesohyl, n – nucleus, sp - spicule.

173x123mm (300 x 300 DPI)

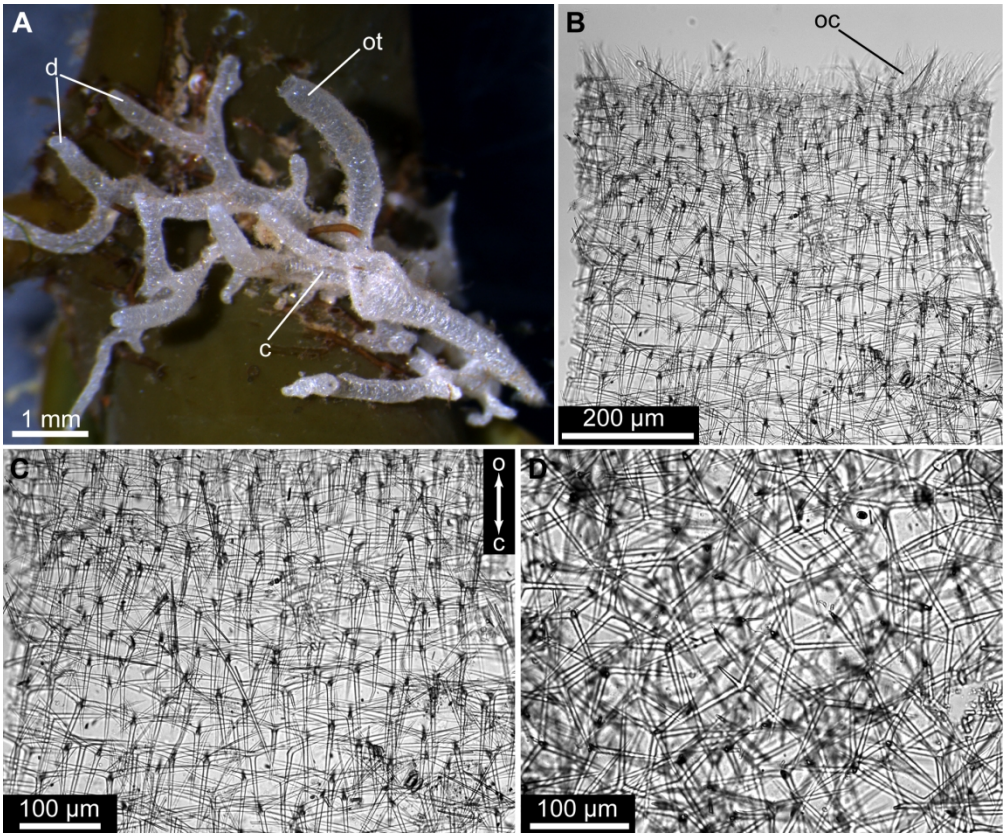

Figure 7. Leucosolenia corallorrhiza (Haeckel, 1872). External morphology and skeleton. A – general morphology (WS11642); B – skeleton of oscular rim (WS11653); C – skeleton of oscular tube (WS11653); D – skeleton of cormus (WS11653). c – cormus, d – diverticulum, o – osculum, oc – oscular crown, ot – oscular tube.

174x144mm (300 x 300 DPI)

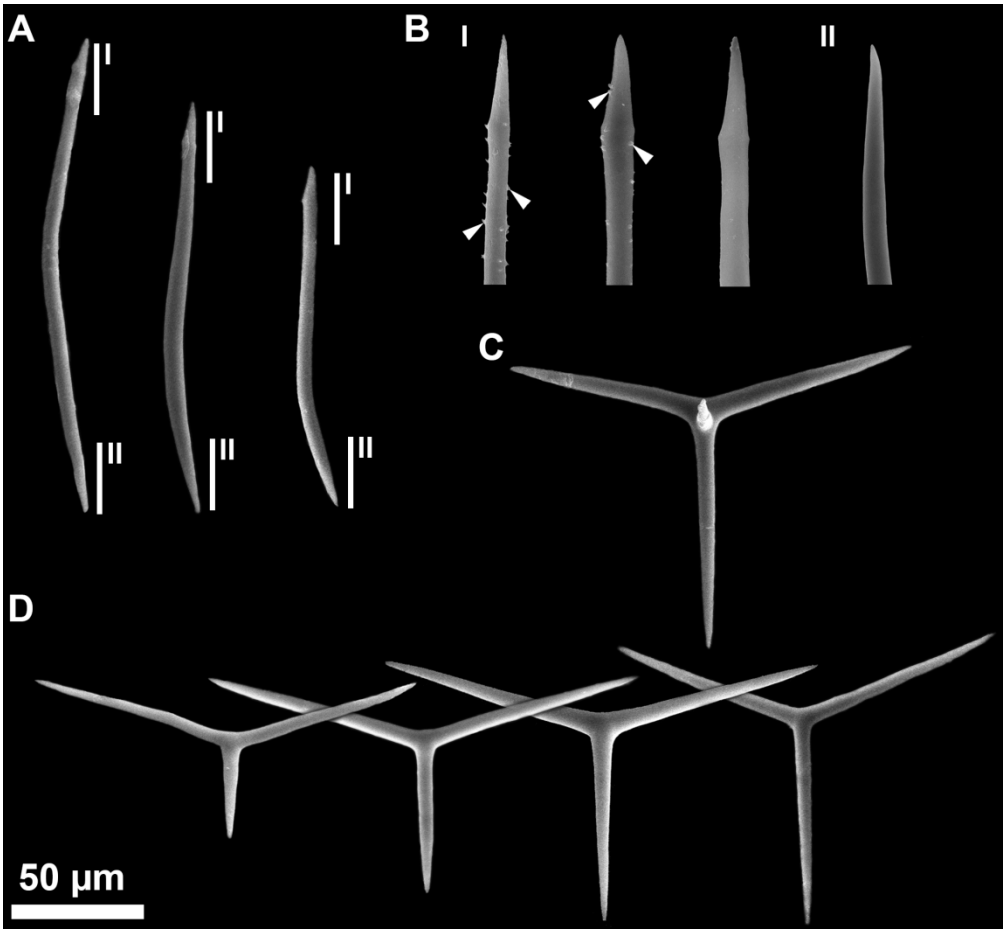

Figure 8. Leucosolenia corallorrhiza (Haeckel, 1872). Spicule types, scanning electron microscopy. A – curved lanceolate diactines; B – tips of diactines, I and II refer to the zones marked on A, white arrowheads mark spines; C – tetractine; D – triactines.

173x160mm (300 x 300 DPI)

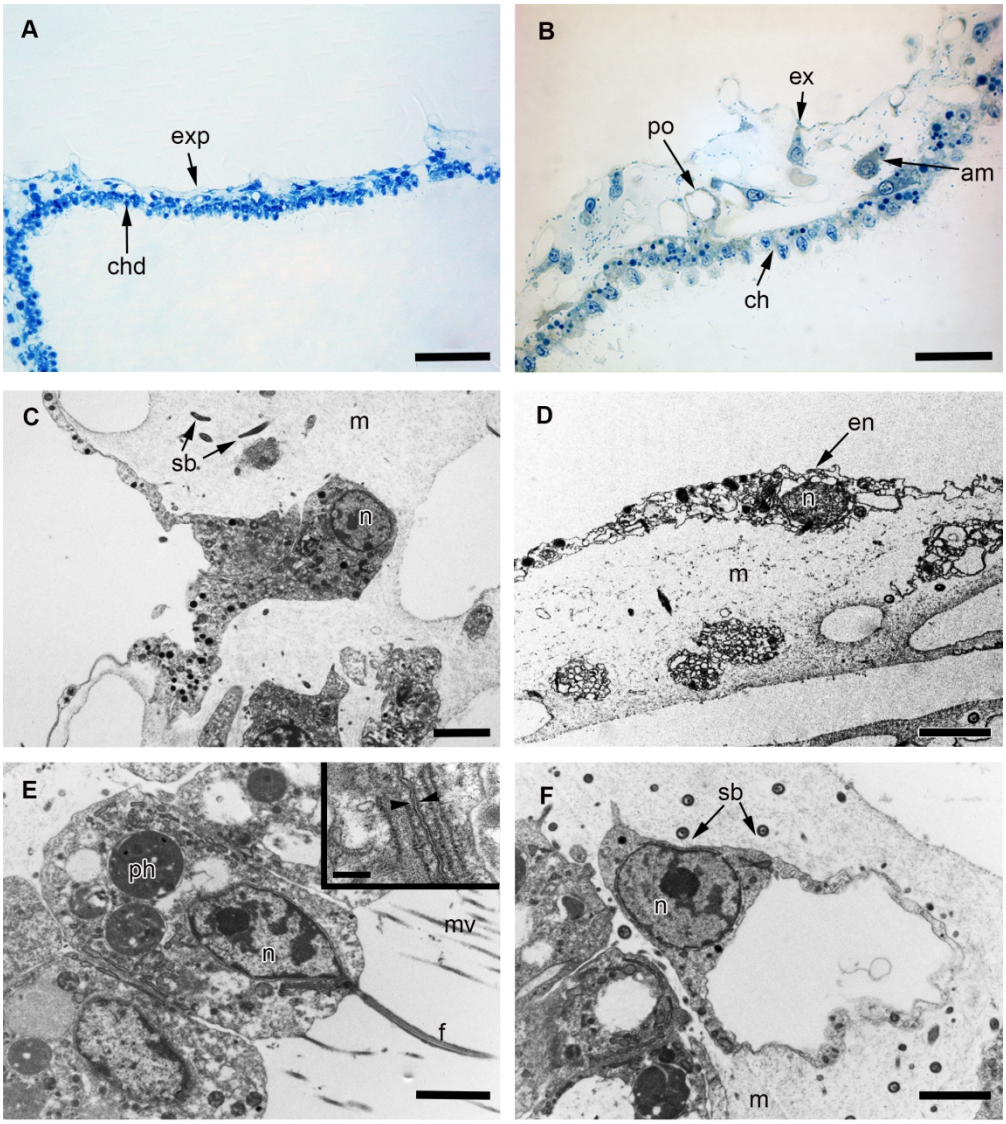

Figure 9. Leucosolenia corallorrhiza (Haeckel, 1872). Body wall structure and cell types of bordering tissues. A, B – semi-thin sections of body wall of sponge; C – exopinacocyte; D – endopinacocyte; E – choanocytes, inset – junctions between choanocytes; F – porocyte. Scale bars: A – 50 μm, B – 20 μm, C - F– 2 μm, inset – 0.2 μm. am – amoebocyte, ch – choanocytes, chd – choanoderm, en – endopinacocyte, exp – exopinacoderm, f – flagellum, m – mesohyl, mv – microvilli, n – nucleus, ph – phagosome, po – porocytes, sb – symbiotic bacteria.

173x194mm (300 x 300 DPI)

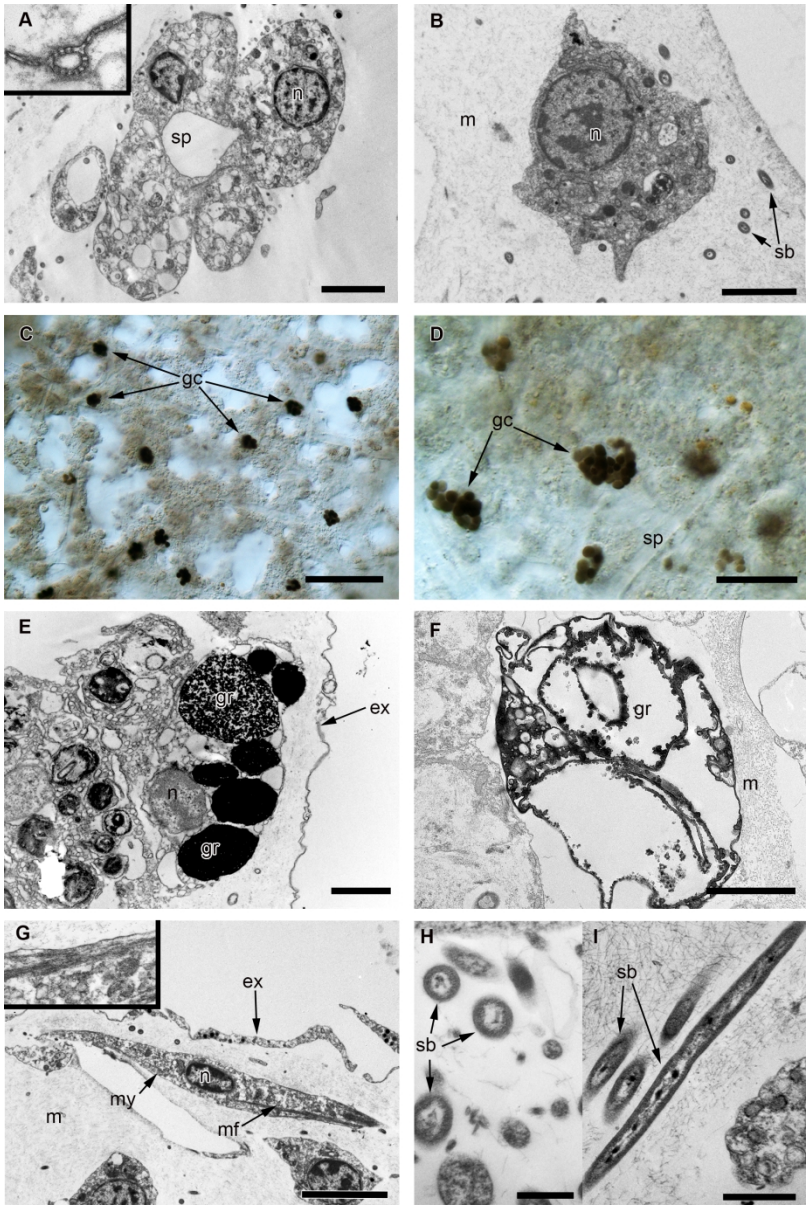

Figure 10. Leucosolenia corallorrhiza (Haeckel, 1872). Mesohyl cell types and symbiotic bacteria. A – sclerocytes, inset – septate junctions between sclerocytes; B – amoebocytes; C, D – granular cells in the body wall; E – granular cell; F – degraded granular cell; G – myocytes, inset - bundles of myofilaments; H, I - symbiotic bacteria, morphotype 1. Scale bars: A, B, E, F – 2 μm, C – 50 μm, C – 20 μm, G – 5 μm, H – 0.5 μm, I – 1 μm. ch – choanocytes, chd – choanoderm, ex – exopinacocyte, exp – exopinacoderm, f – flagellum, gc – granular cells gr – granule, m – mesohyl, mf – myofibrils, mv – microvilli, my – myocytes, n – nucleus, po – porocytes, sb – symbiotic bacteria, sp - spicule.

173x260mm (300 x 300 DPI)

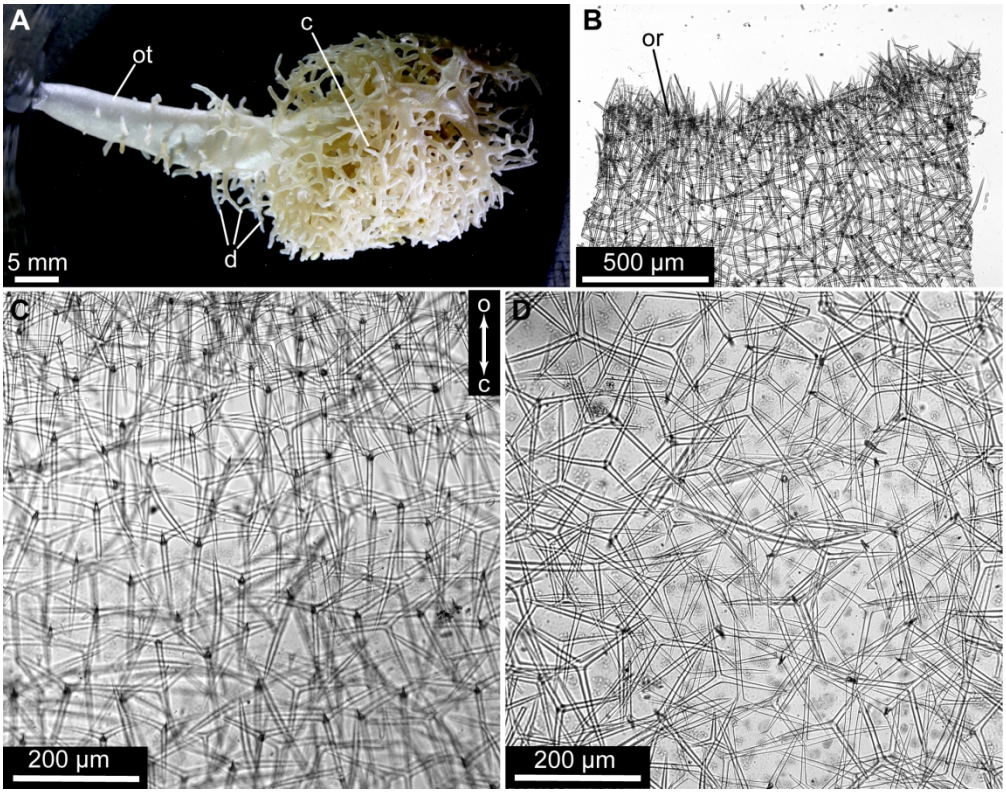

Figure 11. Leucosolenia variabilis Haeckel, 1870. External morphology and skeleton. A – general morphology (WS11731); B – skeleton of oscular rim (WS11731); C – skeleton of oscular tube; D – skeleton of cormus (WS11643). c – cormus, d – diverticulum, o – osculum, or – oscular rim, ot – oscular tube.

174x136mm (300 x 300 DPI)

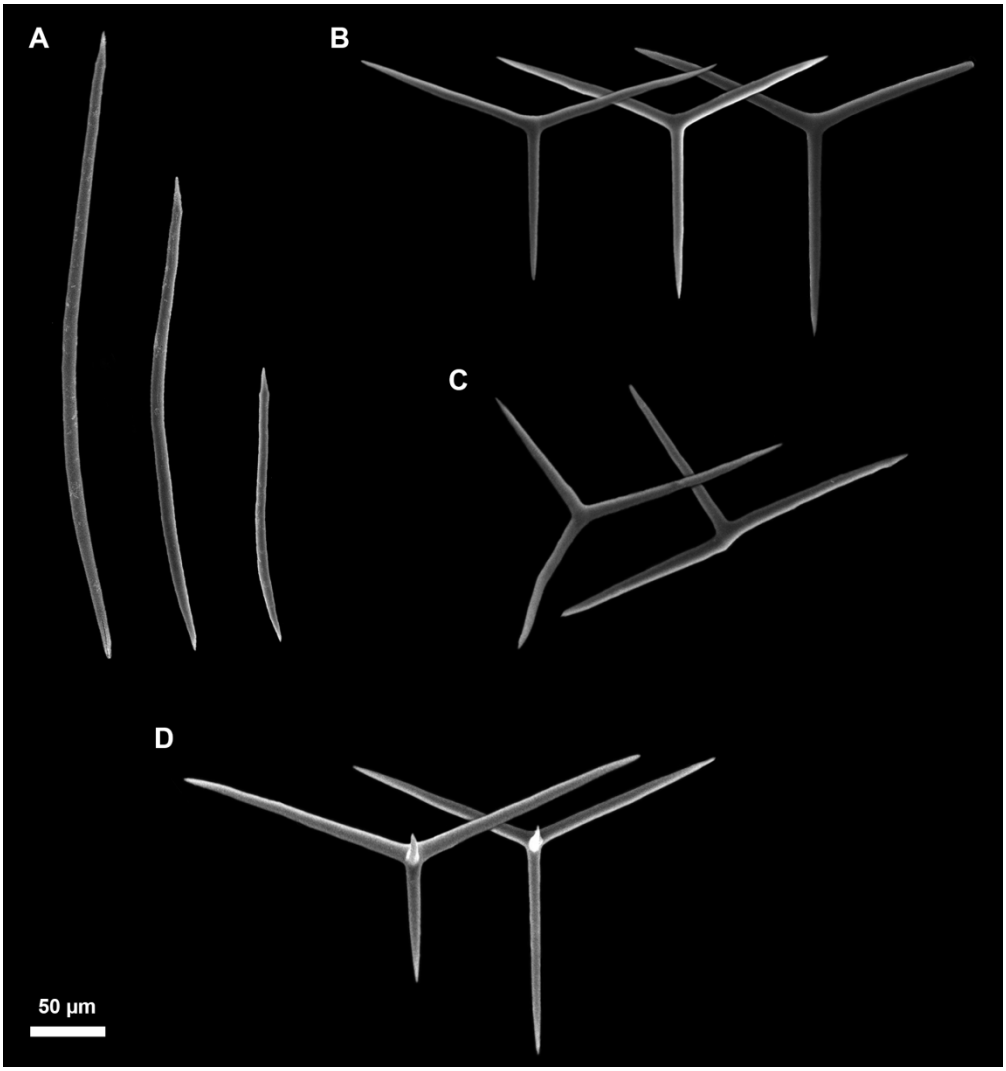

Figure 12. Leucosolenia variabilis Haeckel, 1870. Spicule types, scanning electron microscopy. A – curved smooth lanceolate diactines; B – triactines; C – abnormal triactines; D – tetractine.

173x184mm (300 x 300 DPI)

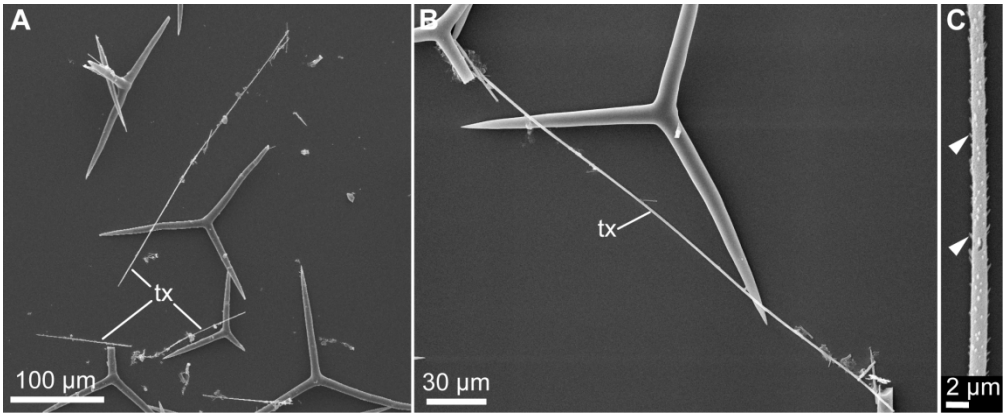

Figure 13. Leucosolenia variabilis Haeckel, 1870. Trichoxeas. A, B – general view of trichoxea fragments; C – enlarge view of trichoxea, white arrowhead marks spines. tx – trichoxeas.

174x71mm (300 x 300 DPI)

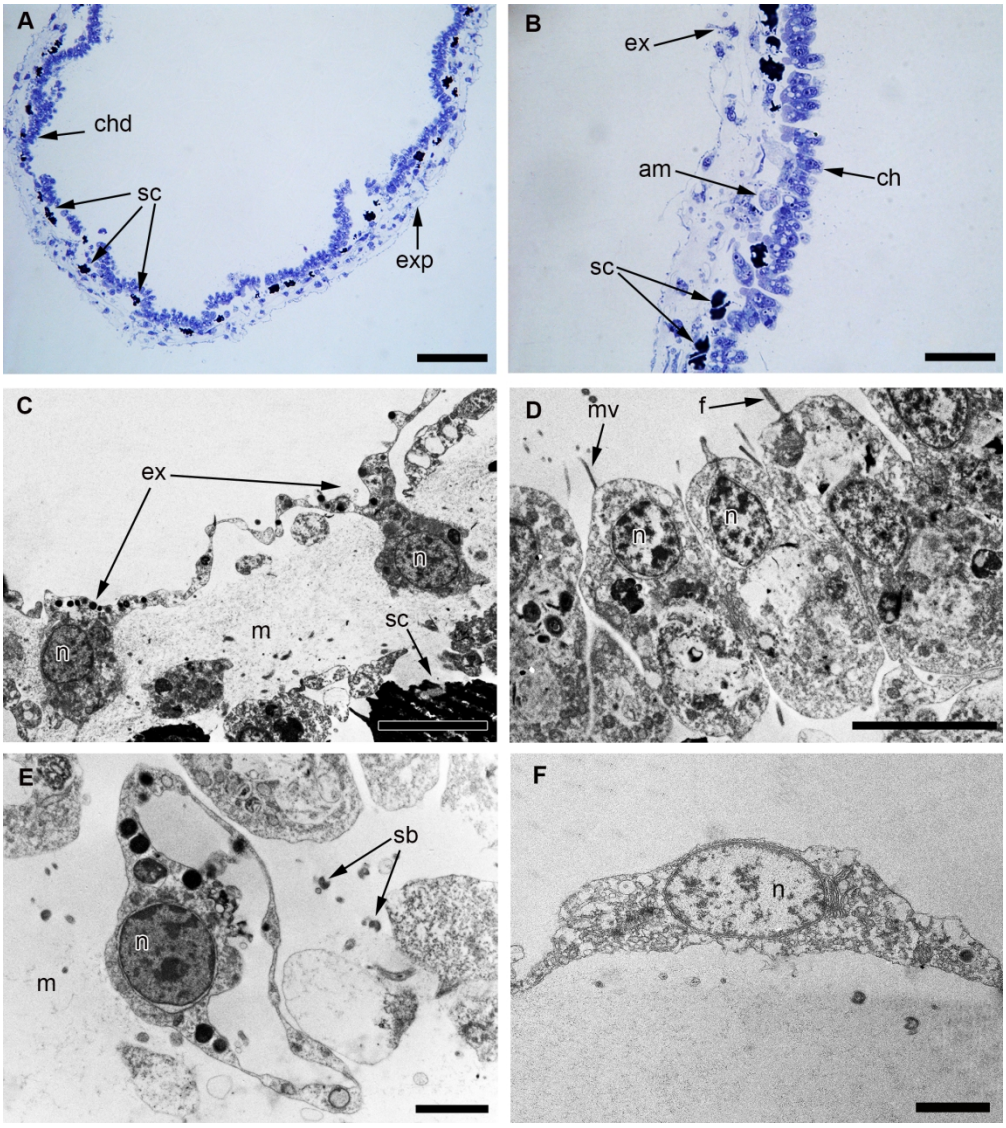

Figure 14. Leucosolenia variabilis Haeckel, 1870. Body wall structure and cell types of bordering tissues. A, B – semi-thin sections of body wall of sponge; C – exopinacocytes; D – choanocytes; E – porocyte; F – endopinacocyte. Scale bars: A - 50 μm, B – 20 μm, C, D – 5 μm, E, F – 2 μm. am - amoeboid cell, ch – choanocytes, chd – choanoderm, ex – exopinacocyte, exp – exopinacoderm, f – flagellum, m – mesohyl, mv – microvilli, n – nucleus, po – porocyte, sb – symbiotic bacteria, sc – spherulous cells.

173x194mm (300 x 300 DPI)

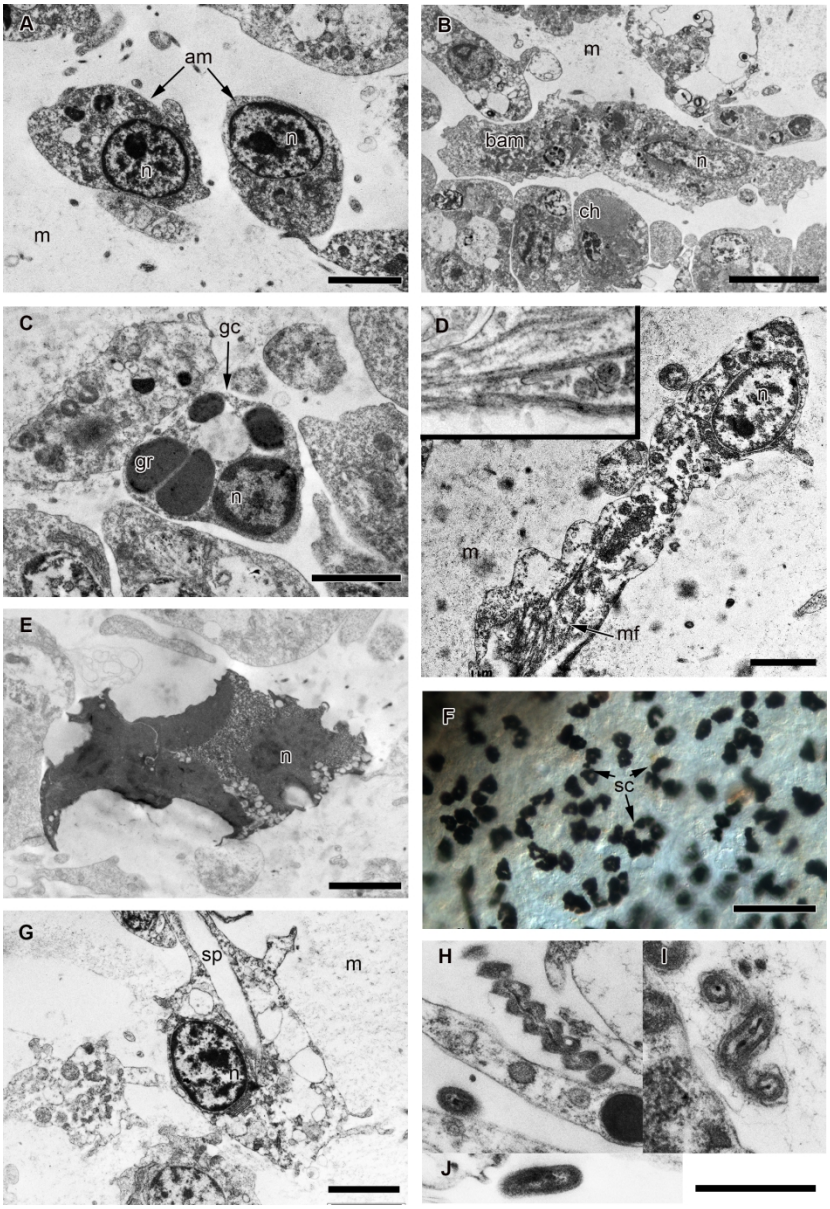

Figure 15. Leucosolenia variabilis Haeckel, 1870. Mesohyl cell types and symbiotic bacteria. A – amoebocytes; B – large amoeboid cell; C – granular cell; D – myocyte, inset - bundles of myofilaments; E – spherulous cell; F – spherulous cells in the body wall; G – sclerocyte; H – symbiotic bacteria, morphotype 1. I – symbiotic bacteria, morphotype 2. J – symbiotic bacteria, morphotype 3. Scale bars: A - 2 μm, B – 5 μm, C-E – 2 μm, F – 50 μm, G – 2 μm, H-J – 1 μm. am - amoebocyte, bam - large amoeboid cell, ch – choanocytes, gc – granular cell, gr – granule, m – mesohyl, mf – myofibrils, n – nucleus, sc – spherulous cells, sp - spicule.

173x253mm (300 x 300 DPI)

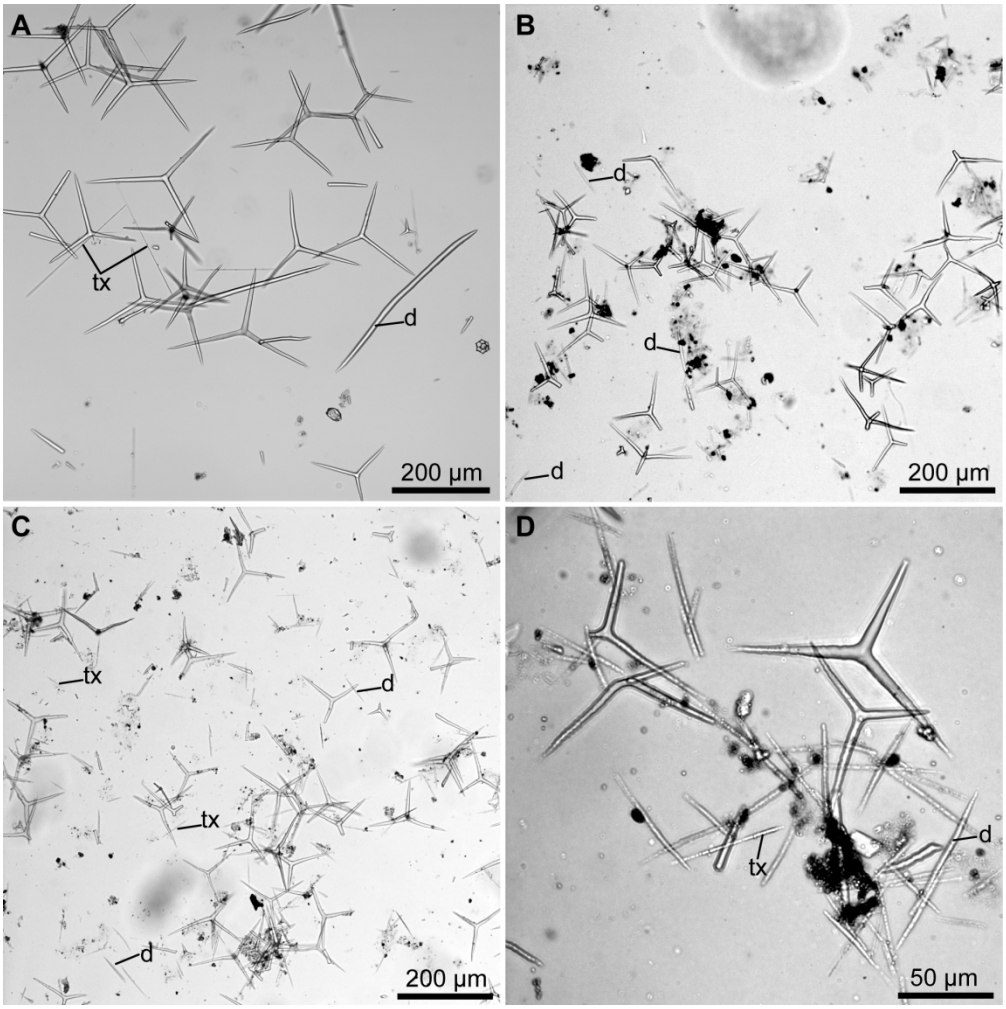

Figure 16. Leucosolenia variabilis Haeckel, 1870. Spicule types in the White Sea specimen (A) and in the specimens from the British Natural History Museum collection (B-D). A – spicules from WS11731; B – spicules from BMNH 1906.12.1.40; C – spicules from BMNH 1906.12.1.50; D – spicules from the syntype BMNH 1910.1.1.421.a. d – diactines, tx – trichoxeas.

174x173mm (300 x 300 DPI)

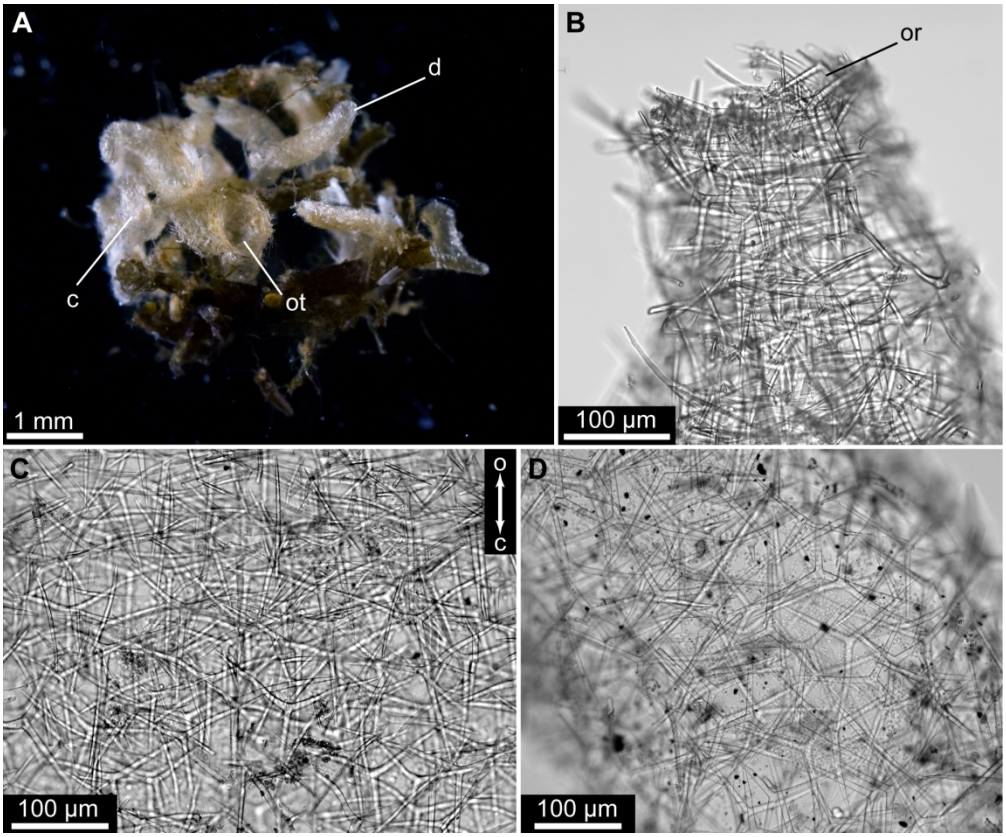

Figure 17. Leucosolenia sp. A. External morphology and skeleton. A – general morphology (WS11752); B – skeleton of oscular rim (WS11770); C – skeleton of oscular tube (WS11770); D – skeleton of cormus (WS11752). c – cormus, d – diverticulum, o – osculum, or – oscular rim, ot – oscular tube.

174x144mm (300 x 300 DPI)

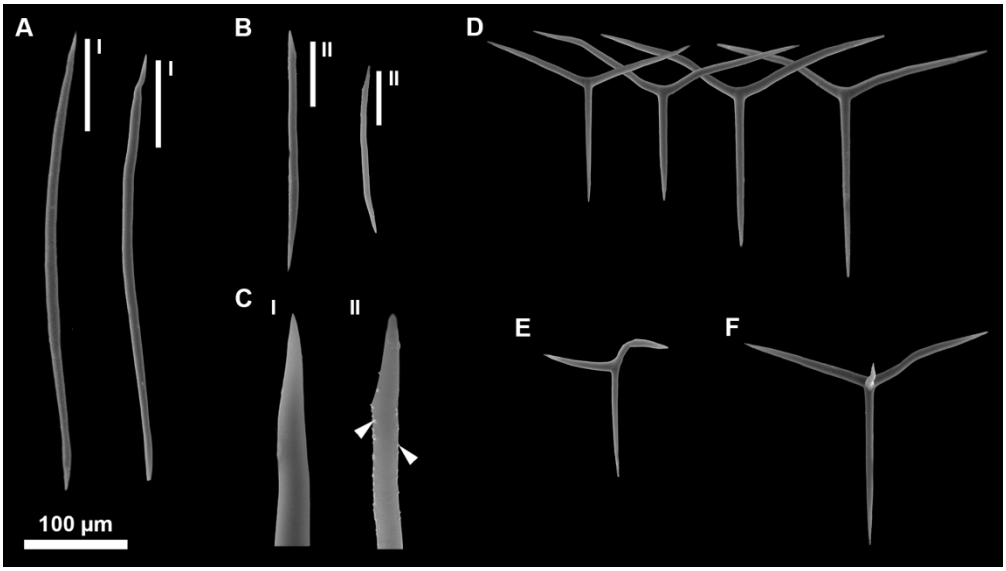

Figure 18. Leucosolenia sp. A. Spicule types, scanning electron microscopy. A – curved smooth diactines; B – curved spiny lanceolate diactines triactines; C – tips of diactines, I and II refer to the zones marked on A and B, white arrowheads mark spines; D – triactines; E – abnormal triactines; F – tetractine.

173x97mm (300 x 300 DPI)

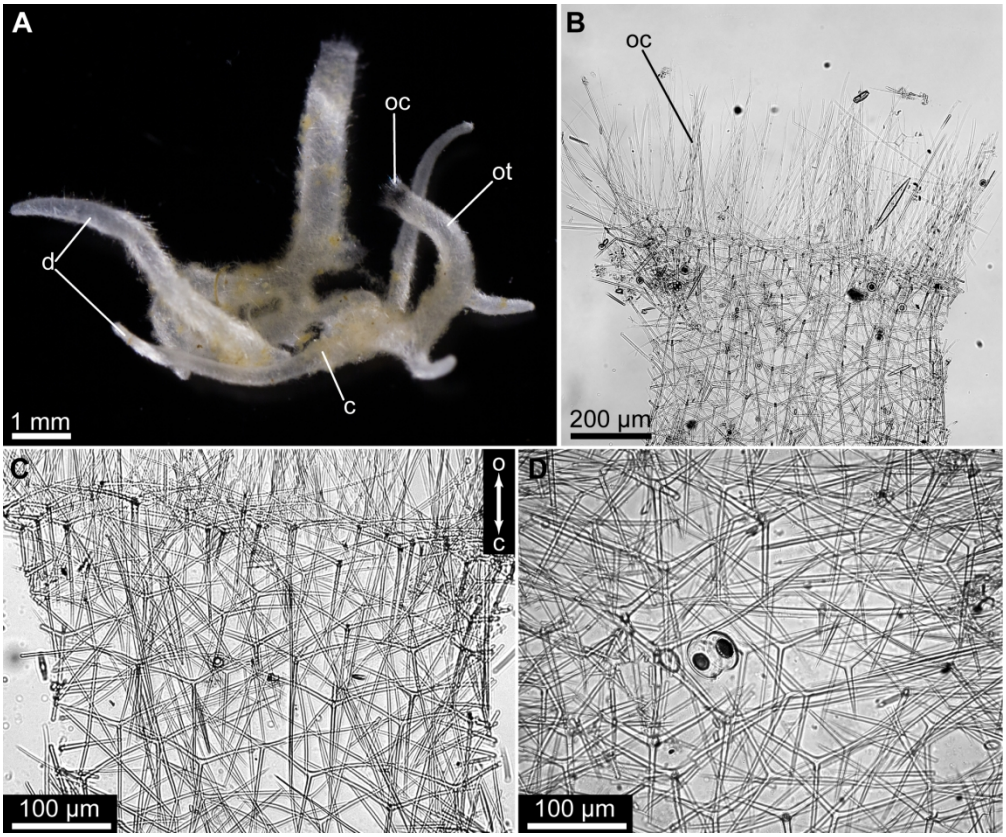

Figure 19. Leucosolenia creepae sp. nov. External morphology and skeleton. A – general morphology (WS11702, holotype); B – skeleton of oscular rim (WS11762); C – skeleton of oscular tube (WS11728); D – skeleton of cormus (WS11655). c – cormus, d – diverticulum, o – osculum, oc – oscular crown, ot – oscular tube.

174x144mm (300 x 300 DPI)

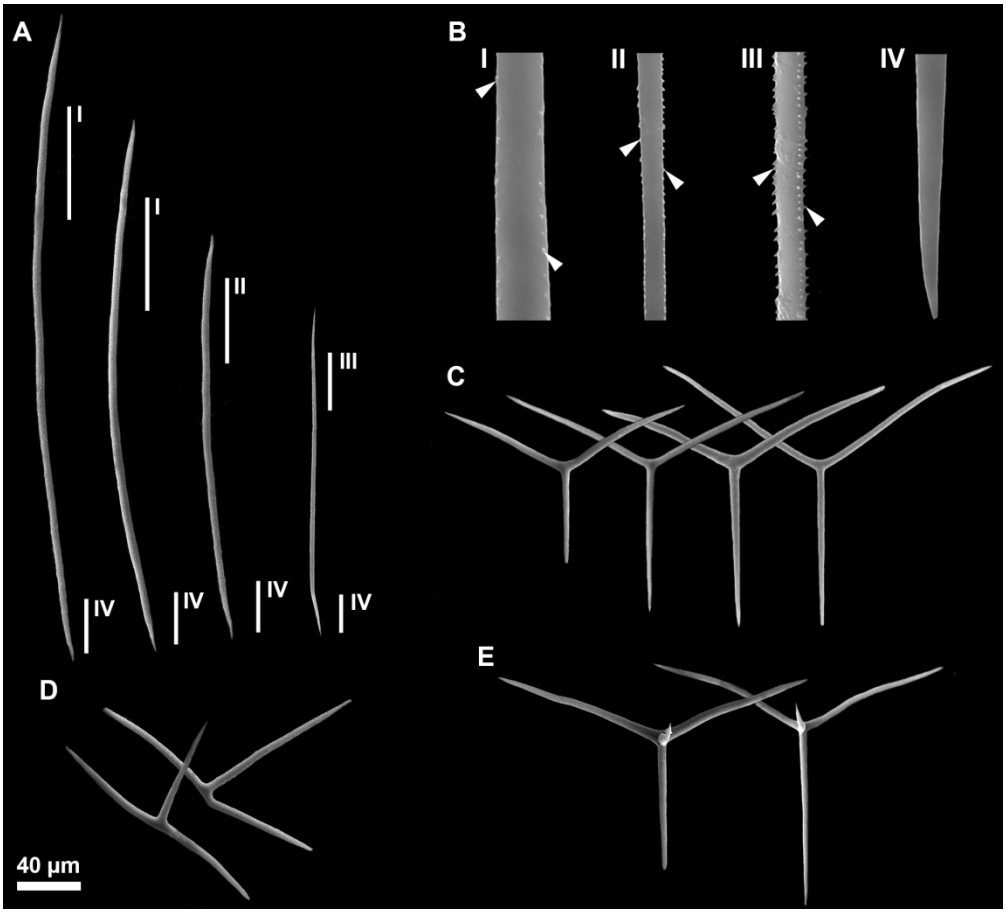

Figure 20. Leucosolenia creepae sp. nov. Spicule types, scanning electron microscopy. A – spiny diactines; B – tips of diactines, I, II, III and IV refer zones marked on A, white arrowheads mark spines; C – triactines; D – abnormal triactines; E – tetractines.

173x157mm (300 x 300 DPI)

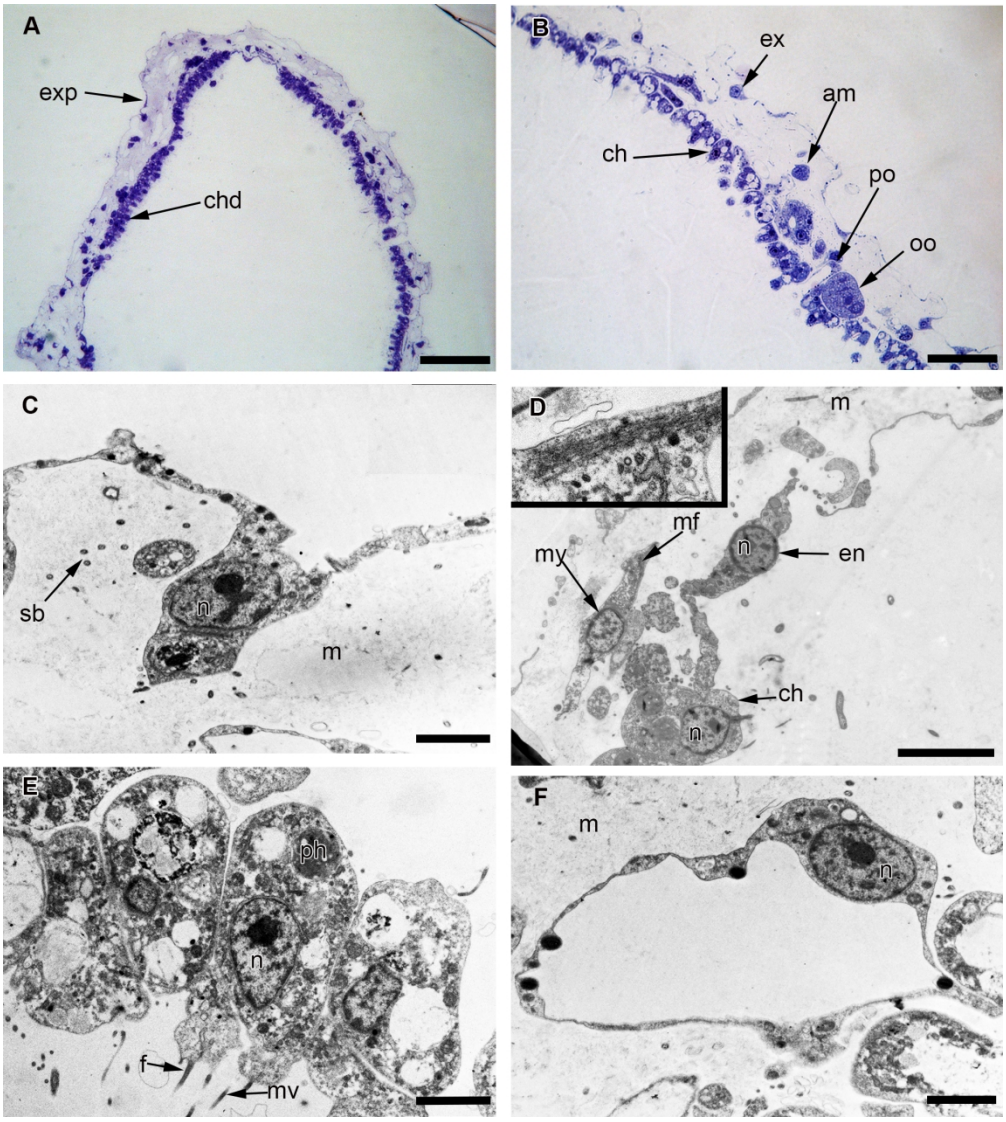

Figure 21. Leucosolenia creepae sp. nov. Body wall structure and cell types of bordering tissues. A, B – semi-thin sections of body wall of sponge; C – exopinacocyte; D – endopinacocyte and myocyte, inset - bundles of myofilaments in the myocyte; E – choanocytes. F – porocyte. Scale bars: A – 50 μm, B – 20 μm, C – 2 μm, D – 5 μm, E, F – 2 μm. am – amoeboid cell, ch – choanocytes, chd – choanoderm, en – endopinacocyte, ex – exopinacocyte, exp – exopinacoderm, f – flagellum, m – mesohyl, mf – myofibrils, mv – microvilli, my – myocytes, n – nucleus, oo – oocyte, ph – phagosome, po – porocyte, sb – symbiotic bacteria.

173x193mm (300 x 300 DPI)

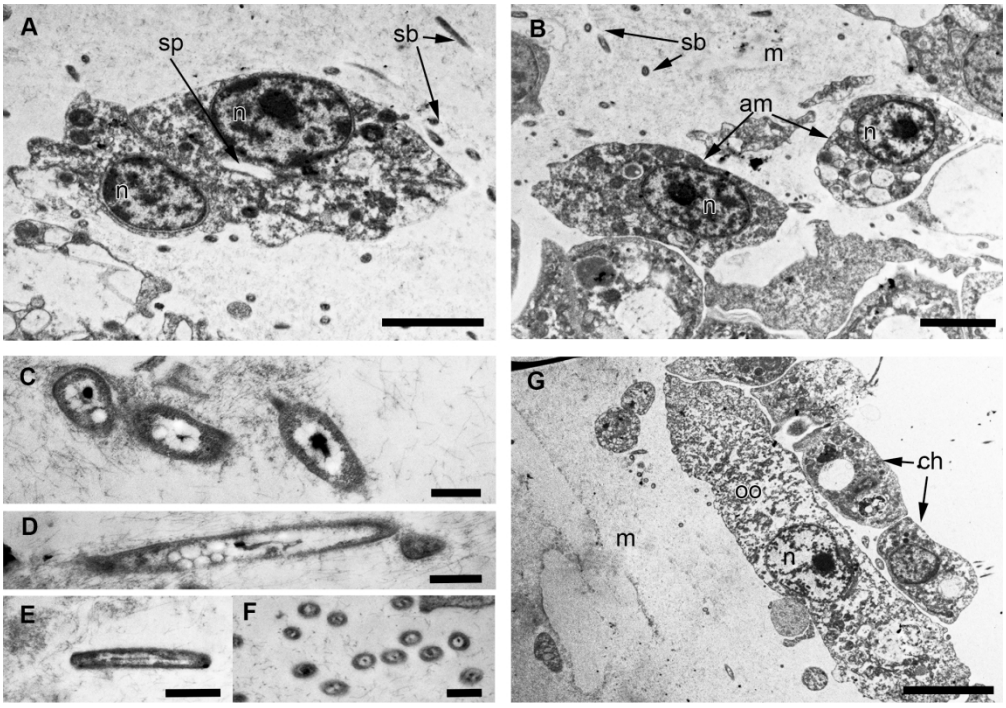

Figure 22. Leucosolenia creepae sp. nov. Mesohyl cell types and symbiotic bacteria. A – sclerocyte; B – amoebocyte; C, D – symbiotic bacteria, morphotype 1; E, F – symbiotic bacteria, morphotype 2; G – young oocyte. Scale bars: A, B – 2 μm, C - F – 0.5 μm, G – 5 μm. am - amoeboid cell, ch – choanocytes, m – mesohyl, n – nucleus, oo – oocyte, sb – symbiotic bacteria, sp – spicule.

173x121mm (300 x 300 DPI)

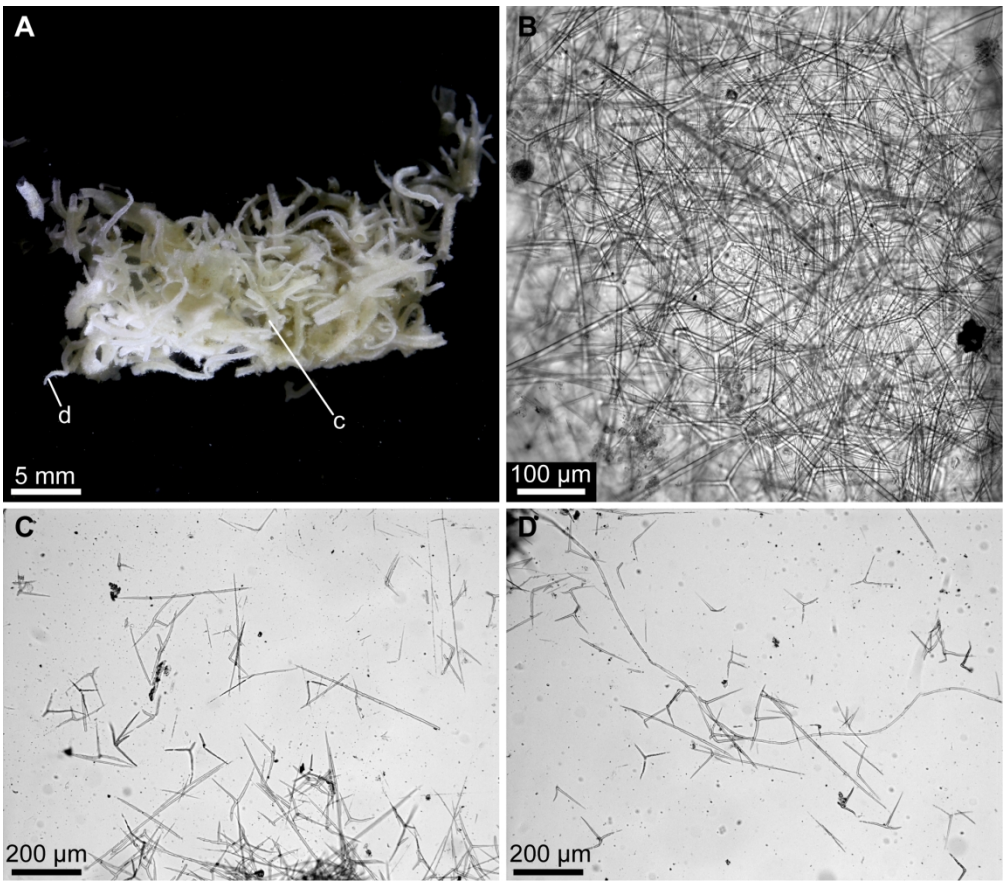

Figure 23. Leucosolenia somesii (Bowerbank, 1874). External morphology and skeleton. A – general morphology (ZMA Por. 17572); B – skeleton of cormus (ZMA Por. 17572); C, D – spicules from BMNH 1956.4.26.35. c – cormus, d – diverticulum.

174x152mm (300 x 300 DPI)

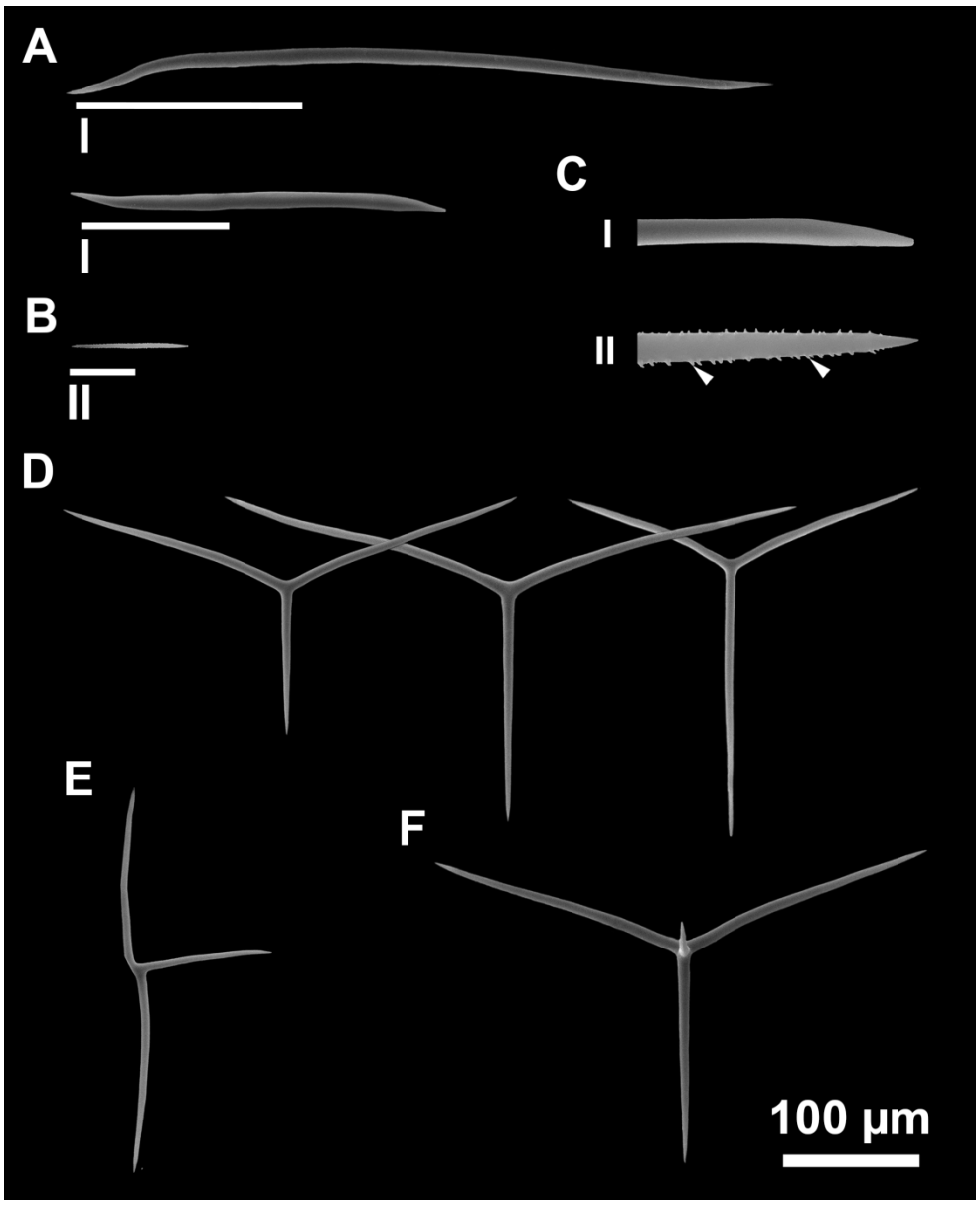

Figure 24. Leucosolenia somesii (Bowerbank, 1874). ZMA Por. 17572. Spicule types, scanning electron microscopy. A – curved smooth diactines; B – straight spiny diactines; C – tips of diactines, I and II refer to the zones marked on A and B, white arrowheads mark spines; D – triactines; E – abnormal triactines; F – tetractines.

173x213mm (300 x 300 DPI)